



University of Kentucky  
UKnowledge

---

University of Kentucky Master's Theses

Graduate School

---

2005

## CYCLE-UP OF MULTIPLE RIFTING EVENT MODELS: HOW LONG DOES IT TAKE TO REACH A STEADY STATE STRESS?

Lokranjith K. Ravi

*University of Kentucky*, [vaavilok@yahoo.com](mailto:vaavilok@yahoo.com)

[Right click to open a feedback form in a new tab to let us know how this document benefits you.](#)

---

### Recommended Citation

Ravi, Lokranjith K., "CYCLE-UP OF MULTIPLE RIFTING EVENT MODELS: HOW LONG DOES IT TAKE TO REACH A STEADY STATE STRESS?" (2005). *University of Kentucky Master's Theses*. 338.  
[https://uknowledge.uky.edu/gradschool\\_theses/338](https://uknowledge.uky.edu/gradschool_theses/338)

This Thesis is brought to you for free and open access by the Graduate School at UKnowledge. It has been accepted for inclusion in University of Kentucky Master's Theses by an authorized administrator of UKnowledge. For more information, please contact [UKnowledge@lsv.uky.edu](mailto:UKnowledge@lsv.uky.edu).

## ABSTRACT OF THESIS

### CYCLE-UP OF MULTIPLE RIFTING EVENT MODELS: HOW LONG DOES IT TAKE TO REACH A STEADY STATE STRESS?

Many geological numerical models are initiated with a background stress state of zero. Often these numerical results are compared directly to geodetic data. Recent work (Kenner and Simons, 2004) has shown that modeled deformation rates can change as the model is ‘cycled-up’ following repeated earthquakes or rifting events. In this study, we investigate model cycle-up in the context of time-dependent deformation following rifting during the 1975-1984 Krafla eruption in Iceland. We consider the number of rifting cycles required for complete cycle-up, variations in cycle-up time at different locations in the model, background stress magnitudes in fully cycled-up models, and errors incurred when the models are not properly cycled-up.

The modeling is done using the commercial software ABAQUS. In ABAQUS a user-defined subroutine is used to apply repeated rifting events within the finite element model. We have generated various 3D models with different fault/rift geometries. The models include (1) a straight rift oriented perpendicular to the far-field velocity boundary conditions, (2) a rift oriented at an angle to the far-field velocities, (3) a model containing two intersecting rifts, one perpendicular to the far-field velocities and the other rift intersecting the first at an angle, and (4) overlapping rift segments in which the overlapped region is bounded by strike-slip faults.

Keywords: Rifting, cycle-up, finite element analysis, Iceland, user-subroutine.

Lokranjith K Ravi

Date:01/12/2005

CYCLE-UP OF MULTIPLE RIFTING EVENT MODELS: HOW  
LONG DOES IT TAKE TO REACH A STEADY STATE STRESS?

By

Lokranjith K Ravi

Dr. Keith Rouch

-----  
(Director of Thesis)

Dr. George Huang

-----  
(Director of Graduate Studies)

01/12/2004

-----  
(Date)

CYCLE-UP OF MULTIPLE RIFTING EVENT MODELS: HOW  
LONG DOES IT TAKE TO REACH A STEADY STATE STRESS?

By

Lokranjith K Ravi

Dr. Shelley J. Kenner

---

(Co-Director of Thesis)

Dr. George Huang

---

(Director of Graduate Studies)

01/12/2004

---

(Date)

## RULES FOR THE USE OF THESES

Unpublished theses submitted for the Master's degree and deposited in the University of Kentucky Library are as a rule open for inspection, but are to be used only with due regard to the rights of the authors. Bibliographical references may be noted, but quotations or summaries of parts may be published only with the permission of the author, or with the usual scholarly acknowledgements.

Extensive copying or publication of the thesis in whole or in part also requires the consent of the Dean of the Graduate School of the University of Kentucky.

THESIS

Lokranjith K Ravi

The Graduate School  
University of Kentucky

2005

CYCLE-UP OF MULTIPLE RIFTING EVENT MODELS: HOW  
LONG DOES IT TAKE TO REACH A STEADY STATE STRESS?

---

THESIS

---

A thesis submitted in partial fulfillment of the requirements  
for the degree of Master of Science in Mechanical Engineering in the  
College of Engineering at the  
University of Kentucky

By

Lokranjith K Ravi

Lexington, Kentucky

Director: Dr. Keith Rouch, Professor of Mechanical Engineering

Lexington, Kentucky

2004

CYCLE-UP OF MULTIPLE RIFTING EVENT MODELS: HOW  
LONG DOES IT TAKE TO REACH A STEADY STATE STRESS?

---

THESIS

---

A thesis submitted in partial fulfillment of the requirements  
for the degree of Master of Science in Mechanical Engineering in the  
College of Engineering at the  
University of Kentucky

By

Lokranjith K Ravi

Lexington, Kentucky

Co-Director: Dr. Shelley J. Kenner, Professor of Geological Sciences

Lexington, Kentucky

2004



***Dedicated to:***

*Lord*

*Shri. Venkateswara Swami*

*Father*

*Shri. Rama Rao Ravi*

*Mother*

*Shri. Swarna Ravi*

*Brother*

*Mr. Venu Madhave Ravi*

**MASTER'S THESIS RELEASE**

**I authorize the University of Kentucky  
Libraries to reproduce this thesis in  
whole or in part for purposes of research.**

**Signed:** \_\_\_\_\_

**Date:** \_\_\_\_\_



## ACKNOWLEDGEMENTS

I am deeply indebted to my advisor, Dr. Shelley J. Kenner for providing me an opportunity to grow in every aspect of my life under her able guidance. I thank her from the bottom of my heart for having given me a chance to be a part of this research. I have greatly benefited from my long hours of interaction with her each day. She has pulled me out of many ignorant situations and has supported and inspired me through my graduation. I am at loss of words to truly honor such a great and exceptional personality.

I am deeply obliged to Dr. Keith Rouch and Dr. Kaveh A. Tagavi for having agreed to be on my Thesis Committee. I thank Dr. Keith Rouch for providing outstanding insights that have guided me to deliver a much better work and supporting my graduate research in the Department of Geological Sciences.

It is only the unparalleled love, support and vision of my parents that has made this work a reality. I dedicate this work to Lord Venkateswara, my mother, father, and brother who has been my source of strength since childhood. They laid a strong foundation to my future, inspired me to take up engineering as a career. Finally, I would like to thank all my friends who have understood and motivated me during the course of this work. It is their unconditional love that has sustained me through the last couple of years.

# TABLE OF CONTENTS

ACKNOWLEDGMENTS.....	iii
TABLE OF CONTENTS.....	iv
LIST OF FIGURES.....	vii
CHAPTER 1: INTRODUCTION.....	2
1.1 PLATE TECTONICS.....	3
1.1(a) Converging Plate Boundaries.....	3
1.1(b) Transform Plate Boundaries.....	3
1.1(c) Diverging Plate Boundaries.....	4
1.2 FINITE ELEMENT ANALYSIS.....	6
1.2(a) What is Finite Element Analysis? .....	7
1.2(b) Introduction to ABAQUS .....	9
CHAPTER 2: RIFTING MODELS .....	11
2.1 HOW DOES RIFTING START? .....	13
2.1.1 Plate Tectonics and Boundaries .....	13
2.1.2 Types of Plate Boundaries .....	14
2.1.2a Transform Boundaries .....	14
2.1.2b Divergent Boundaries .....	15
2.1.2c Convergent Boundaries .....	16
2.2 GEOLOGY OF ICELAND .....	17
2.3 REVIEW OF PUBLISHED LITERATURE .....	19
2.4 INTRODUCTION TO SIMPLE RIFTING MODELS .....	21
2.4.1 Straight Rift Model .....	22

2.4.2 Inclined Rift Model .....	23
2.4.3 Intersecting Rift Model .....	24
2.4.4 Skewed Rift Model and Double Kink Rift Model.....	25
2.4.5 Box Rift Model .....	27
CHAPTER 3: PRE- AND POST-PROCESSING OF RIFTING MODELS .....	28
3.1 DEVELOPING PRE- AND POST-PROCESSORS OF FINITE ELEMENT RIFTING MODELS .....	29
3.2 BOUNDARY CONDITIONS .....	32
3.3 ELEMENT SELECTION .....	33
3.3.1a Family .....	34
3.3.1b Degrees of Freedom .....	34
3.3.1c Number of Nodes .....	34
3.3.1d Formulation .....	35
3.3.1e Integration .....	35
3.3.2 Naming Convention .....	36
3.4 MODELING AND MESHING ISSUES .....	37
3.4.1 Modeling .....	37
3.4.2 Meshing .....	38
3.4.3 Virtual Topology.....,	39
CHAPTER 4: MULTIPLE RIFTING EVENTS: CYCLE-UP OF RIFTING MODELS...40	
4.1 USER SUBROUTINES IN ABAQUS.....	41
4.2 NEED FOR USER SUBROUTINE IN THE MODEL .....	42
4.2a What Does the Subroutine Do? .....	43
4.3 MULTI POINT CONSTARINT USER SUBROUTINE (*MPC) .....	44

4.3a Variables to be Defined .....	45
4.3b User Subroutine Interface .....	46
4.3c Variables Passed in for Information .....	47
4.4 USER INPUTS TO USER SUBROUTINE .....	48
4.4a During Loading .....	48
4.4b During Rifting .....	50
CHAPTER 5: RESULTS AND DISCUSSION.....	51
5.1 EXPERIMNET 1: STRAIGHT RIFT MODEL .....	54
5.2 EXPERIMNET 2: INCLINED RIFT MODEL .....	63
5.3 EXPERIMNET 3: INTERSECTING RIFT MODEL .....	71
5.4 EXPERIMNET 4: BOX RIFT MODEL .....	79
5.5 EXPERIMENT 5&6: SKEWED RIFT MODEL & DOUBLE KINK MODEL...	86
CHAPTER 6: CONCLUSIONS.....	88
6.1 CONCLUSIONS.....	89
CHAPTER 7: SCOPE OF FUTURE WORK.....	91
7.1 FUTURE WORK.....	92
APPENDIX A: GLOSSARY.....	94
APPENDIX B: USER INPUT FILE .....	99
APPENDIX C: GEOLOGICAL TIME SCALE .....	103
REFERENCES.....	104
VITA.....	107

## LIST OF FIGURES

Figure 1.: Earth cutaway.....	2
Figure 1.1b:Map of Iceland and the diverging plate boundaries .....	4
Figure 2.1.2a: The cross-section of the main types of plate boundaries.....	15
Figure 2.1.2b: Diverging plate boundaries.....	16
Figure 2.2: Geology of Iceland.....	17
Figure 2.4.1: Straight Rift Model.....	23
Figure 2.4.2: Inclined Rift Model.....	24
Figure 2.4.3: Intersecting Rift Model.....	25
Figure 2.4.4a: Skewed Rift Model.....	26
Figure 2.4.4b: Double Kink Model.....	26
Figure 2.4.5: Box Rift Model.....	27
Figure 3.3.1a: Element Families.....	34
Figure 3.3.1c: Linear and quadratic brick element.....	35
Figure 4.2a: Schematic model.....	43
Figure 5.1a: Straight Rift Model Assembly .....	54
Figure 5.1b: Top View of Straight Rift Model.....	55
Figure 5.1c: Shaded Model with Loads and Boundary Conditions .....	55
Figure 5.1d: Meshed Model.....	56
Figure 5.1e: Model at the End of the Initial Step.....	57
Figure 5.1f: Model Mises Stresses at the End of the 1 <sup>st</sup> Loading Step.....	58
Figure 5.1g: Model Mises stresses at the End of the 8 <sup>th</sup> Rifting Step .....	58
Figure 5.1h: Top View of the Rift/Fault with Mises Stresses at the End of 8 <sup>th</sup> Rifting Step .....	59



Figure 5.1i: Displacement of the Nodes on the Rift During the 16 Step Analysis ...	60
Figure 5.1j: Cycle-Up and Subsequent steady State Mises Stress for the Right Hand Bottom Node on the Front Face of the Model .....	61
Figure 5.1k: Cycle-Up and Subsequent Steady State Mises Stress for a Node Located at the Base of the Rift on the Front Face of the Model .....	62
Figure 5.1l: Cycle-Up and Subsequent Steady State Mises Stress for a Node Located in the Middle of the Front Face of the Model .....	63
Figure 5.2a: Inclined Rift Model Assembly .....	64
Figure 5.2b: Top View of Inclined Rift Model.....	64
Figure 5.2c: Shaded Model with Loads and Boundary Conditions .....	65
Figure 5.2d: Meshed Model.....	65
Figure 5.2e: Model at the End of the Initial Step.....	66
Figure 5.2f: Model Mises Stresses at the End of the 1 <sup>st</sup> Loading Step.....	66
Figure 5.2g: Model Mises stresses at the End of the 8 <sup>th</sup> Rifting Step .....	67
Figure 5.2h: Top View of the Rift/Fault with Mises Stresses at the End of 8 <sup>th</sup> Rifting Step .....	67
Figure 5.2i: Displacement of the Nodes on the Rift During the 16 Step Analysis ...	68
Figure 5.2j: Cycle-Up and Subsequent steady State Mises Stress for the Right Hand Bottom Node on the Front Face of the Model .....	69
Figure 5.2k: Cycle-Up and Subsequent Steady State Mises Stress for a Node Located at the Base of the Rift on the Front Face of the Model .....	70
Figure 5.2l: Cycle-Up and Subsequent Steady State Mises Stress for a Node Located in the Middle of the Front Face of the Model .....	71

Figure 5.3a: Intersecting Rift Model Assembly .....	72
Figure 5.3b: Top View of Intersecting Rift Model.....	72
Figure 5.3c: Shaded Model with Loads and Boundary Conditions .....	73
Figure 5.3d: Meshed Model.....	73
Figure 5.3e: Model at the End of the Initial Step.....	74
Figure 5.3f: Model Mises Stresses at the End of the 1 <sup>st</sup> Loading Step.....	74
Figure 5.3g: Model Mises stresses at the End of the 8 <sup>th</sup> Rifting Step .....	75
Figure 5.3h: Top View of the Rift/Fault with Mises Stresses at the End of 8 <sup>th</sup> Rifting Step.....	75
Figure 5.3i: Displacement of the Nodes on the Rift During the 16 Step Analysis ..	76
Figure 5.3j: Cycle-Up and Subsequent steady State Mises Stress for the Right Hand Bottom Node on the Front Face of the Model .....	77
Figure 5.3k: Cycle-Up and Subsequent Steady State Mises Stress for a Node Located at the Base of the Rift on the Front Face of the Model .....	78
Figure 5.3l: Cycle-Up and Subsequent Steady State Mises Stress for a Node Located in the Middle of the Front Face of the Model .....	78
Figure 5.4a: Box Rift Model Assembly .....	79
Figure 5.4b: Top View of Box Rift Model.....	80
Figure 5.4c: Shaded Model with Loads and Boundary Conditions .....	80
Figure 5.4d: Meshed Model.....	81
Figure 5.4e: Model at the End of the Initial Step.....	81
Figure 5.4f: Model Mises Stresses at the End of the 1 <sup>st</sup> Loading Step.....	82
Figure 5.4g: Model Mises stresses at the End of the 8 <sup>th</sup> Rifting Step .....	82

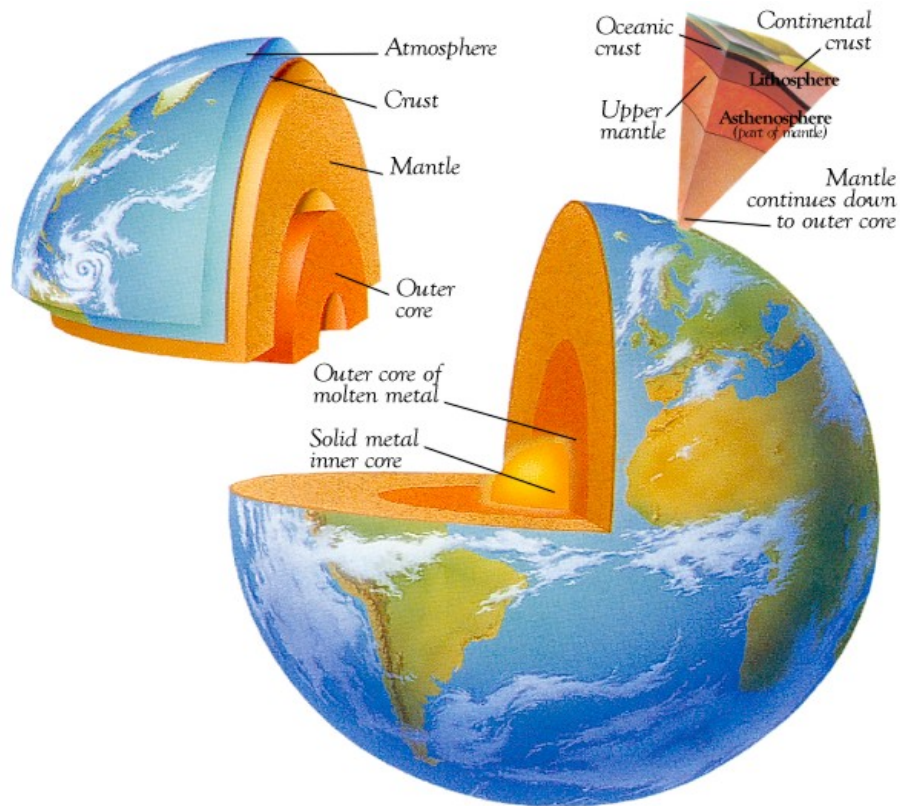
Figure 5.4h: Top View of the Rift/Fault with Mises Stresses at the End of 8 <sup>th</sup> Rifting Step .....	83
Figure 5.4i: Displacement of the Nodes on the Rift During the 16 Step Analysis ...	83
Figure 5.4j: Cycle-Up and Subsequent steady State Mises Stress for the Right Hand Bottom Node on the Front Face of the Model .....	84
Figure 5.4k: Cycle-Up and Subsequent Steady State Mises Stress for a Node Located at the Base of the Rift on the Front Face of the Model .....	85
Figure 5.4l: Cycle-Up and Subsequent Steady State Mises Stress for a Node Located in the Middle of the Front Face of the Model .....	86
Figure 5.5a: Skewed Rift Model.....	86
Figure 5.5b: Double Kink Model.....	87
Figure 7.1: Model with a complex rift pattern.....	92
Figure 7.2: Parts of the complex model.....	93

# **CHAPTER ONE**

## ***INTRODUCTION***

1.3 PLATE TECTONICS.....	3
1.1(a) Converging Plate Boundaries.....	3
1.1(b) Transform Plate Boundaries.....	3
1.1(c) Diverging Plate Boundaries.....	4
1.4 FINITE ELEMENT ANALYSIS.....	6
1.2(a) What is Finite Element Analysis? .....	7
1.2(b) Introduction to ABAQUS .....	9

# 1. INTRODUCTION



**Earth cutaway**

FIG 1. Sections of the earth have been removed to show its internal structure.

Image by: Colin Rose, Dorling Kindersley

The earth consists of several layers. The three main layers are the core, the mantle and the crust. The core is the inner part of the earth, the crust is the outer part and between them is the mantle. The lithosphere is comprised of both crust and a part of the upper mantle. The lithosphere has varying thickness and is brittle down till ~15 km. Below this layer it is viscoelastic over long time scales. It easily fractures at low temperatures having an average thickness of 25 km. The thickness of the lithosphere beneath continents ranges

up to 30 km and is thinner beneath oceanic ridges and rift valleys. Below the lithosphere is the asthenosphere\* and its thickness ranges from 100-200 km. The lithosphere is not entirely brittle. In this study we will be discussing the rifting events in Iceland. We will include both lithosphere and asthenosphere as these layers are diverging at this location. In the discussions to follow the terms denoting “\*” are better explained in Appendix A.

## **1.1 PLATE TECTONICS**

Plate tectonics is a synthesis of geological and geophysical observations in which the earth’s crust is conceived to be divided into six or more large rigid plates, each of which rotates about its own pole of rotation. The movement of these crustal plates are thought to produce regions of tectonic activity along their margins. These regions are believed to be the site of most large earthquakes, volcanism, the formation of island arcs and mid-oceanic ridges\*. The theory of plate tectonics was formulated during the late 1960’s.

### ***1.1(a) Converging Plate Boundaries***

Converging plate boundaries are where plates run into each other. The most common type are where oceanic lithosphere\* subducts beneath continental lithosphere. Several mechanisms contribute to the generation\* of magmas\* in this environment

### ***1.1(b) Transform Plate Boundaries***

Transform plate boundaries are a different class of plate boundaries, where in the plates move horizontally past each other on strike-slip faults. Lithosphere is neither created nor

destroyed. Transform plate boundaries are shearing zones where plates move past each other without diverging or converging.

### 1.1(c) *Diverging Plate Boundaries*

Diverging plate boundaries are where plates move away from each other. These include oceanic ridges\* or spreading centers\*, and rift valleys\*. Oceanic Ridges are areas where the mantle ascends due to rising convection currents. Decompression melting is a process that involves the upward movement of the earth's mantle to an area of lower pressure. The reduction in overlying pressure enables the rock to melt, leading to magma formation. Decompression melting thus results in generating magmas that intrude and erupt at the oceanic ridges to create new oceanic crust. Iceland is one of the few areas where the diverging plate boundaries are evident on land.

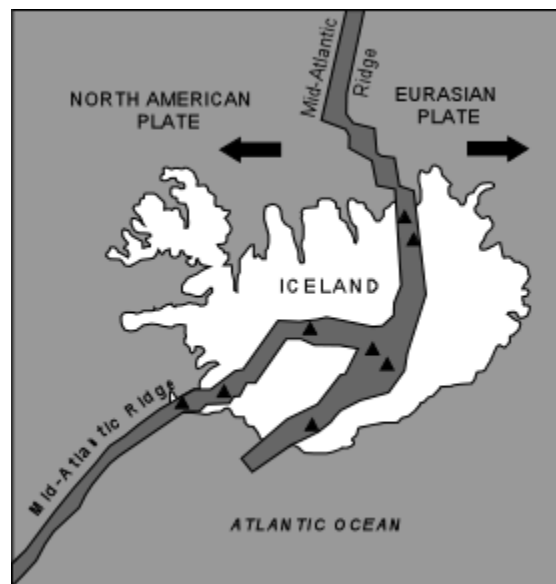


FIG 1.1c Map of Iceland and the diverging plate boundaries

(U.S. Geological Survey. [www.usgs.gov](http://www.usgs.gov))

In Iceland, we can observe the Mid Atlantic Ridge\* above sea level as well as its associated volcanism. The anomalous elevation of this segment of mid-ocean ridge is due to the fact that the ridge is centered on a hotspot\*, generally interpreted as a mantle plume\*. The ridge drifts away from the hotspot due to plate motion over periods of millions of years. Periodically, rifting is reestablished over the hotspot, abandoning the old ridge segment. Iceland is a result of a rare combination of tectonic processes, a hot spot located beneath a mid-ocean ridge and the slow-spreading\* Mid-Atlantic ridge. At Iceland, the ridge is splitting the island apart at a rate of 3.2 cm/yr and creating new crust at the edges of the Eurasian and North American plates. The rifting\* causes numerous fissure eruptions\*. ( Jacoby, W., Bjornsson, A., and Moller, D., (eds.) 1980)

Based on the above facts, which are stunningly interesting, modeling rift-intrusion events and crustal deformation in Iceland, especially over multiple rifting cycles, with multiple intersecting rifts, is an extremely difficult job.

The engineering goals of this study are: (1) To develop finite element models of rift-intrusion events which would aid in better understanding of crustal deformation in Iceland. (2) Understanding cycle-up of multiple rifting events. (3) Handling contact surfaces, rifting surfaces and intersecting rifts/faults. (4) Developing pre- and post-processors to facilitate model development and analysis. The scientific goal of this study is make an in-depth understanding of multiple rifting events with intersecting rifts/faults and its effects.



To achieve the engineering and scientific goals as stated above we use finite elements. The essence of the finite element method is to break large, complex model into smaller interconnected components called “elements”. Each element has a function which is assumed to satisfy the required differential equation over the volume of the element. Since the differential equations are only solved for over the volume of the element, this leads to a piecewise representation of the actual response of the overall model. More elements in the model assist in better results. The modeling and analysis is carried out using ABAQUS, a commercial software package.

### **1.2 FINITE ELEMENT ANALYSIS:**

The Finite Element Method is a versatile numerical method used to solve many types of problems found in engineering and the Earth Sciences. It is well adapted for problems of slow flow, crustal deformation, viscoelasticity and elasticity, particularly where the geometry and constitutive properties of the relevant volumes are complicated. Typical problem areas of interest in engineering and mathematical physics that are solvable by the use of the finite element method include structural analysis, heat transfer, fluid flow, mass transport, and electromagnetic potential. This method is used to solve complex problems that are difficult to satisfactorily solve by other analytical methods. It actually originated as a method of analyzing the stress distribution in different systems.

### **1.2(a) *What is Finite Element Analysis?***

The Finite Element Analysis (FEA) is a numerical technique used to obtain approximate solutions to a wide variety of engineering problems where the variables are related by means of algebraic, differential and integral equations. It is a computer-based numerical technique for calculating the strength and behavior of the model under consideration. It can be used to calculate deformation, stress, buckling behavior and many other phenomena. It can be used to analyze either small or large-scale deformation under loading or applied displacement. It can analyze elastic deformation, quasi-static flow or plastic deformation.

In the finite element method, a model is broken down into many small simple blocks or elements. The behavior of an individual element can be described with a relatively simple set of equations. Just as the set of elements would be joined together to build the whole structure, the equations describing the behaviors of the individual elements are joined into an extremely large set of equations that describe the behavior of the whole model. The computer can solve this large set of simultaneous equations. From the solution, the computer extracts the behavior of the individual elements. From this, the stress and deformation of the model can be inferred.

The concept of Finite Element Analysis was initially proposed by Courant in 1941 (Cook, R.D., Malkus, D.S., and Plesha, M.E.). In a work published in 1943, he used the principle of stationary potential energy and piecewise polynomial interpolation over triangular subregions to study the Saint-Venant torsion problem. Approximately ten years later engineers had set up stiffness matrices and solved the equations with the help of

digital computers. The exact behavior of a structure at any point can be approximated by using the numerical solutions at discrete points, called nodes. The nodes are connected by the elements. The approximate solution for each element is represented by a continuous function, which leads to a system of algebraic equations. The complete solution is then generated by assembling the elemental solutions, allowing for the continuity at the inter-elemental boundaries.

The term "finite element" distinguishes the technique from the use of infinitesimal "differential elements" used in calculus, differential equations, and partial differential equations. Finite element analysis is a way to deal with structures that are more complex than can be dealt with analytically using partial differential equations. FEA deals with complex boundaries better than finite difference equations will, and gives answers to "real world" structural problems. It has been substantially extended in scope during the roughly 40 years of its use. There are numerous element types that could be chosen for a given structure. The selection of the appropriate element type depends on the problem at hand. An element or mesh that works fine in a particular situation may not be as good for a different situation. The engineer should select the best element for a problem understanding well both the nature of the element behavior and the problem itself. The numerical hand calculations using this method become increasingly difficult with the complexity in the geometry of the structure and with increasing number of nodes. For this reason, several finite element computer programs have been developed by research organizations that can produce reliable approximate solutions, at a small fraction of the cost of more rigorous, closed-form analyses.

Out of all the numerous computer programs currently available to analyze finite element problems, ABAQUS is very popular commercial software. ABAQUS can be efficiently used to analyze a number of models in most of the above mentioned areas in slow flow, crustal deformation, viscoelasticity, engineering and mathematical physics.

### **1.2(b) *Introduction to ABAQUS***

Finite Element Analysis is done principally with commercially purchased software. We make use of ABAQUS. It is a suite of powerful engineering simulation programs, based on the finite element method, which can solve problems ranging from relatively simple linear analyses to the most challenging nonlinear simulations. ABAQUS contains an extensive library of elements that can model virtually any geometry. It has an equally extensive list of material models that can simulate the behavior of most typical engineering materials including metals, rubber, polymers, composites, reinforced concrete, crushable and resilient foams, and geotechnical materials such as soils and rock. Designed as a general-purpose simulation tool, ABAQUS can be used to study more than just structural (stress/displacement) problems. Use of any finite element program requires familiarity with the interface of the program in order to create and load the models, and to review the results. To do the work well requires experience, comprehension of the models and their classical (manual analytical) analysis, an understanding of a variety of FEA modeling issues, and an appreciation of the specialized field in which the design work is taking place.

ABAQUS can simulate problems in such diverse areas as heat transfer, crustal deformation, acoustics, soil mechanics (coupled pore fluid-stress analyses), and piezoelectric analysis. ABAQUS is simple to use even though it offers the user a wide range of capabilities. The most complicated problems can be modeled easily. In most simulations, even highly nonlinear ones, the user need only provide the engineering data such as the geometry of the structure, its material behavior, its boundary conditions, and the loads applied to it. In a nonlinear analysis ABAQUS automatically chooses appropriate load increments and convergence tolerances. Not only does it choose the values for these parameters, it also continually adjusts them during the analysis to ensure that an accurate solution is obtained efficiently. The user rarely has to define parameters for controlling the numerical solution of the problem.

## **CHAPTER TWO**

### ***RIFTING MODELS***

2. RIFTING .....	12
2.1 HOW DOES RIFTING START? .....	13
2.1.1 Plate Tectonics and Boundaries .....	13
2.1.2 Types of Plate Boundaries .....	14
2.1.2a Transform Boundaries .....	14
2.1.2b Divergent Boundaries .....	15
2.1.2c Convergent Boundaries .....	16
2.2 GEOLOGY OF ICELAND .....	17
2.3 REVIEW OF PUBLISHED LITERATURE .....	19
2.4 INTRODUCTION TO SIMPLE RIFTING MODELS .....	21
2.4.1 Straight Rift Model .....	22
2.4.2 Inclined Rift Model .....	23
2.4.3 Intersecting Rift Model .....	24
2.4.4 Skewed Rift Model & Double Kink Rift Model.....	25
2.4.5 Box Rift Model .....	27

## **2. RIFTING**

A rift is a place where the Earth's lithosphere expands. Rifts are frequently found at divergent plate boundaries between two tectonic plates. Rifting is the process by which the new lithosphere is made. A Continental rift is the belt or zone of the continental lithosphere where the extensional deformation (rifting) is occurring. These zones have important consequences and geological features, and if the rifting is successful, lead to the formation of new ocean basins. In general, Continental crust is split by diverging plate boundaries. A divergent plate boundary is a condition between two tectonic plates where the plates move away from one another. These areas form in the middle of the continents but soon transform to a ocean basins. Therefore most divergent plate boundaries, the Mid-Atlantic Ridge and the boundary between the African Plate and the Arabian Plate, exist between oceanic plates and are often called oceanic rifts or mid-ocean ridges as a result. Hence, rifting can be described as a process that occurs when land sinks between two parallel extensional faults.

The face of the earth has seen many great rifts which include, the Great Rift Valley in Africa, the Mid-Atlantic Ridge, rifts throughout the Basin and Range in North America and the rift in the middle of the Gulf of Corinth in Greece. The Great Rift Valley in Africa is an outcome of the rifting events that took place at the African and Arabian tectonic plates. The mid-Atlantic Ridge, an area of concern in this thesis, is an underwater mountain range in the Atlantic Ocean that runs from Iceland to Antarctica. It is the longest mountain range on Earth. This ridge is an oceanic rift which resulted from the separation of the North American Plate and the Eurasian Plate. The Basin and Range

Province is a peculiar topography that extends east from Nevada all the way to the Colorado Plateau. The basins are the down fallen blocks of crust and the ranges are the up-thrusted slabs of crust. The Gulf of Corinth was created by the expansion of a tectonic rift. It is a body of water separating Peloponnese from western mainland Greece.

## **2.1 HOW DOES RIFTING START?**

This happened to be the topic of discussion over the years. A certain group attribute rifting to up-lifting of the crust over a hot-spot. Certainly parts of the East African rift system are very elevated, compared with other regions, suggesting that the up-lifting reflects an underlying hot low-density mantle. In some cases, mantle is rising to high levels beneath the rift. So, rifting can take place without extensive uplift. Material in the mantle is thought to flow convectively. This is the process which drives plate tectonic motions. To rift a continent apart it needs the rifts associated with various possible thermal domes to link together. As continents drift slowly over hotspots the hotspots weaken the plate and these weakened zones become the sites of continental rifting.

### ***2.1.1 Plate Tectonics and Boundaries:***

Tectonics is the study of earth's structural features. The study of Tectonic Plates is called plate tectonics. This theory of Geology is developed to explain continental drift, the spreading of the sea floor, volcanic eruptions and how mountains are formed. The earth's crust is made of a number of moving plates which are moving relative to each other. The main features of plate tectonics are:



- The Earth's crust consists of nine large plates and twelve small ones.
- The ocean floors move continuously, spreading from the center, sinking at the edges, and regenerating in the mantle.
- Convection currents in the mantle beneath the plates move the crustal plates in different directions.
- The source of heat driving the convection currents is radioactivity deep in the Earth's mantle and the remnant heat resulted from the original formation of the Earth.

### **2.1.2 Types of Plate Boundaries:**

Plate boundaries can be broadly classified into three different categories based on the movement of the plates relative to one another. They are:

- a) Transform Boundaries
- b) Divergent Boundaries
- c) Convergent Boundaries

**2.1.2a Transform Boundaries:** These plate boundaries can also be referred to as conservative plate boundaries. Here the plates slide past each other. The relative motion of the plates is either left-lateral\* or right-lateral\* as one plate moves parallel to the other. The surfaces in contact are rough and hence the plates can not slip over one another due to friction. The huge amounts of energy released, when the stress accumulated over a period of time exceeds the limiting value of friction, causes earthquakes. The San Andreas Fault in North America is a good example of transform plate boundaries.

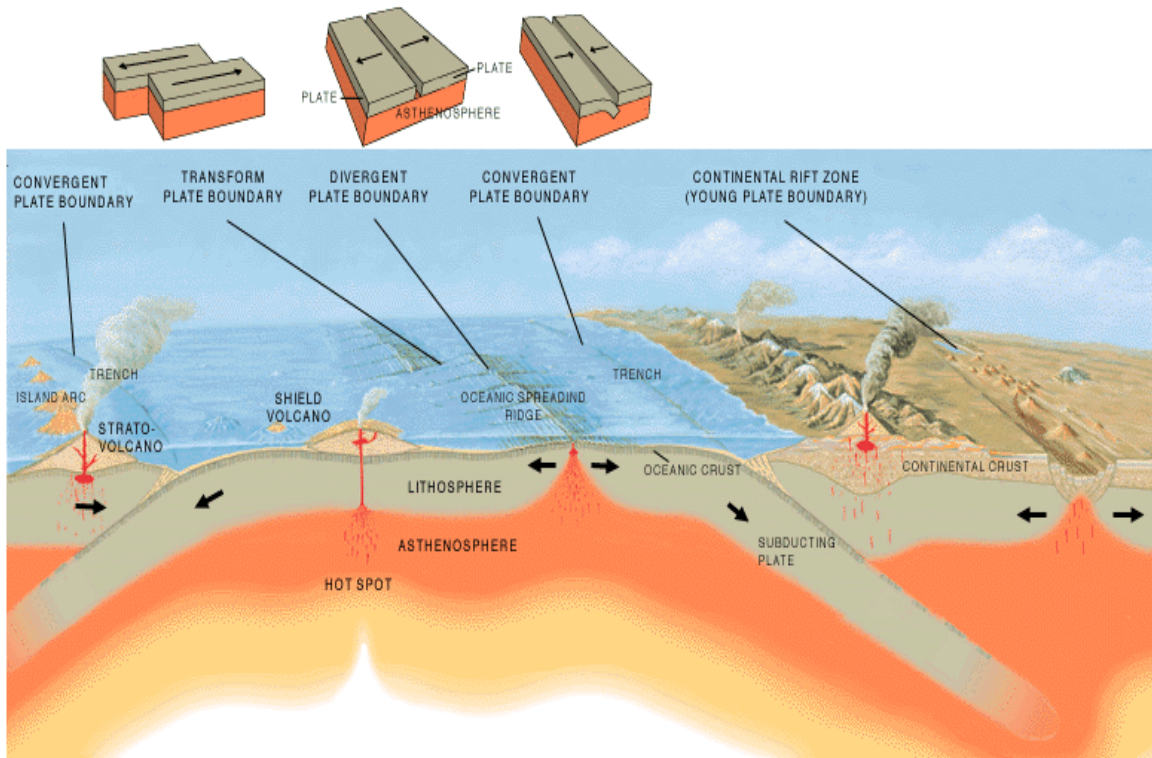


FIG 2.1.2a The cross-section of the main types of plate boundaries. Illustration by Jose F.Vigil from *This Dynamic Planet* -- a wall map produced jointly by the U.S. Geological Survey, the Smithsonian Institution, and the U.S. Naval Research Laboratory.

**2.1.2b Divergent Boundaries:** These plate boundaries can also be referred to as constructive plate boundaries. Here the plates slide apart from one another. As the plates move apart they create space which eventually is filled with new crustal material from molten magma. Large convective currents bring very large quantities of hot asthenospheric material near the surface and the kinetic energy is sufficient to break the lithosphere apart. Oceanic ridges are areas where the mantle ascend due to convective currents. The Mid-Atlantic Ridge system under Iceland is a typical result of the diverging plate boundaries in oceanic lithosphere. The Great Rift Valley in Africa is an example of diverging plate boundaries in continental lithosphere. These boundaries create huge fault

zones in the oceanic ridge system. In Iceland the oceanic ridge is above the sea level. In this study we model the multiple rifting events in Iceland.

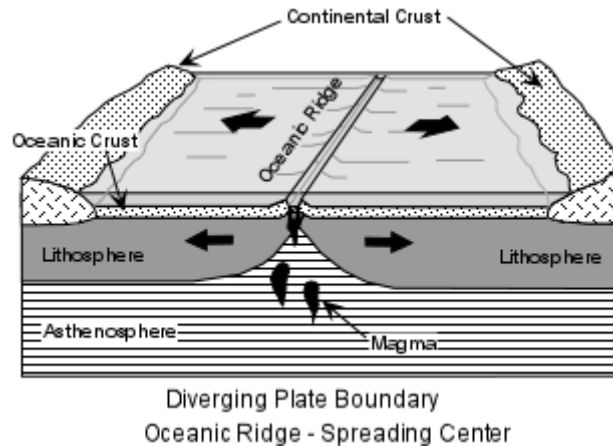


FIG 2.1.2b (U.S. Geological Survey. [www.usgs.gov](http://www.usgs.gov))

**2.1.2c Convergent Boundaries:** These plate boundaries can also be referred to as destructive plate boundaries. Here the plates run into each other. An ideal example for convergent plate boundaries is where the oceanic lithosphere subducts. We find island arcs when a dense oceanic lithosphere subducts beneath another. Japan is a good example for island arcs. A continental margin arc is formed when the oceanic lithosphere subducts beneath the continental lithosphere. One such example being the Andes. When two continental lithospheric plates converge the result in fold-thrust mountain ranges. One such example being Himalayas.

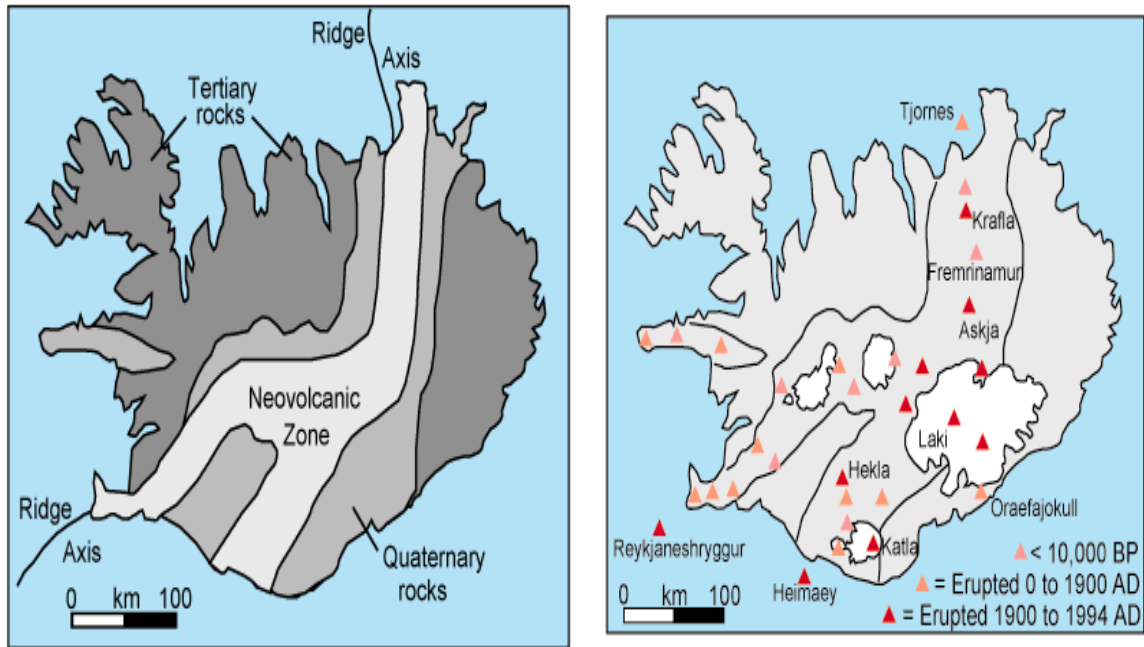


FIG 2.2 Geology of Iceland. Map based on Simkin and Siebert (1994).

## **2.2 GEOLOGY OF ICELAND:**

Iceland can be divided into three zones based on the age of the basaltic rocks\*. Tertiary (70,000,000 to 2,000,000 years ago. See Geological timescale in Appendix C) flood basalts make up most of the northwest quadrant of the island. This stack of lava flows is at least 3,000 m thick. Quaternary (2-3 million years ago. See Geological timescale in Appendix C) flood basalts and hyaloclastites\* are exposed in the central, southwest and east parts of the island. The quaternary rocks are cut by the neovolcanic zone, areas of active rifting that contain most of the active volcanoes. The rifts (or grabens\*) are topographic depression bordered by and containing many faults. Fissure swarms\* make up most of the neovolcanic zone. The swarms are 5-10 km wide and 30-100 km long. The rift zones

have opened about 30 m in the last 3,000-5,000 years (McClelland et al. 1989; Jacoby et al. 1980). The neovolcanic zone compose about one-third of the area of Iceland.

Iceland is one of the most active volcanic regions on Earth. Thorarinsson (1967) estimated that one-third of the lava erupted since 1500 A.D. was produced in Iceland. Iceland has 35 volcanoes that have erupted in the last 10,000 years. On average, a volcano erupts about every 5 years. Eleven volcanoes have erupted between 1900 and 1998: Krafla, Askja, Grimsvotn, Loki-Fogrufljoll, Bardarbunga, Kverkfjoll, Esjufjoll, Hekla, Katla, Surtsey, and Heimaey (Fig. 2.2). Most of the eruptions were from fissures or shield volcanoes\*.

The consequences of plate movement are easy to see around Krafla Volcano, in the northeastern part of Iceland. Here, existing ground cracks have widened and new ones appear every few months (W. Jacquelyne Kious and Robert I. Tilling, [26]). From 1975 to 1984, numerous episodes of rifting (surface cracking) took place along the Krafla fissure zone. Some of these rifting events were accompanied by volcanic activity. Between 1975 and 1984, the displacements caused by rifting totaled about 7 m (W. Jacquelyne Kious and Robert I. Tilling, [26]).

### **2.3 REVIEW OF PUBLISHED LITERATURE:**

Modern day science has undergone many changes to provide a better understanding of geological and geophysical events. There are many significant efforts that threw light on rifting events in Iceland and its geology. Most of the older models are analytical elastic half-space or elastic layer over visco-elastic half-space. A Mogi source (volumetric point source) is used to represent a volume change [2, 23]. The boundary element method has been employed by Hackman et al. [25] 1990 assuming linear elastic behavior. Finally, an extremely simple model using the finite element method was introduced by Jacoby et al. [24] but the results were considered less accurate than comparable analytic methods. Discrete rifting events were not considered.

Pollitz and Sacks [1] discussed, using inversion methods and the correspondence principle, the viscosity structure beneath Iceland and states that, the dynamics of crustal rifting in Iceland depends to a greater extent on the lower crustal rheology, which controls the intensity of the upper crustal stress concentration and time of heat diffusion from the underlying mantle plume. Pollitz and Sacks [1] utilized horizontal and vertical displacement vectors using the Global Positioning System (GPS) campaigns in northeast Iceland since 1986. In their model the elastic part is fixed by external constraints and modeling is carried out in terms of steady state tectonic loading plus postseismic relaxation following the 1975-1984 Krafla rifting event. Pollitz and Sacks [1] draw a conclusion that the lower and upper mantle viscosities of about  $3 \times 10^{19}$  Pa-s and  $3 \times 10^{18}$  Pa-s respectively were the closest match with the data.

Hofton and Foulger [2] presented the post-rifting anelastic deformation around the spreading plate boundary of north Iceland in 1996. In their study of the data, the results from the 1992 GPS survey differed with those from 1987 and 1990. This revealed that the maximum rift expansion rate near the rift was 4.5 cm/year which is in great conflict with the time-averaged spreading rate of 1.8 cm/year in north Iceland. Three different models were applied by Hofton and Foulger [2] to study the postrifting ground deformation. The best model that explained the above conflict was the one with a viscoelastic half-space. This model had a viscosity of  $1.1 \cdot 10^{18}$  Pa-s, a relaxation time of 1.7 years, and the elastic layer thickness was 10 km for northeast Iceland. The results from modeling by Hofton and Foulger [2] had great implications and did shed light on the fundamentals of deformation around spreading plate boundaries. They conclude by saying that elastic-viscoelastic models can account for deformation effects of the Krafla episode and can be used when modeling deformations in other regions of Iceland.

Lynch and Richards [3] dealt with finite element models of stress orientations in strike-slip fault zones. They made use of finite element models to study the stresses in an elastic layer overlying a viscoelastic shear zone of finite width. The dimensions of the model under consideration by Lynch and Richards [3] were 300 km in width, 400 km in length, and 50km in depth. In their model, stress on the fault accumulates naturally as the far-field velocity boundary conditions are enforced on the edges of the model. They have provided valuable information in terms of maximum compressive stress orientations, angles of principal stress axes and had provided insight on the distribution of strain in the

lower crust. This paper provides an insight in to the dimensions of the finite model being modeled in this study using a commercial software package ABAQUS.

In 1985 Bjornsson [4] discussed the dynamics of crustal rifting in north-east Iceland. From his discussion we know that the crustal thickness in the axial rift zone of north-east Iceland ranges from 8 to 10 km. The crust thickens with increasing age and is 20 to 30 km thick in the older areas of the axial rift zone. Bjornsson proposes that, at the crust asthenosphere interface there is a partial molten basaltic layer a few kilometers thick which partially decouples the crust from the mantle. The Krafla rifting is attributed to local tensional stress that has been accumulated over a period of time near the plate boundaries due to the slow retreat of the plates. This accounts for crustal thinning and subsidence. The local tensional stress accumulated is then released in a rifting episode.

#### **2.4 INTRODUCTION TO SIMPLE RIFT MODELS:**

Modeling of a rifting event, in particular rifting in Iceland is a complex problem. Applying the same principles of finite elements we have broken this complex problem into many small and simple ones. The levels of complexity in the rift patterns are built up from the simple models. The input files for all the rift models are coded in the PYTHON script. We have built a general code in MATLAB that could produce the desired model as per the user specifications. This subject is dealt in detail in the chapters to follow. In all the models we have used same rheology in all the layers for better comparison. The simple



models we have considered for better understanding of the rifting problems in general are:

- A straight rift model
- An inclined rift model
- An intersecting rift model
- Skewed rift model
- Double kink model
- Box rift model

#### ***2.4.1 Straight Rift Model:***

A straight rift model includes a straight rift that is oriented perpendicular to the far-field velocity boundary conditions. This rift is located right in the center of the top crustal surface and extends into the upper mantle. The model accommodates various rheologies for the crust and the mantle. The mantle is further divided into different layers and can have different rheologies for each layer. These rheologies are user-defined and are passed to the general code along with the other model parameters. Depending on the complexity of the model various parts of the model are built and are then assembled. Here in this model we build the two parts of the crust divided by the rift separately in addition to the mantle and then assemble all these pieces to form an entire model. The figure below better explains a straight rift model.

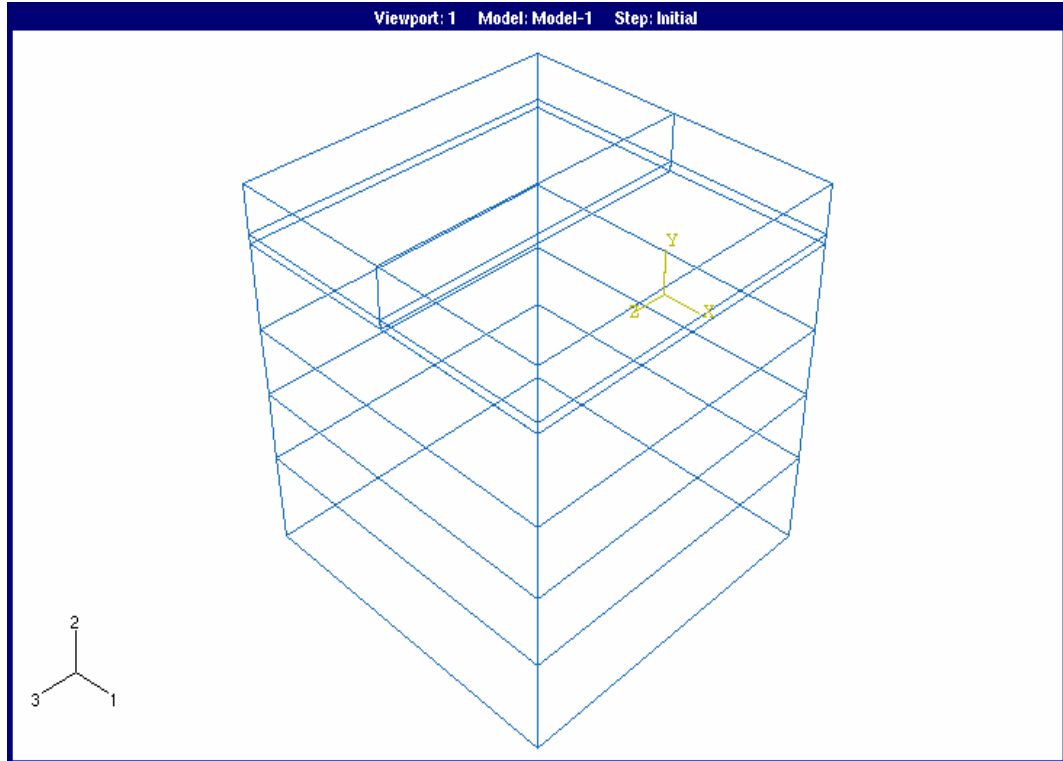


FIG 2.4.1 Straight Rift Model

### ***2.4.2 Inclined Rift Model:***

Moving a step ahead in the direction of complexity are the inclined rift models. In an inclined rift model the rift is oriented at an angle to the far-field velocity boundary conditions. Based on the user specification of the point list the model is generated with the required rift inclination. An example of an inclined rift model is shown in figure

2.4.2

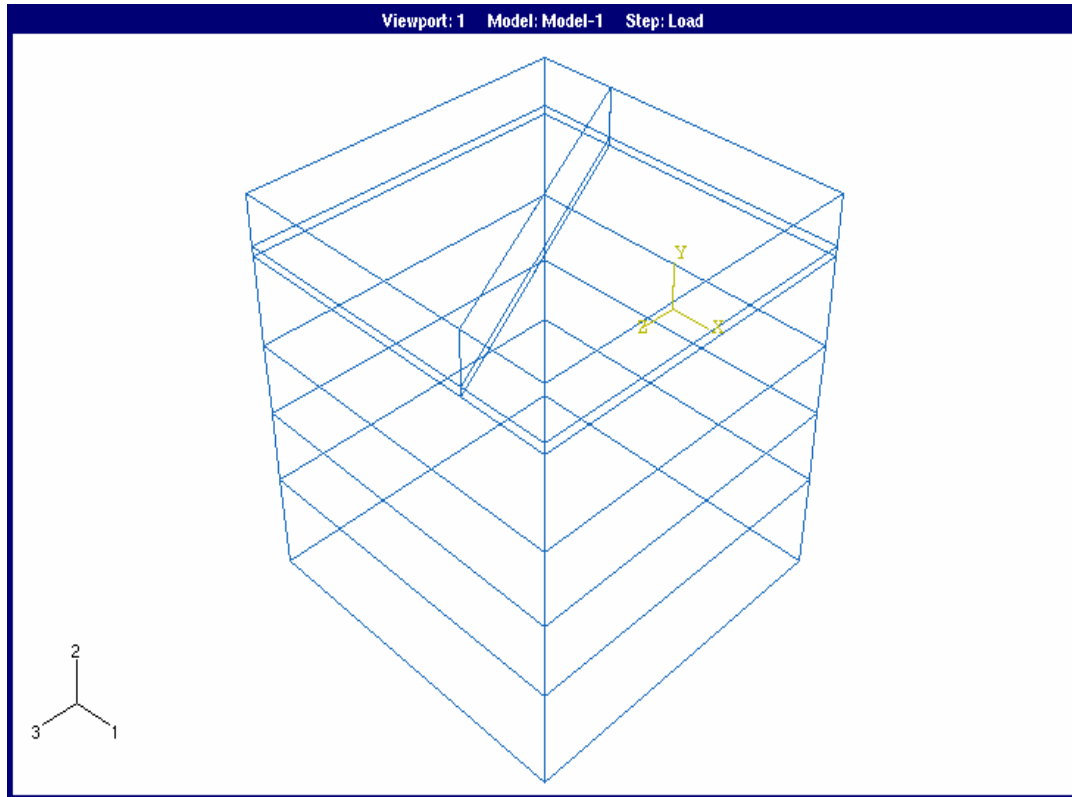


FIG 2.4.2 Inclined Rift Model

### ***2.4.3 Intersecting Rift Model:***

To better understand the behavior of intersecting rifts, we have considered two individual rift patterns intersecting at a point. In this model a straight rift is intersected by another inclined rift at a point. This drives the complexity to a higher level. We have used a better mesh to handle the meshing issues more thoroughly and generated the same corresponding nodes on either side of the rift to ensure proper functionality of the user-subroutine. An example of an intersecting rift is shown in figure 2.4.3

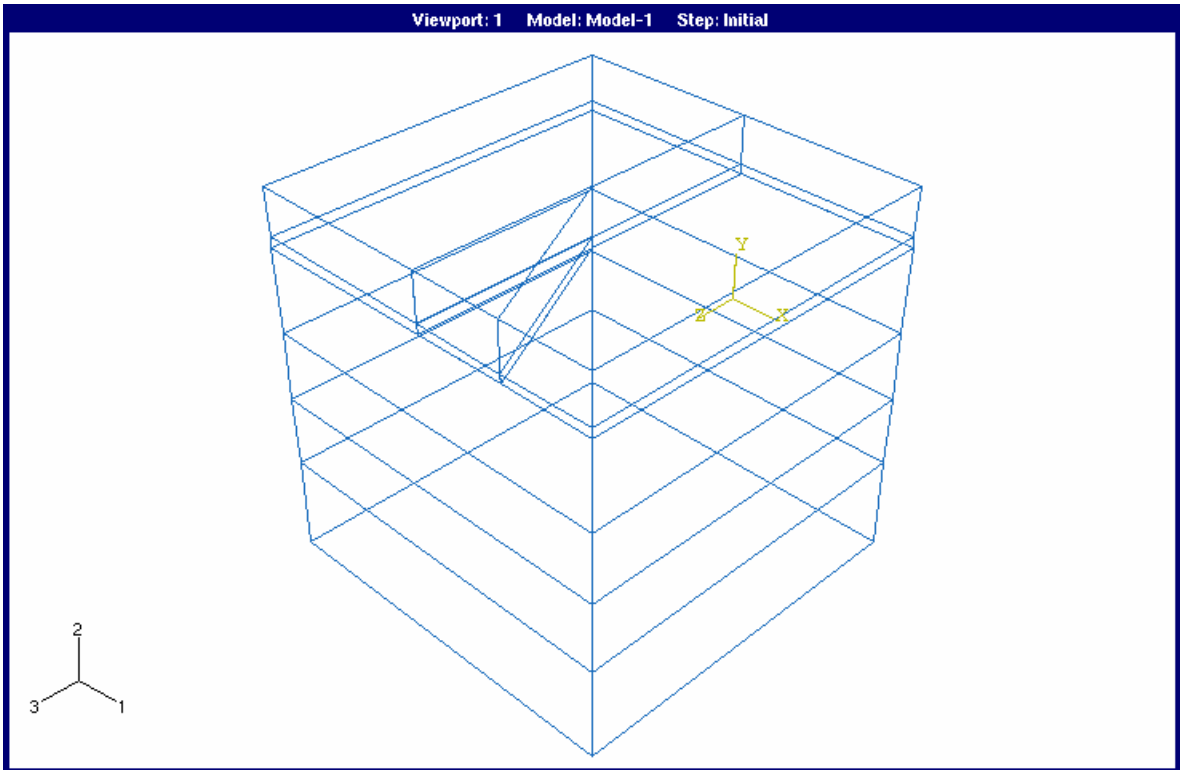


FIG 2.4.3 Intersecting Rift Model

***2.4.4 Skewed Rift Model:***

The complexity of the rifting problem is at a higher degree when we deal with skewed rift models. In these models we have a single rift inclined at two different angles to the far-field velocity boundary conditions. These models help us understand rifting issues that involve corners and intersecting rifts. An example of an skewed rift model is shown in figure 2.4.4a figure 2.4.4b shows a model with further complexity having two kinks in the rift pattern.

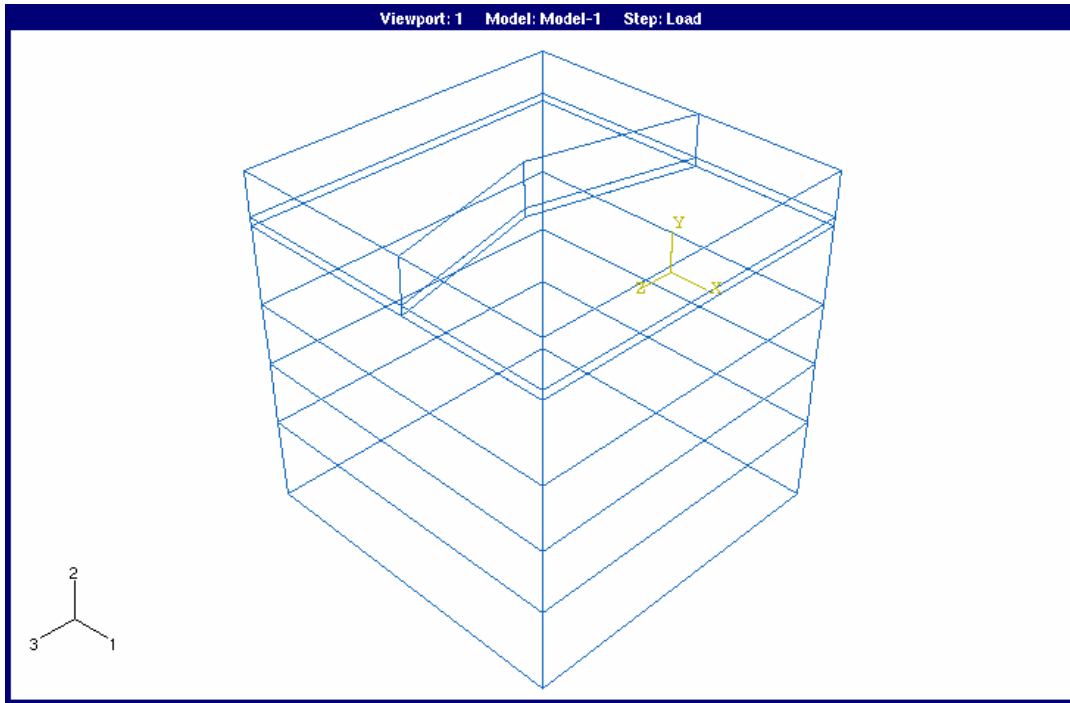


FIG 2.4.4a Skewed Rift Model

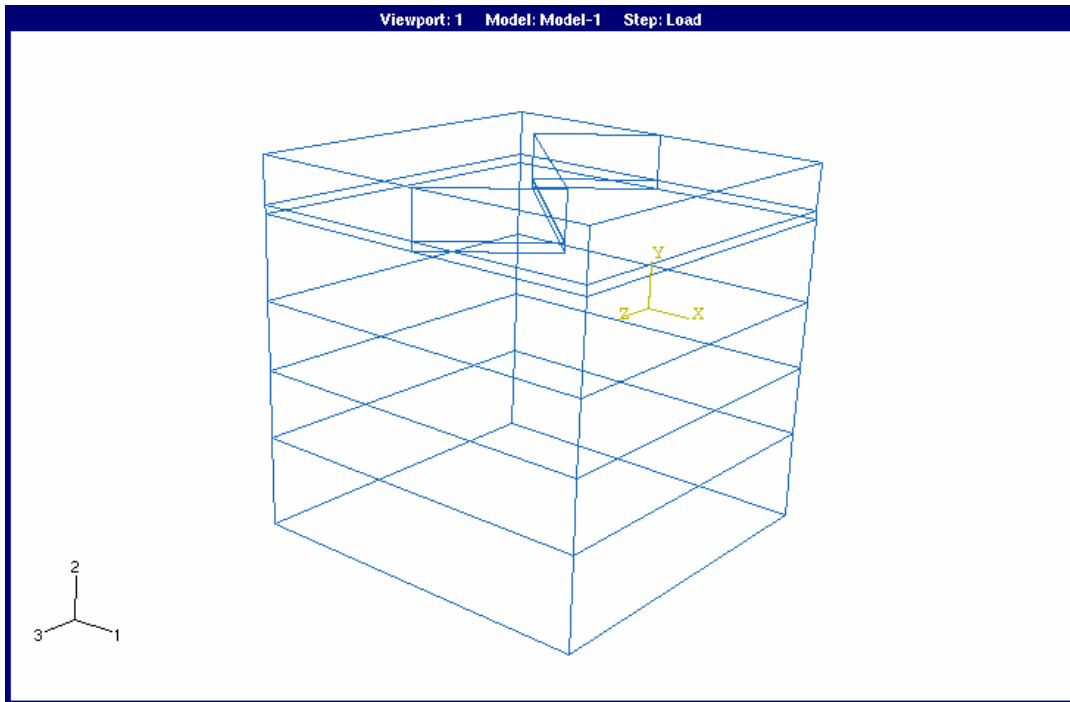


FIG 2.4.4b Double Kink Model

### **2.4.5 Box Rift Model:**

The box rifting problem has a rift pattern close to the 1<sup>st</sup> order model Dr. Kenner and Dr. Simons would compare real data to similar models. It is a higher degree of complexity when we deal with box rift models. In these models we have a straight rift intersected at two different location by “U” rift pattern. These models help us understand rifting issues that involve corners, multiple polygons, and intersecting rifts. An example of a box rift model is shown in figure 2.4.5.

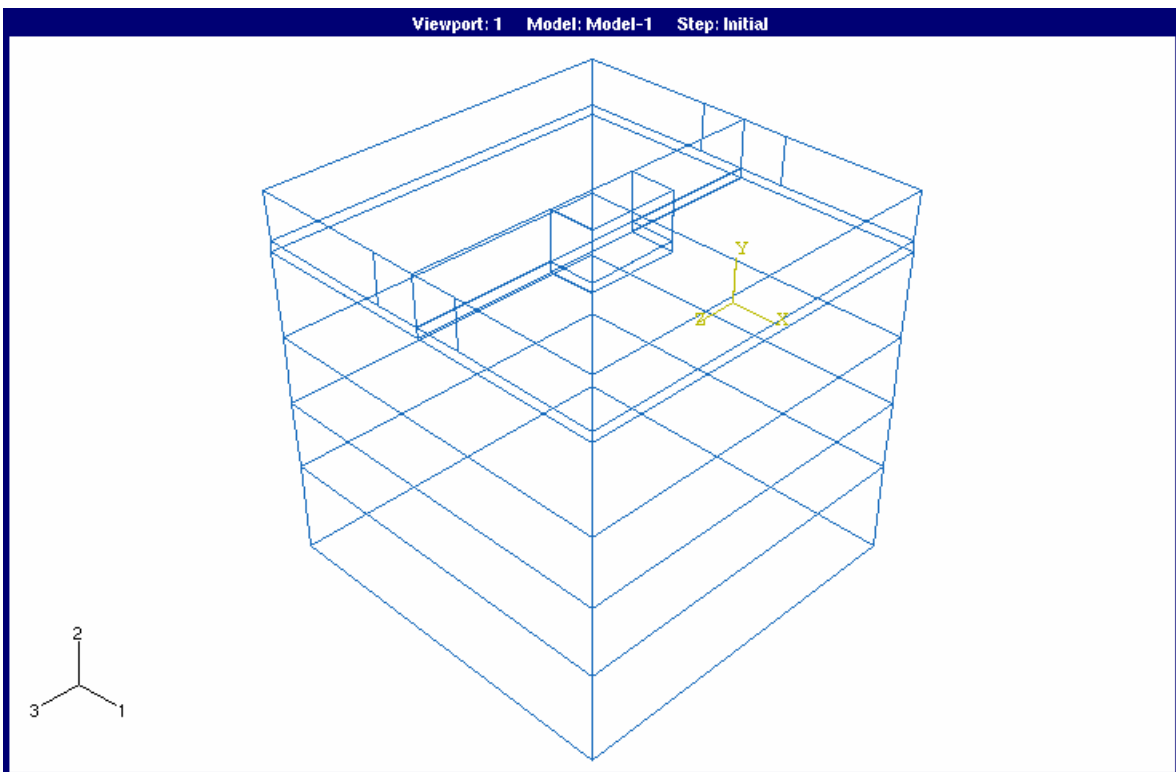


FIG 2.4.5 Box rift Model

## **CHAPTER THREE**

# ***PRE- AND POST-PROCESSING OF RIFTING MODELS***

3.1 DEVELOPING PRE- AND POST-PROCESSORS OF FINITE ELEMENT RIFTING MODELS .....	29
3.2 BOUNDARY CONDITIONS .....	32
3.3 ELEMENT SELECTION .....	33
3.3.1a Family .....	34
3.3.1b Degrees of Freedom .....	34
3.3.1c Number of Nodes .....	34
3.3.1d Formulation .....	35
3.3.1e Integration .....	35
3.3.2 Naming Convention .....	36
3.4 MODELING AND MESHING ISSUES .....	37
3.4.1 Modeling .....	37
3.4.2 Meshing .....	38
3.4.3 Virtual Topology.....,	39

### **3.1 DEVELOPING PRE- AND POST-PROCESSORS OF FINITE ELEMENT RIFITING MODELS**

In many cases a significant percentage of the time spent on a FEM analysis is devoted to the pre- and post processing stages. ABAQUS pre-and postprocessor is a command- and menu-driven interactive tool, whose main functions include

- Geometry modeling and mesh generation
- Specification of boundary and initial conditions
- Specification of material properties
- Step definition for analysis
- Generating output based on step definition
- Read and re-format the various data files produced by the analysis
- Computation of derived quantities
- Summary of information on the calculated results

Abaqus-cae is both a pre-processor and post-processor, and is developed to replace Abaqus/Pre and Abaqus/Post modules. It is a consistent interface for creating, submitting, monitoring, and evaluating results from Abaqus/Standard and Abaqus/Explicit simulations. Abaqus-cae is made up of several modules, where each module defines a logical aspect of the modeling process:

- *Part module* -- creating and importing parts, importing mesh from output databases and input files
- *Property module* -- defining material properties, defining sections and assigning sections to parts or regions of parts



- *Assembly module* -- assembling instances of parts to create a model
- *Step module* -- creating and managing analysis steps
- *Interaction module* -- defining interactions between regions of a model or between the model and its surroundings. Surface data is defined in this module.
- *Load/BC/IC module* -- defining and managing the loads, boundary conditions and initial conditions
- *Mesh module* -- generating meshes
- *Job module* -- creating, managing, submitting and monitoring analysis jobs
- *Visualization module* -- viewing models and results of analyses

As the models generated in this study are very diverse in nature, it would be a tedious process to build every single model from scratch. To overcome this difficulty we have generated a pre-processor, using Python as the scripting language. This has been carried out by making use of MATLAB, ABAQUS AND PYTHON. The preprocessor is developed in a flexible manner to handle all the requirements of the user. Arbitrary fault geometries can be input as well as rheological layering at depth. It builds the model to the user specifications and is adaptive to all the needs of the user. Arbitrary fault geometries can be input as well as rheological layering at depth.

The coding is been done in Matlab which generates a “.py” file. This Python file is used as the input file (run script file) in Abaqus which eventually generates the desired model in the pre-processor and the “.odb” file (e.g. Abaqus output file) and the desired results in the post-processor.

I have made use of three files, namely:

1) mktstmodel.m

2) ursmktstmpvw.m

3) trail3.m

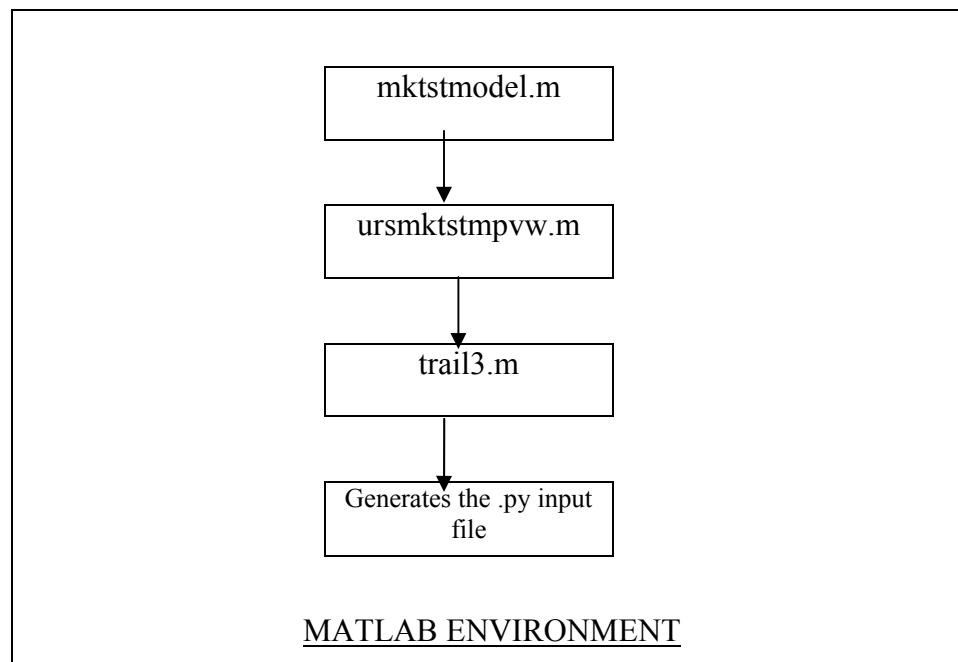
The “mktstmodel.m” generates trial mapview geometry for testing geometry and mesh building techniques in abaqus cae and generates the “.py” input file.

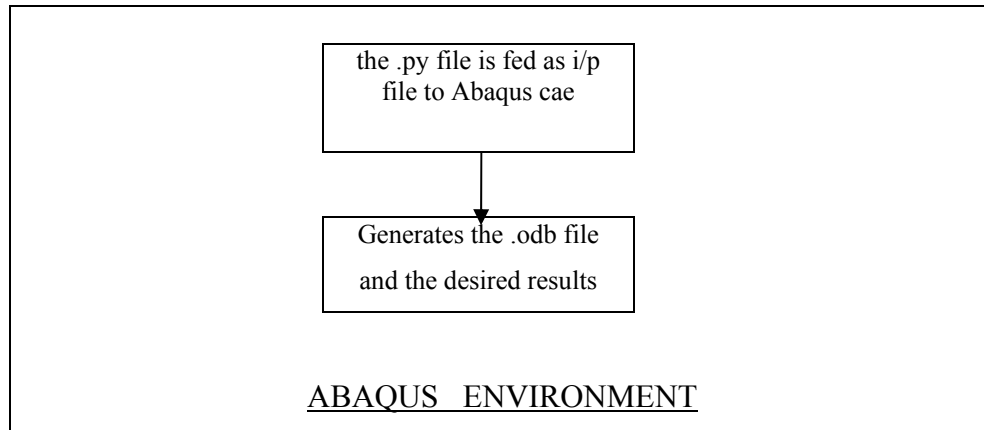
The “ursmktstmpvw.m” file has the data given by the user telling us the crack pattern, rheology at various depths, number of layers, crustal depth and so on that are needed to build a model as per the requirements of the user.

The “trail3.m” file uses the user given data and the data from the mktstmodel.m file to generate a ABAQUS CAE .py script file to create the surfaces defined by the user.

All the files are attached in the Appendix D for reference.

The flow of activities in Matlab and Abaqus Environment are as follows.





### **3.2 BOUNDARY CONDITIONS:**

Boundary conditions are defined in the Load/BC/IC module. Boundary conditions considered in the model generation and analysis are plate velocities and displacement boundary conditions on the sides of the model. The following boundary conditions are applied in various steps. The units of velocity are km/yr.

Step1 (Initial):  $v_1=v_2=v_3=0$  on the sides of the model, thus constraining the displacement in all three directions.

Step2 (Load1):  $v_1=1e-5$  and  $v_2=v_3=0$  on the eastern side and  $v_1= -1e-5$  and  $v_2=v_3=0$  on the western side.

Step3 (Rift1):  $v_1=1e-5$  and  $v_2=v_3=0$  on the eastern side and  $v_1= -1e-5$  and  $v_2=v_3=0$  on the western side.

Step4 (Load2):  $v_1=1e-5$  and  $v_2=v_3=0$  on the eastern side and  $v_1= -1e-5$  and  $v_2=v_3=0$  on the western side.

Step5 (Rift2):  $v_1=1e-5$  and  $v_2=v_3=0$  on the eastern side and  $v_1= -1e-5$  and  $v_2=v_3=0$  on the western side.

And so on...

The steps definition is done in a cyclic manner. There is a loading step for 200 years followed by a rifting step for 20 years. This cycle of loading and rifting is done till the model attains a steady state.

A tie constraint is used to tie the non-seismogenic zone of the lower mantle. We have defined rough friction as the contact property. As the rifting surfaces move away from each other in the lithosphere the contact surface interactions are defined between the rift surfaces using multi-point constraints.

### **3.3 ELEMENT SELECTION:**

In ABAQUS, the element that is been made use of is “C3D8R”, an 8-noded linear brick element, reduced integration with hourglass control. Five aspects of an element characterize its behavior:

- Family
- Degrees of freedom (directly related to the element family)
- Number of nodes
- Formulation
- Integration

Each element in ABAQUS has a unique name. The element name identifies each of the five aspects of an element.

### 3.3.1a Family

One of the major distinctions between different element families is the geometry type that each family assumes. The first letter or letters of an element's name indicate to which family the element belongs. The figure below shows the commonly used element families.

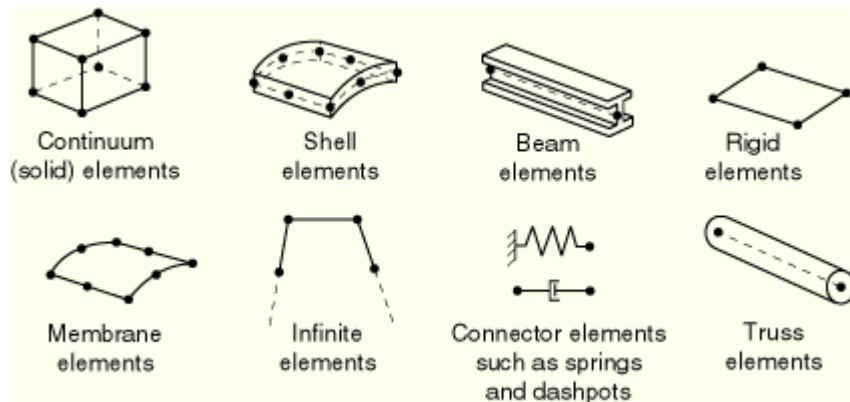


FIG 3.3.1a Element Families

### 3.3.1b Degrees of freedom

The degrees of freedom are the fundamental variables calculated during the analysis. For a stress/displacement simulation the degrees of freedom are the translations and, for shell and beam elements, the rotations at each node.

### 3.3.1c Number of nodes

Displacements or other degrees of freedom are calculated at the nodes of the element. At any other point in the element, the displacements are obtained by interpolating from the

nodal displacements. Typically, the number of nodes in an element is clearly identified in its name. The 8-node brick element is called C3D8. The figure below shows a linear and quadratic brick elements.

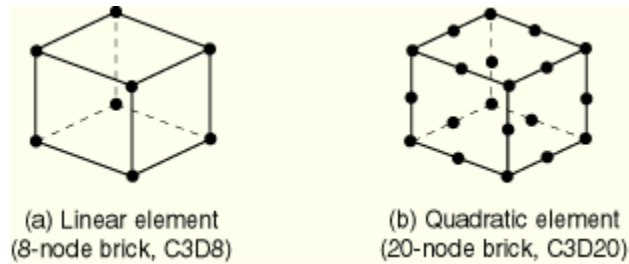


FIG 3.3.1c Linear and Quadratic Brick Element

### ***3.3.1d Formulation***

An element's formulation refers to the mathematical theory used to define the element's behavior. All of the stress/displacement elements in ABAQUS/Standard are based on the Lagrangian or material description of behavior: the element deforms with the material. In the alternative Eulerian, or spatial, description elements are fixed in space as the material flows through them.

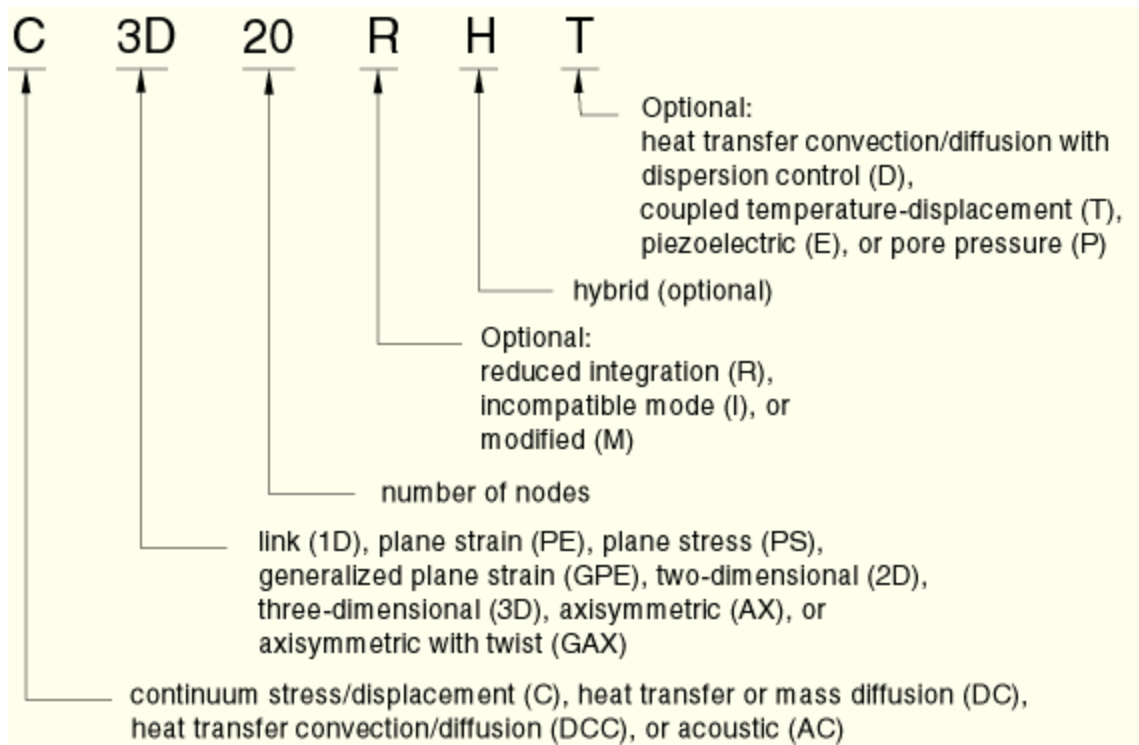
### ***3.3.1e Integration***

ABAQUS uses numerical techniques to integrate various quantities over the volume of each element, thus allowing complete generality in material behavior. Using Gaussian quadrature for most elements, ABAQUS evaluates the material response at each integration point in each element. When using continuum elements, you must choose

between full or reduced integration, a choice that can have a significant effect on the accuracy of the element for a given problem.

### 3.3.2 Naming convention

One-dimensional, two-dimensional, three-dimensional, and axisymmetric solid elements in ABAQUS are named as follows (Abaqus/Standard User Manual):



C3D8R is a 8-node linear brick, reduced integration with hourglass control. Active degrees of freedom are 1, 2, 3 ( $u_x, u_y, u_z$ ).

### **3.4 MODELING AND MESHING ISSUES:**

#### ***3.4.1 Modeling:***

Finite Element Analysis is fundamentally an approximation. The underlying mathematical model may be an approximation of the real physical system. There is a great deal of complexity in modeling the Earth's physics. Material property definition and selection of the material is an approximation of reality. The finite element itself approximates what happens in its interior with interpolation formulas. The interior of a 2-D or 3-D finite element has been mapped to the interior of an element with a perfect shape, so a severely distorted element can not deform in a manner that has an accurate match to the real physical response. Integration over the body of the element is often approximated depending on the element. The continuity of deformation between connected elements is interrupted at some level. Elements approximate the local shape of the real body. Badly shaped elements can give less accurate results. Numerical analysis difficulties such as poor matrices may reduce the accuracy of calculated results. A linear analysis is an approximation of the real behavior of what happens in the Earth's crust.

The loading of the model is an approximation of what happens in the real world. It is very difficult to arrive at a particular loading condition in designing a rifting model. It has many loading conditions, which can not be accounted for, that make a significant contribution towards causing the rifting event. The boundary conditions approximate how the model is supported by the material around it. The material properties assumed are approximate. The dimensioning of the model is a major approximation in the design of the rifting models. The rift pattern is approximated with models approximating to the real



physical rifting zones. Many details are idealized, simplified, or unknown. Element results may be reported at integration points or nodes, not continuously evaluated with the interpolation functions over the whole element interior. Stress and strain results are based on the derivatives of the displacement solution, amplifying the errors.

The result of an analysis contains the accumulated errors due to all of the contributing approximations. Good analysis and interpretation of results requires knowing of an acceptable approximation, and development of a complete list of what should be evaluated.

#### ***3.4.2 Meshing:***

Generating a good quality refined mesh is a major issue. The mesh should be fine enough for good detail where information is needed, but not too fine, or the analysis will require considerable time and space in the computer. A mesh should have well-shaped elements - only mild distortion and moderate aspect ratios. This can require considerable thought and intervention, despite Abaqus's automatic meshing. We have put considerable effort into the generation of well-shaped meshes. Investigated automatic meshing controls, and re-meshing individual areas and volumes until the result looks "just right". Virtual topology was a handy tool in producing considerable meshing. To save time and space on the computer we have generated fine mesh around the areas of interest and had a coarse mesh in other areas.

Most finite elements are stiffer than the real physical elements. A coarse mesh is less sensitive to and hides stress concentrations. A fine mesh generally gives an answer closer to the exact solution. To get better results around the rift zone we had a fine mesh around the rifting areas. A fine mesh also results in larger models, more data storage, and longer model solution and display times.

### ***3.4.3 Virtual Topology :***

Complex CAD models usually have detailed surface features that can be meshed only using very fine element densities. Even with high mesh densities, long and thin “sliver” surfaces often lead to poorly shaped elements that can result in analysis failure when the element quality checks are performed. In addition, with finer meshes there is a corresponding increase in the time that it takes for the analysis to complete. Version 6.3 of ABAQUS/CAE has a powerful new capability called “virtual topology” that permits small, unimportant features that may lead to poorly shaped elements or meshing failures to be abstracted away easily. Virtual topology can be used effectively to simplify the surface representation of a model without modifying the underlying geometry. A good boundary mesh is important since it affects the tetrahedral meshing success rate and mesh quality.

The virtual model created allows unimportant details (vertices and edges) to be ignored during meshing. In effect, ABAQUS/CAE creates a simpler, virtual representation of the part and applies the mesh to that representation. Using virtual topology, virtual features can be created very quickly. Virtual topology increases the range of parts that can be meshed and increases the usability of the resulting mesh.

## **CHAPTER FOUR**

# ***MULTIPLE RIFTING EVENTS: CYCLE-UP OF RIFTING MODELS***

4.1 USER SUBROUTINS IN ABAQUS .....	41
4.2 NEED FOR USER SUBROUTINE IN THESE MODEL .....	42
4.2a What Does the Subroutine Do? .....	43
4.3 MULTI POINT CONSTARINT USER SUBROUTINES (*MPC) .....	44
4.3a Variables to be Defined .....	45
4.3b User Subroutine Interface .....	46
4.3c Variables Passed in for Information .....	47
4.4 USER INPUTS TO USER SUBROUTINE .....	48
4.4a During Loading .....	48
4.4b During Rifting .....	50

## **4.1 USER SUBROUTINES IN ABAQUS:**

User subroutines are provided to increase the functionality of several ABAQUS options for which data line usage alone may be too restrictive. They are written as FORTRAN code and must be included in a model through an execution command line option. A subroutine is a procedure whose purpose is to produce some side effect, such as modifying a set of arguments and/or global variables, or performing input/output. For example, a subroutine is invoked either with a call statement or as a defined assignment. For example, a call statement or a defined assignment to invoke a subroutine of the form \*MPC, USER, MODE=NODE (MPC stands for multi point constraint). User subroutines provide an extremely powerful and flexible tool for analysis. ABAQUS uses \* keywords for various operations to be carried out in model generation through an input file. \*MPC option is used to impose constraints between different degrees of freedom of the model. Including the USER and MODE parameters on the \*MPC option, indicates that multi-point constraints will be defined in user subroutine \*MPC in nodal mode. (ABAQUS Standard User's Manual)

A subroutine defines a complete process and is self contained. It has an initial subroutine statement, a specification part, an execution part that comprises the algorithm, any internal procedures that perform ancillary processes, and an END statement. When a subroutine is invoked, its execution begins with the first executable construct in the subroutine. Data objects and other entries may be communicated to and from the subroutine through argument association, host association, or common storage

association. One or more user subroutines can be included in a model by using the user option on the abaqus execution procedure to specify the name of a fortran source or object file that contains the subroutines.

#### **4.2 NEED FOR USER SUBROUTINE IN THESE MODELS:**

Boundary conditions have to be enforced on the rift surfaces which enable the surfaces on either side of the rift to move as a single surface during loading and to move in equal and opposite directions during rifting. The boundary conditions need to be ON during loading steps and have to be OFF during the rifting steps. In other words, the boundary conditions on the rift surfaces need to be ON or OFF subject to the time step during analysis. To accomplish this requirement in the model we make use of user-subroutine. Here the subroutine is coded to specify equal and opposite motion during rifting and single surface motion during loading thus accomplishing the ON and OFF conditions during different steps in the processing. The ON and OFF conditions during different steps in the processing are therefore enforced using the subroutine.

#### 4.2a What Does The Subroutine Do?

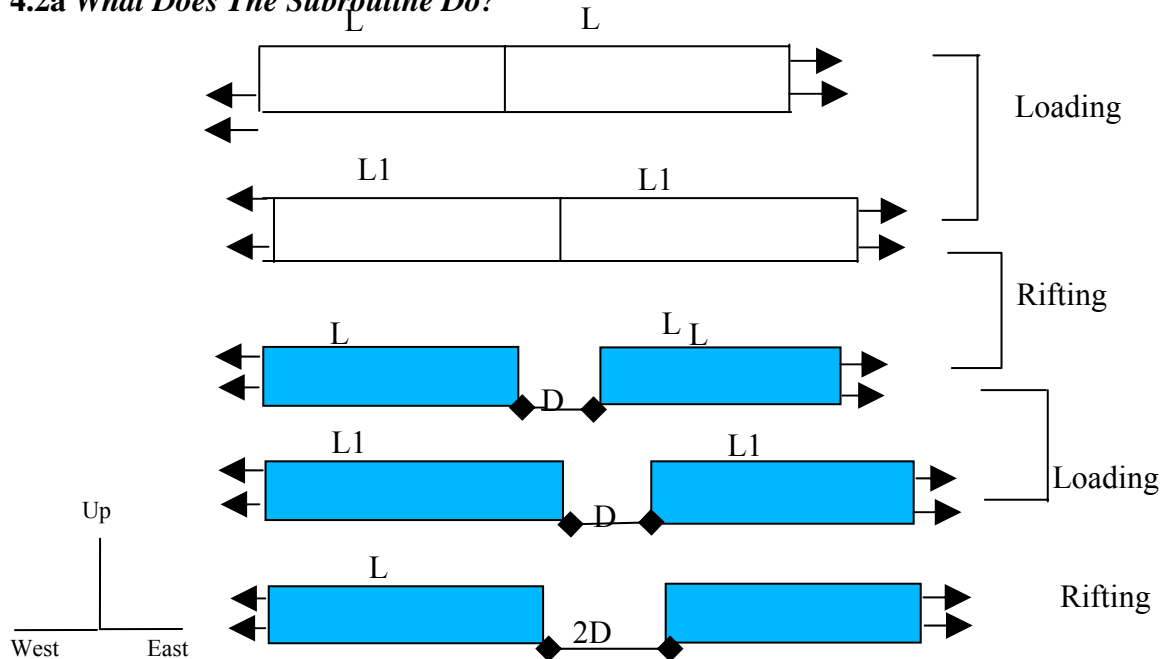


FIG 4.2a Schematic model

The above figure helps us in understanding what the subroutine does in more detail. It is the front view of a block with a rift in the middle and has velocity boundary conditions applied on either side. During analysis we have cyclic loading and rifting steps. During loading the nodes on both the rift surfaces should be moving in the same direction as if they are in tied contact. During rifting the nodes on the fault surfaces should move apart equally but in opposite directions

Thus, when the second cycle of loading starts, though the two blocks are apart by a distance  $D$ , they should be acting as if they are in tied contact. The blocks will be stressed while loading, and will move in the same direction. When the second rift takes place the stress is released and the blocks move apart by a distance  $2D$ .

To enforce these multi point constraints on the rift surfaces we have developed a \*MPC user subroutine which does the above task.

#### 4.3 MULTI-POINT CONSTRAINT USER SUBROUTINES (\*MPC)

There are two methods for coding this routine, depending on the value of the MODE parameter on the \*MPC option. If MODE=DOF (the default value), the subroutine operates in a *degree of freedom* mode. In this mode each call to this subroutine allows one individual degree of freedom to be constrained. If MODE=NODE, the subroutine operates in a *nodal* mode. In this mode each call to this subroutine allows a set of constraints to be imposed all at once; that is, on multiple degrees of freedom for the dependent node. In either case, the routine will be called for each \*MPC constraint or set of constraints (ABAQUS Standard User's Manual).

In this study, we make use of the NODE mode as we have to impose a set of constraints all at once. The set of constraints can be quite general and nonlinear. The constraints have the form

$$f_i(u^1, u^2, u^3, \dots, u^N, \text{ geometry, temperature, field variables}) = 0 \quad i = 1, 2, \dots, \text{NDEP},$$

where NDEP is the number of dependent degrees of freedom that are involved in the constraint and should have a value between 1 and MDOF, which is the number of active degrees of freedom per node in the analysis (ABAQUS/Standard User's Manual 20.2.2).

The constraint equation for the model during RIFTING is:

$$(\mathbf{u}_i)_{\text{Master}} = - (\mathbf{u}_i)_{\text{Slave}}$$

The constraint equation for the model during LOADING is:

$$(\mathbf{u}_i)_{\text{Master}} = (\mathbf{u}_i)_{\text{Slave}}$$

#### ***4.3a Variables To Be Defined:***

User must provide two items of information in subroutine \*MPC. The first being a matrix of degree of freedom identifiers [JDOF(MDOF,N)] at the nodes that are listed on the corresponding \*MPC constraint data line and the second being the matrices representing the linearized constraint function with respect to the degrees of freedom involved [A(MDOF,MDOF,N)]. Matrices are defined in the section to follow.

JDOF(MDOF,N)

Matrix of degrees of freedom identifiers at the nodes involved in the constraint. Before each call to the user-subroutine \*MPC, ABAQUS will initialize all of the entries of JDOF to zero. All active degrees of freedom for a given column (first index ranging from 1 to MDOF) must be defined starting at the top of the column with no zeros in between. A zero will mark the end of the list for that column. The number of nonzero entries in



the first column will implicitly determine the number of dependent degrees of freedom (NDEP).

A(MDOF,MDOF,N)

Submatrices of coefficients of the linearized constraint function. Before each call to the user-subroutine \*MPC, ABAQUS will initialize all of the entries of A to zero; therefore, only nonzero entries need to be defined.

#### **4.3b User Subroutine Interface:**

The subroutine interface is as follows:

```
SUBROUTINE MPC(UE,A,JDOF,MDOF,N,JTYPE,X,U,UNIT,MAXDOF,  
* LMPC,KSTEP,KINC,TIME,NT,NF,TEMP,FIELD,LTRAN,TRAN)  
C  
INCLUDE 'ABA_PARAM.INC'  
C  
DIMENSION UE(MDOF),A(MDOF,MDOF,N),JDOF(MDOF,N),X(6,N),  
* U(MAXDOF,N),UNIT(MAXDOF,N),TIME(2),TEMP(NT,N),  
* FIELD(NF,NT,N),LTRAN(N),TRAN(3,3,N)  
  
    user coding to define JDOF, UE, A and, optionally, LMPC  
RETURN  
END (ABAQUS/Standard User's Manual, Version6.3, 20.2.2)
```

### **4.3c Variables Passed In For Information:**

MDOF: Number of active degrees of freedom per node in the analysis.

N: Number of nodes involved in the constraint. The value of N is defined as the number of nodes given on the corresponding \*MPC data line.

JTYPE: Constraint identifier given on the corresponding \*MPC data line. (i.e MODE= NODE or OFF ).

X(6,N): An array containing the original coordinates of the nodes involved in the constraint.

U(MAXDOF,N): An array containing the values of the degrees of freedom at the nodes involved in the constraint. These values will either be the values at the end of the previous iteration or the current values based on the linearized constraint equation, depending at which stage of the iteration the user subroutine is called.

UNIT(MAXDOF,N): An array containing the values of the degrees of freedom at the nodes involved in the constraint at the beginning of the current iteration. This information is useful for decision-making purposes when the user does not want the outcome of a decision to change during the course of an iteration.

MAXDOF: Maximum degree of freedom number at any node in the analysis. For example, for a thermally coupled analysis with continuum elements, MAXDOF is equal to 11.

KSTEP: Step number.

KINC: Increment number within the step.

TIME(1): Current value of step time.

TIME(2): Current value of total model time.

These definitions can be found in ABAQUS/Standard User's Manual, Version 6.3, 20.2.2.

#### **4.4 USER INPUTS TO USER SUBROUTINE:**

The matrix of degree of freedom identifiers [JDOF(MDOF,N)] and the matrices representing the linearized constraint function with respect to the degrees of freedom involved [A(MDOF,MDOF,N)] for the coded user-subroutine are defined for different steps as follows.

##### ***4.4a During Loading:***

The constraint equations are generated based on the model behavior during loading and rifting steps. During loading the displacement on the master and slave surfaces are equal

and in the same direction. The model is pulled apart on either side by the far-field boundary conditions and as the model is loaded the displacements on the nodes on the master and slave move in the same direction.

The constraint equations during loading are:

$$f_1(\mathbf{u}^m, \mathbf{u}^s) = u^m_X - u^s_X = 0$$

$$f_2(\mathbf{u}^m, \mathbf{u}^s) = u^m_Y - u^s_Y = 0$$

$$f_3(\mathbf{u}^m, \mathbf{u}^s) = u^m_Z - u^s_Z = 0$$

where superscript ‘m’ represents the master surface and superscript ‘s’ represents the slave surface.

Sub-matrices of coefficients of the linearized constraint function are as follows

$$A(1:3, 1:3, 1) = \begin{matrix} 1 & 0 & 0 \\ 0 & 1 & 0 \\ 0 & 0 & 1 \end{matrix}$$

$$A(1:3, 1:3, 2) = \begin{matrix} -1 & 0 & 0 \\ 0 & -1 & 0 \\ 0 & 0 & -1 \end{matrix}$$

Matrix of degrees of freedom identifiers at the nodes involved in the constraint are :

$$\text{JDOF}(1:3, 1) = \text{JDOF}(1:3, 2) = [1 \ 2 \ 3]^T$$

#### **4.4b During Rifting:**

During rifting the displacement on the master and slave surfaces are equal and opposite.

The model is pulled apart on either side by the far-field velocity boundary conditions resulting in the displacement of the master and slave nodes when the rift opens.

The constraint equations are

$$f_1(\mathbf{u}^m, \mathbf{u}^s) = u^m_X + u^s_X = 0$$

$$f_2(\mathbf{u}^m, \mathbf{u}^s) = u^m_Y + u^s_Y = 0$$

$$f_3(\mathbf{u}^m, \mathbf{u}^s) = u^m_Z + u^s_Z = 0$$

Sub-matrices of coefficients of the linearized constraint function are as follows

$$\text{A}(1:3, 1:3, 1) = \begin{matrix} 1 & 0 & 0 \\ 0 & 1 & 0 \\ 0 & 0 & 1 \end{matrix} = \text{A}(1:3, 1:3, 2)$$

Matrix of degrees of freedom identifiers at the nodes involved in the constraint are :

$$\text{JDOF}(1:3, 1) = \text{JDOF}(1:3, 2) = [1 \ 2 \ 3]^T$$

## **CHAPTER FIVE**

### ***RESULTS AND DISCUSSION***

5.1 EXPERIMNET 1: STRAIGHT RIFT MODEL .....	54
5.2 EXPERIMNET 2: INCLINED RIFT MODEL .....	63
5.3 EXPERIMNET 3: INTERSECTING RIFT MODEL .....	71
5.4 EXPERIMNET 4: BOX RIFT MODEL .....	79
5.5 EXPERIMENT 5&6: SKEWED RIFT MODEL & DOUBLE KINK MODEL...	86

## RESULTS & DISCUSSION

Various experiments have been carried out to study the cycle-up process over multiple rifting event models and how long it takes to reach the steady state stress. The Earth is not at zero stress and hence the Earth processes should be modeled at a steady state stress value. This is not always the case. The target of this study is to investigate increasingly complex rift models. Experiments conducted include models with different rift patterns by ascending degree of complexity. The motivating factors that contributed to this study are:

- Identification of various factors that contribute to model cycle-up.
- Evaluation of effects of changes in rheology, far-field boundary conditions, and fault/rift pattern on model cycle-up.
- Quantification of variations in model cycle-up time and steady state stress at different location in the model.

The highlights of the experiments conducted are:

- ABAQUS/Standard is the modeling and analysis tool used.
- A \*MPC user-subroutine is developed to model multiple rifting events along the same rift.
- Model uses 8-noded linear brick element with reduced integration and hourglass control.

- Models are 400 km in rift perpendicular direction, 400 km in rift parallel direction, and 800 km in depth.
- The bottom of each rift is 120 km in depth.
- A loading step takes 200 yrs and the corresponding rifting step takes 20 yrs.
- A viscosity value of  $\sim 1.2 * 10^{19}$  Pa-s is used in all the models considered.
- Pre- and Post-Processing is done in MATLAB and ABAQUS environments.
- The model is automatically generated from geologically based user-defined parameters.
- The Bottom of the model is allowed to move in the vertical direction so that Poisson's effects are present.
- All layers below the rupture surface have same rheology. This is the case for all the models.
- In the experiments conducted we have studied 8 loading steps and 8 rifting steps. The analysis is carried out in 16 cycles.

The following contour plots give stress in terms of Mises Stress. The definition of Mises Stress is given below:

$$\sigma_v = \sqrt{\frac{(\sigma_1 - \sigma_2)^2 + (\sigma_2 - \sigma_3)^2 + (\sigma_3 - \sigma_1)^2}{2}}$$

where  $\sigma_1$ ,  $\sigma_2$ , and  $\sigma_3$  are the principal stresses.



## 5.1 EXPERIMENT 1: STRAIGHT RIFT MODEL

The straight rift model is the simplest model under consideration. The rift pattern runs parallel to the east- west boundaries and is perpendicular to the far-field velocity boundary conditions. The figure 5.1a better explains the model assembly and figure 5.1b shows the orientation of the rift pattern on the surface of the earth i.e in mapview. All layers below the rupture surface have the same rheology. This is the case for all models discussed in this thesis.

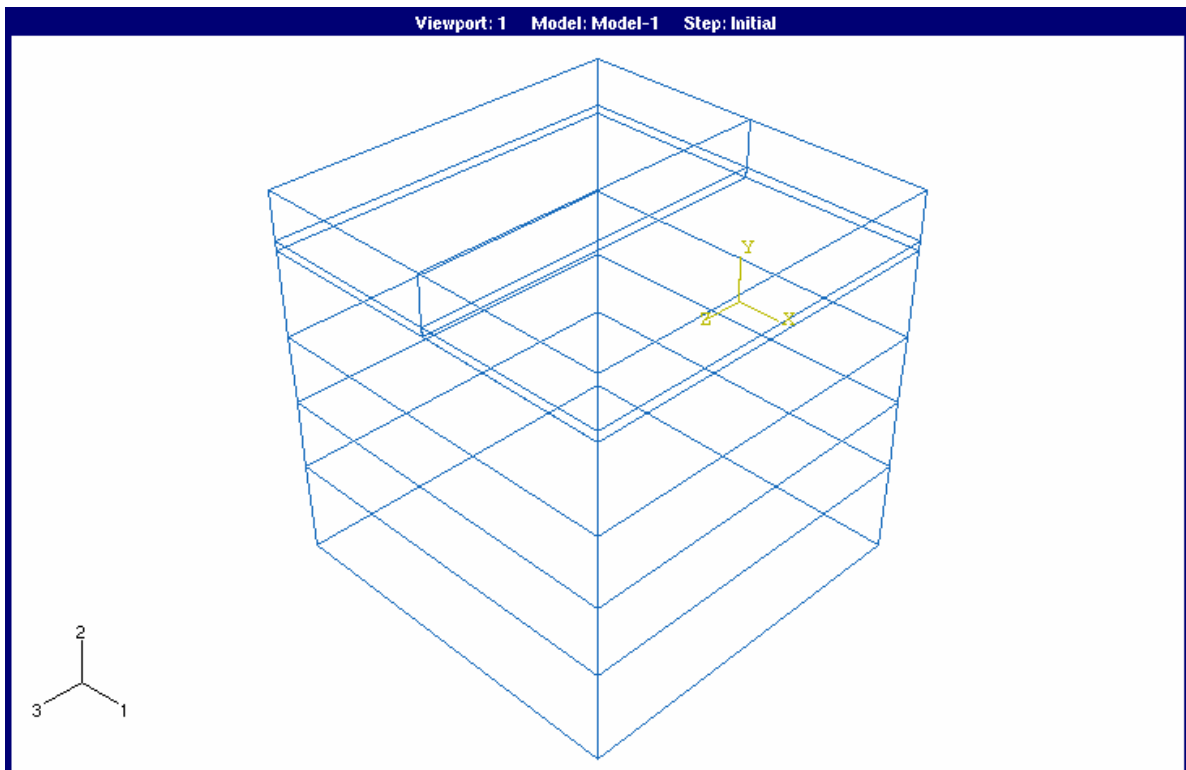


FIG 5.1a Straight Rift Model Assembly

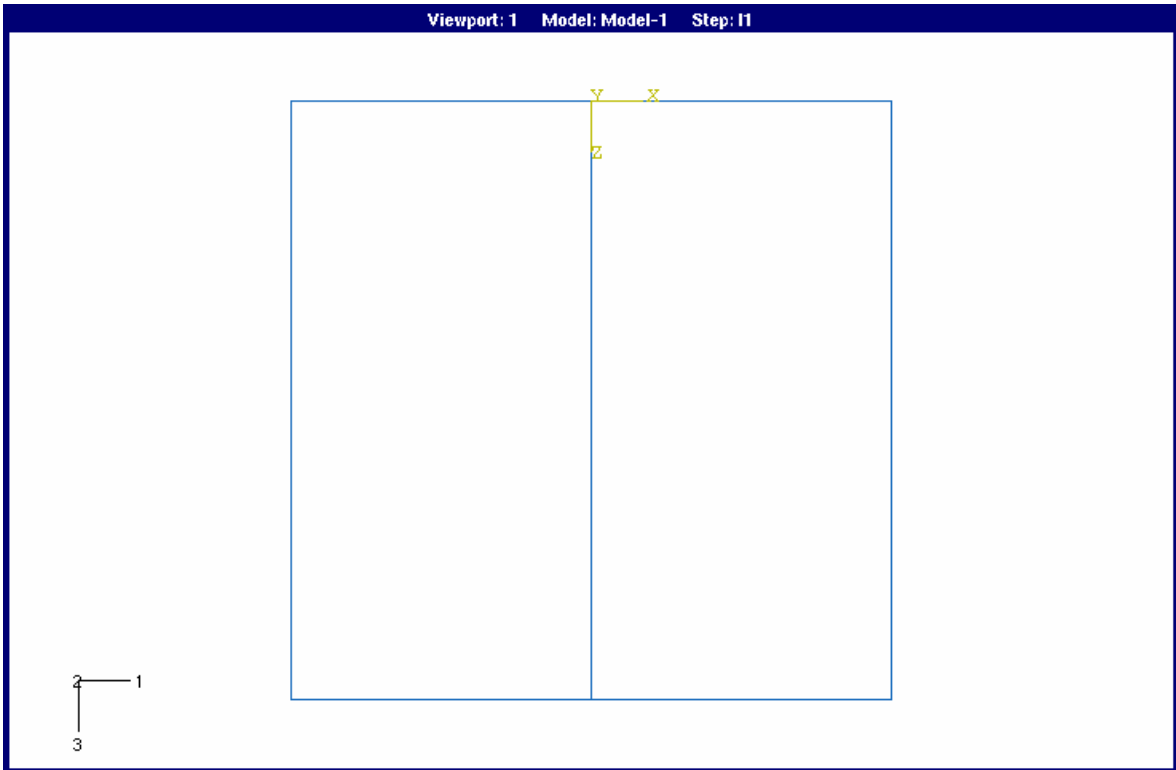


FIG 5.1b Top View of Straight Rift Model

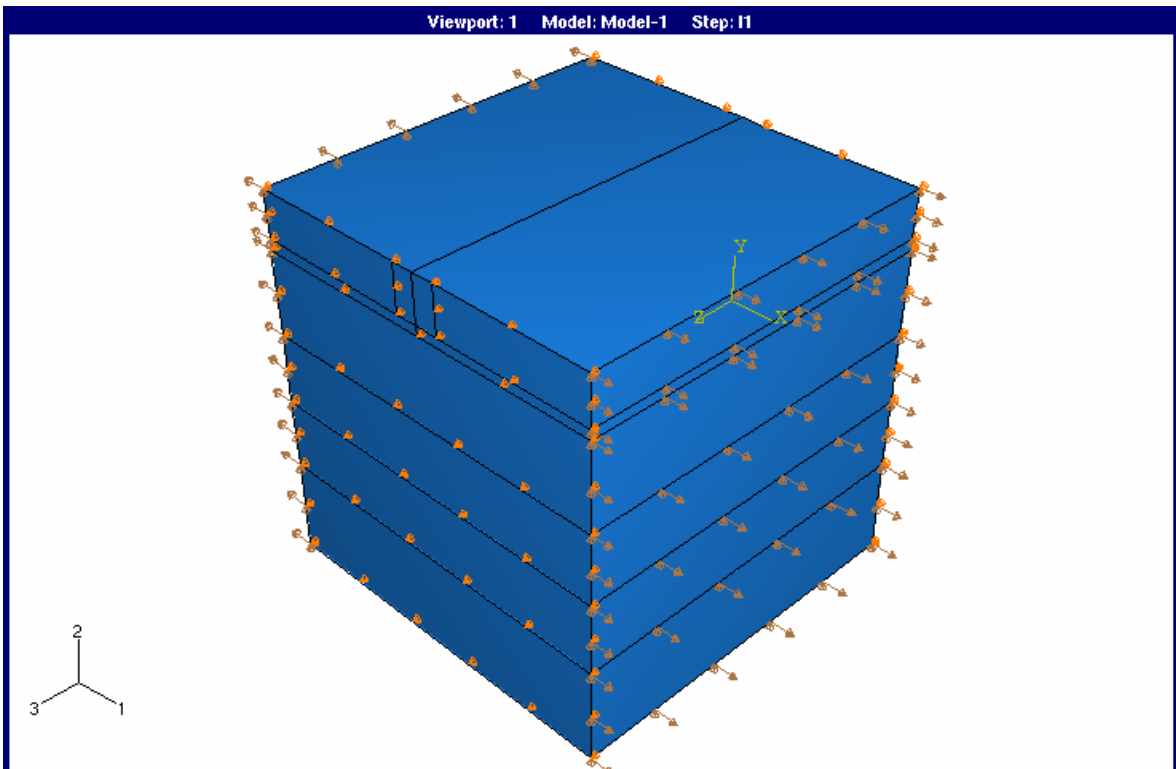


FIG 5.1c Shaded Model with Loads and Boundary Conditions

Figure 5.1c represents the velocity and displacement boundary conditions applied on the model. The model has a velocity BC applied in the 1-direction, and is free to move in 2-direction to account for Poisson's effect. The displacement in the 3- direction (North-South) is constrained as there is infinite material on the sides of the model.

Figure (FIG 5.1d) is the meshed model. We have used C3D8R element. It is a 8-node linear brick, reduced integration with hourglass control. The model is meshed uniformly and with a small seed\* number resulting in a fine mesh.

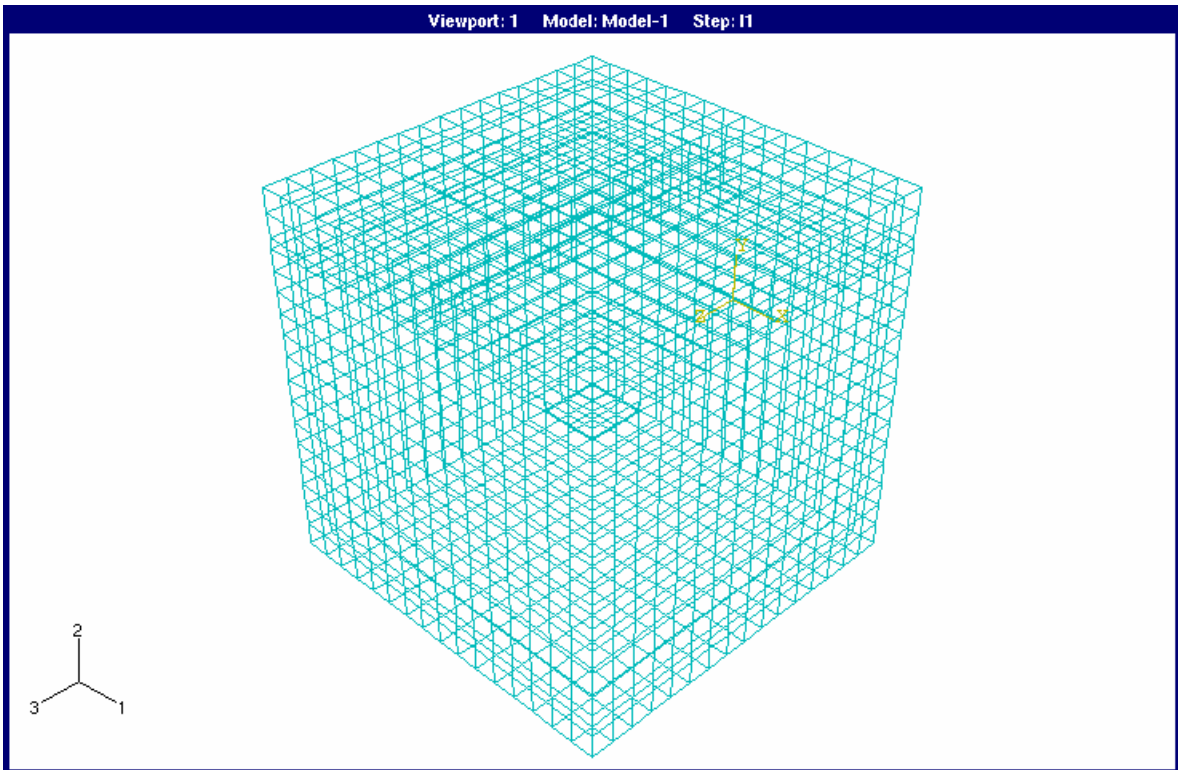


FIG 5.1d Meshed Model



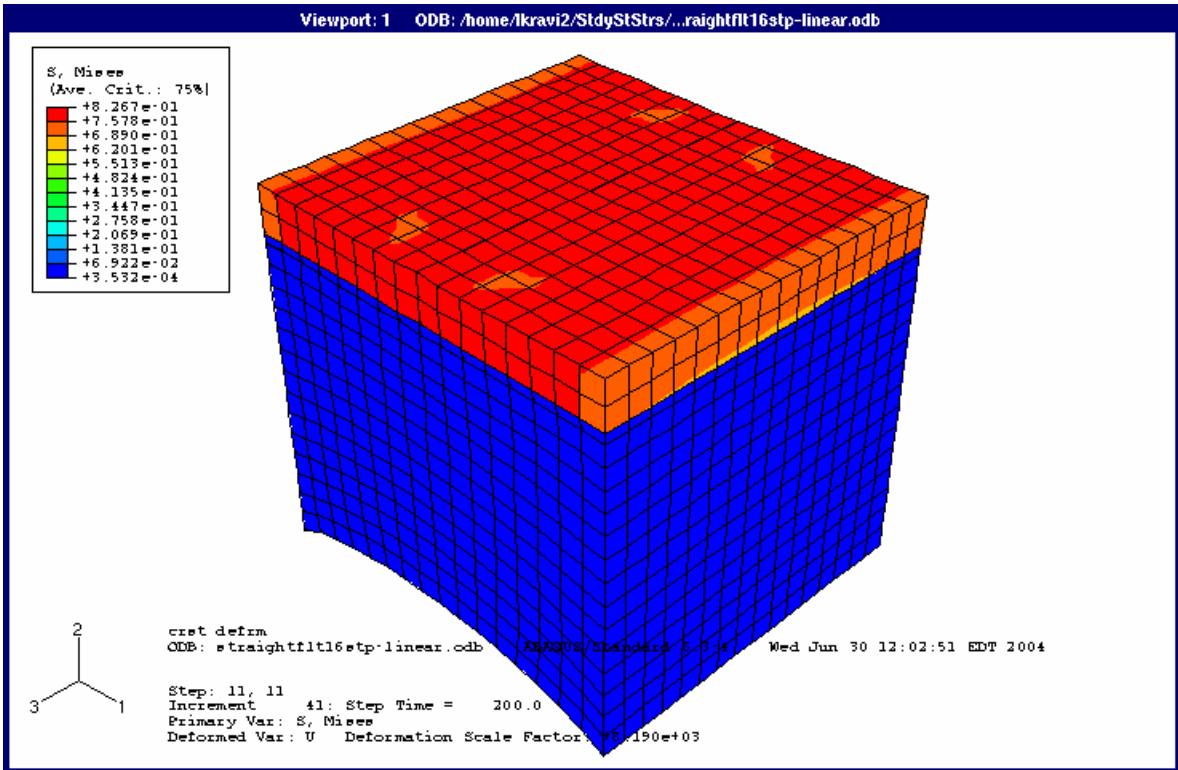


FIG 5.1f Model Mises Stresses at the End of the 1<sup>st</sup> Loading Step

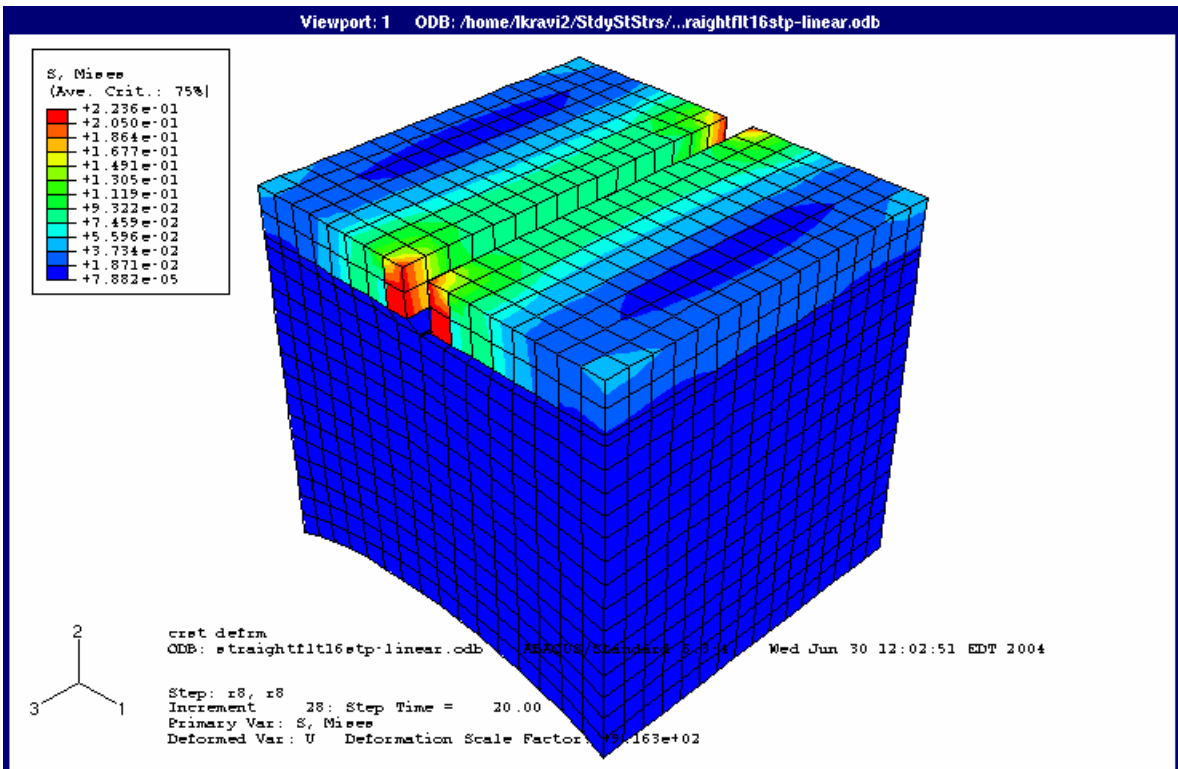


FIG 5.1g Model Mises stresses at the End of the 8<sup>th</sup> Rifting Step

Figure 5.1g is a contour plot of Mises stress distribution at the end of the eighth rifting step. The distribution of the stresses around the model are studied through these contour plots and similar plots can be used to monitor the distribution of stress in various steps of the analysis.

Figure 5.1h represents the stress contours on the crustal surface of the straight rift model. It is the top view of the rift pattern showing the detailed Mises stress distribution on the top surface of the model at the end of the 16<sup>th</sup> step.

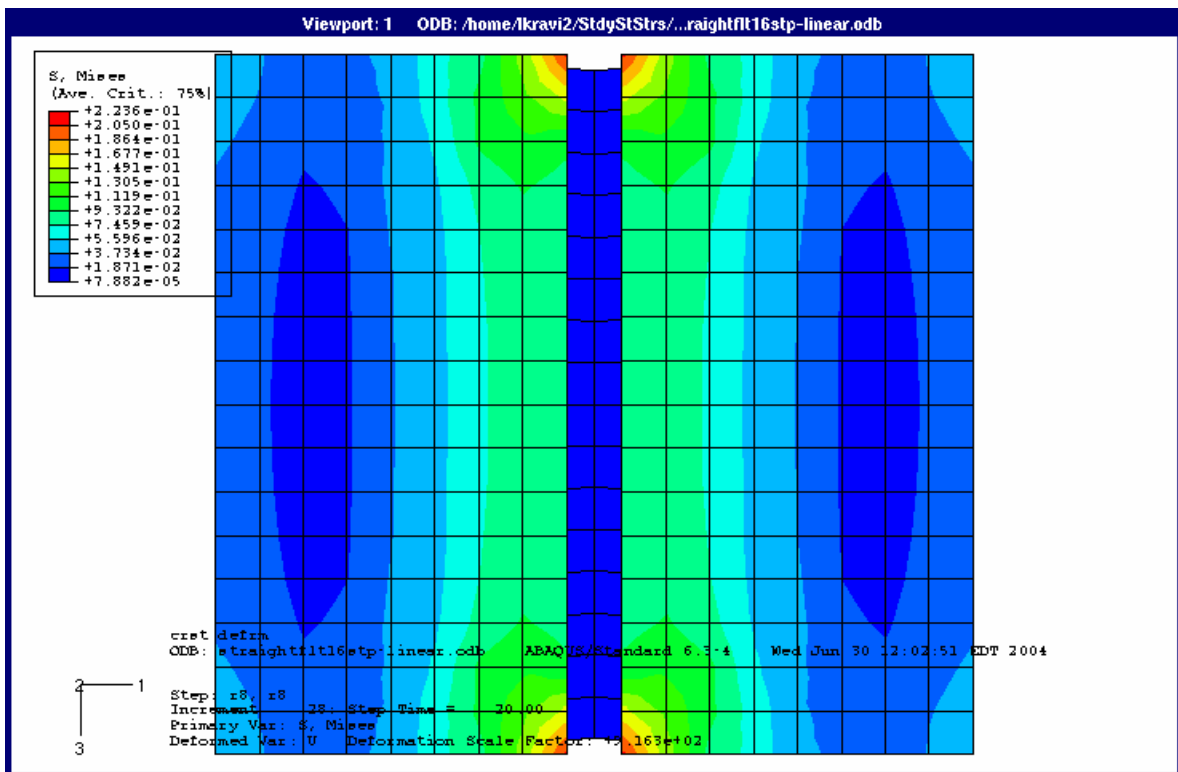


FIG 5.1h Top View of the Rift/Fault with Mises Stresses at the End of 8<sup>th</sup> Rifting Step

Figure 5.1i represents the displacement of the nodes on either side of the rift pattern during the 16 step analysis. This plot helps to better understand the cycle-up process and

function of the user-subroutine. The first horizontal line in the plot shows that the rift is tied together in the 1<sup>st</sup> loading step and displacements are in the same direction. As the rift is oriented symmetrically on the surface, the nodes remain in the same location. During the 1<sup>st</sup> rifting step the nodes on either side of the rift displace in the same magnitude but in the opposite direction, i.e the rift opens. The cycle-up of the model and functionality of the subroutine is emphasized by the symmetry in the repetitive steps.

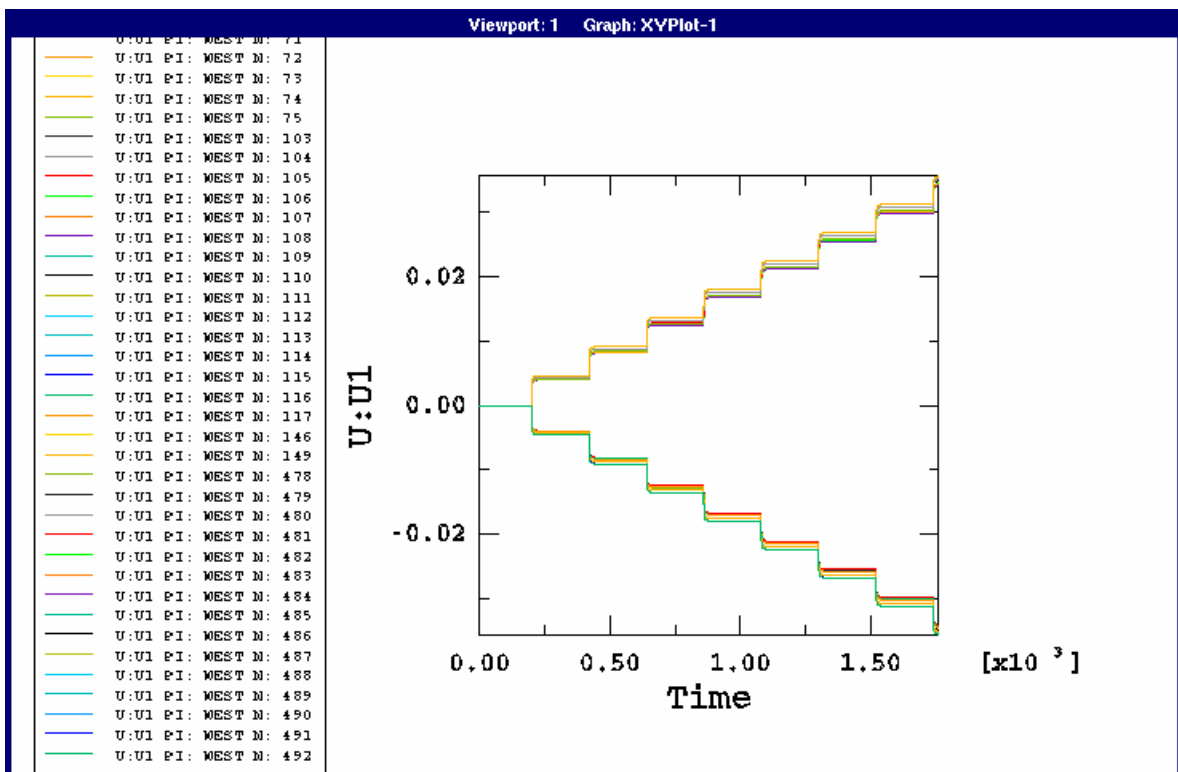


FIG 5.1i Displacement of the Nodes on the Rift During the 16 Step Analysis

Figures 5.1j, 5.1k, and 5.1l represent the Time Vs Mises Stress distribution during the 16 step analysis (8 loading and 8 rifting cycles) of the entire model at different locations. They represent the steady state stress attained and the number of cycles it took to reach the steady state stress.

Figure 5.1j represents steady State Mises Stress and the number of cycles it took to reach the steady state stress at right hand bottom node on the front face of the model. The steady state Mises stresses for this node is  $23.5 \times 10^{-3}$  MPa and its corresponding cycle time is 10 cycles (i.e 5 loading steps and 5 rifting steps).

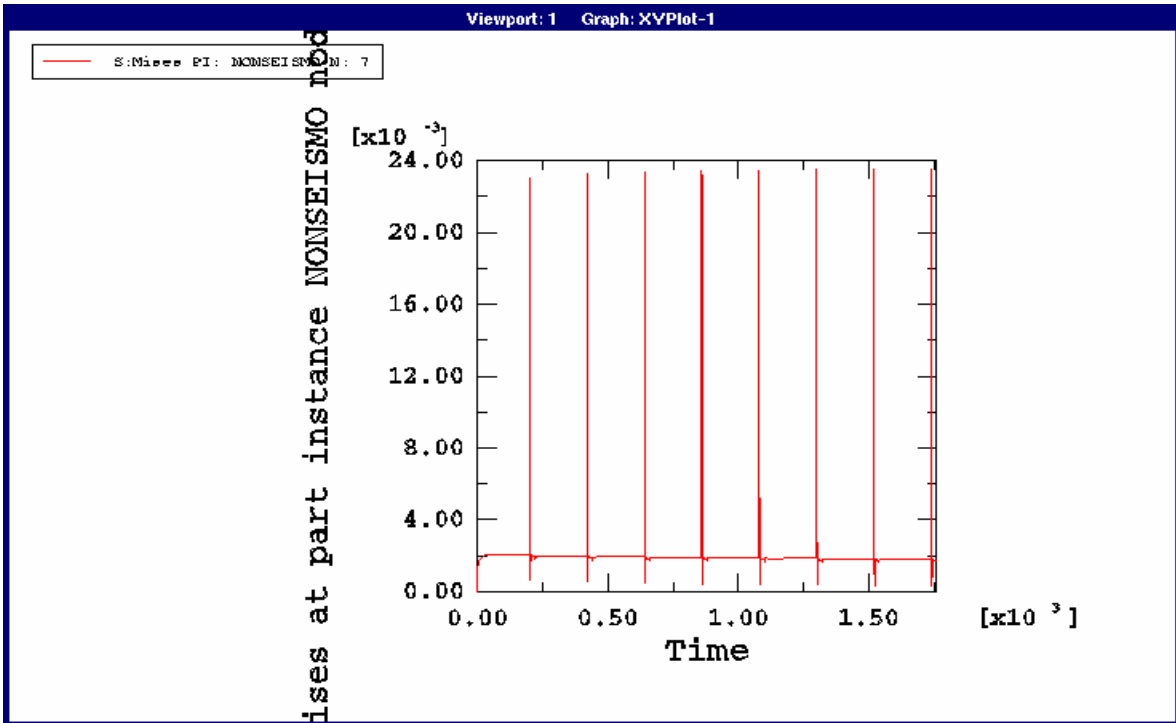


FIG 5.1j Cycle-Up and Subsequent steady State Mises Stress for the Right Hand Bottom Node on the Front Face of the Model.

Figure 5.1k represents steady State Mises Stress and the number of cycles it took to reach the steady state stress for the node located at the base of the rift (120 km) on the front face of the model. The steady state Mises stresses for this node are 0.9 MPa and its corresponding cycle time is 8 cycles (i.e 4 loading steps and 4 rifting steps).



Figure 5.11 represents steady State Mises Stress and the number of cycles it took to reach the steady state stress for the node located in the middle of the front face of the model. The depth of this node is 350 km below the tip of the rift on the front face of the model. The steady state Mises stresses for this are  $21.0 \times 10^{-3}$  MPa and its corresponding cycle time is 4 cycles (i.e 2 loading steps and 2 rifting steps). The difference between cycles and steps will not be defined again for later models.

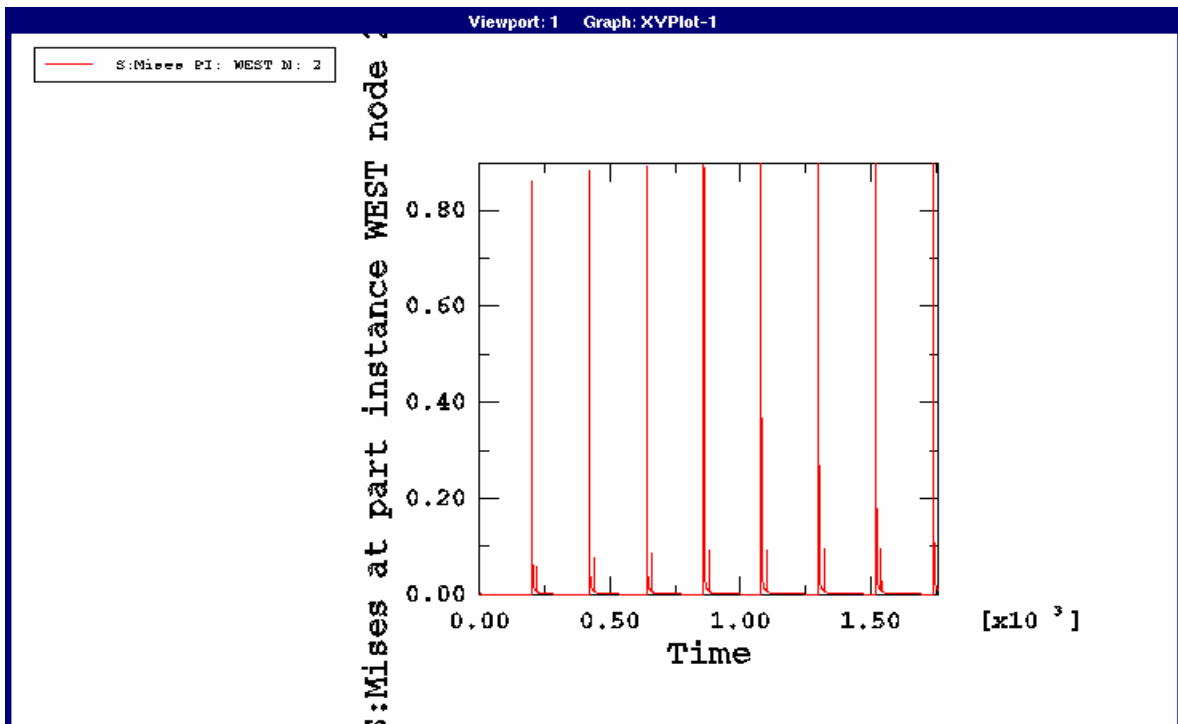


FIG 5.1k Cycle-Up and Subsequent Steady State Mises Stress for a Node Located at the Base of the Rift on the Front Face of the Model.

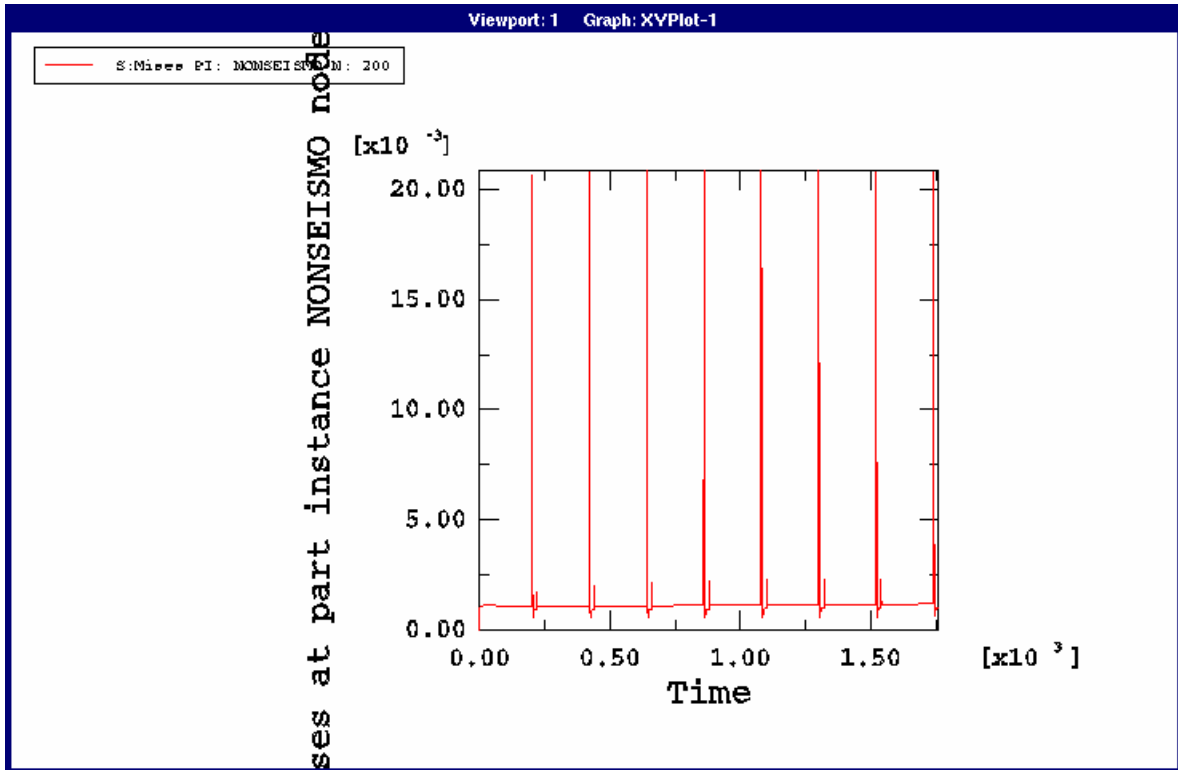


FIG 5.11 Cycle-Up and Subsequent Steady State Mises Stress for a Node Located in the Middle of the Front Face of the Model.

## 5.2 EXPERIMENT 2: INCLINED RIFT MODEL

Moving to a model with greater complexity are the inclined rift models. In an inclined rift model the rift is oriented at an angle to the far-field velocity boundary conditions. Plots from 5.2a to 5.2 l in this experiment are similar to the those explained in the straight rift model.

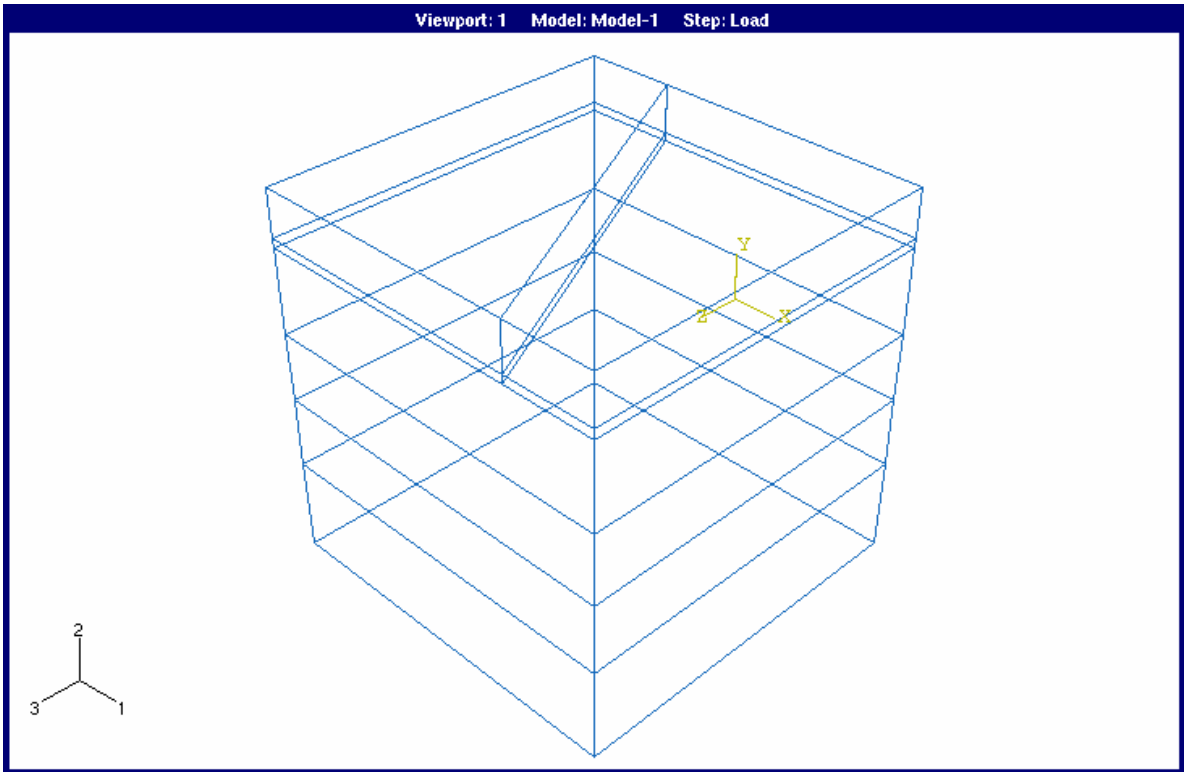


FIG 5.2a Inclined Rift Model Assembly

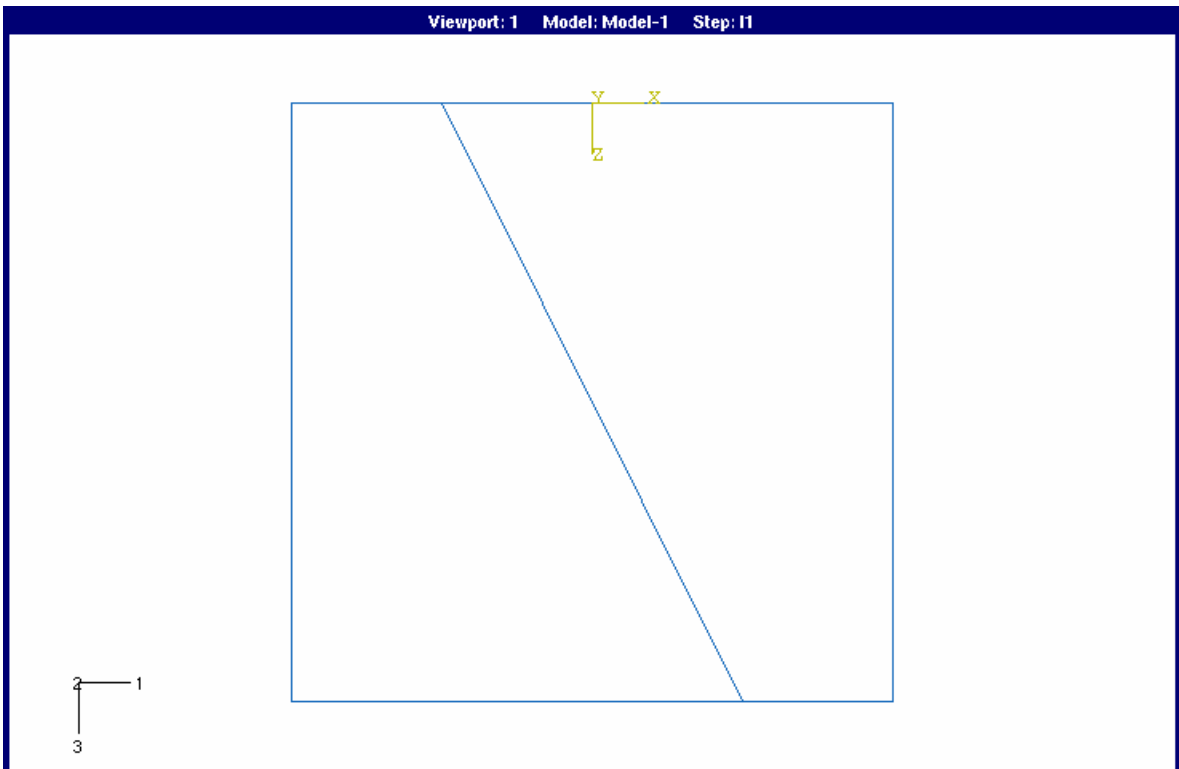


FIG 5.2b Top View of the Inclined Rift Model

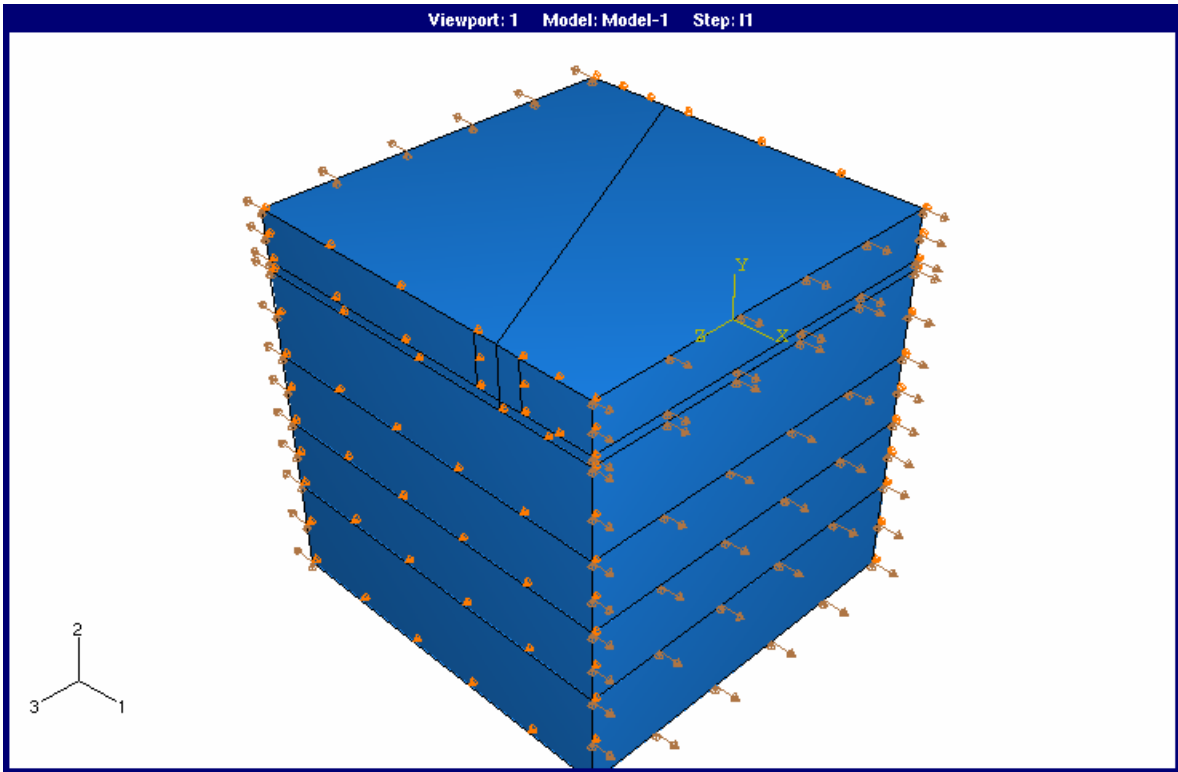


FIG 5.2c Shaded Model with Loads and Boundary Conditions

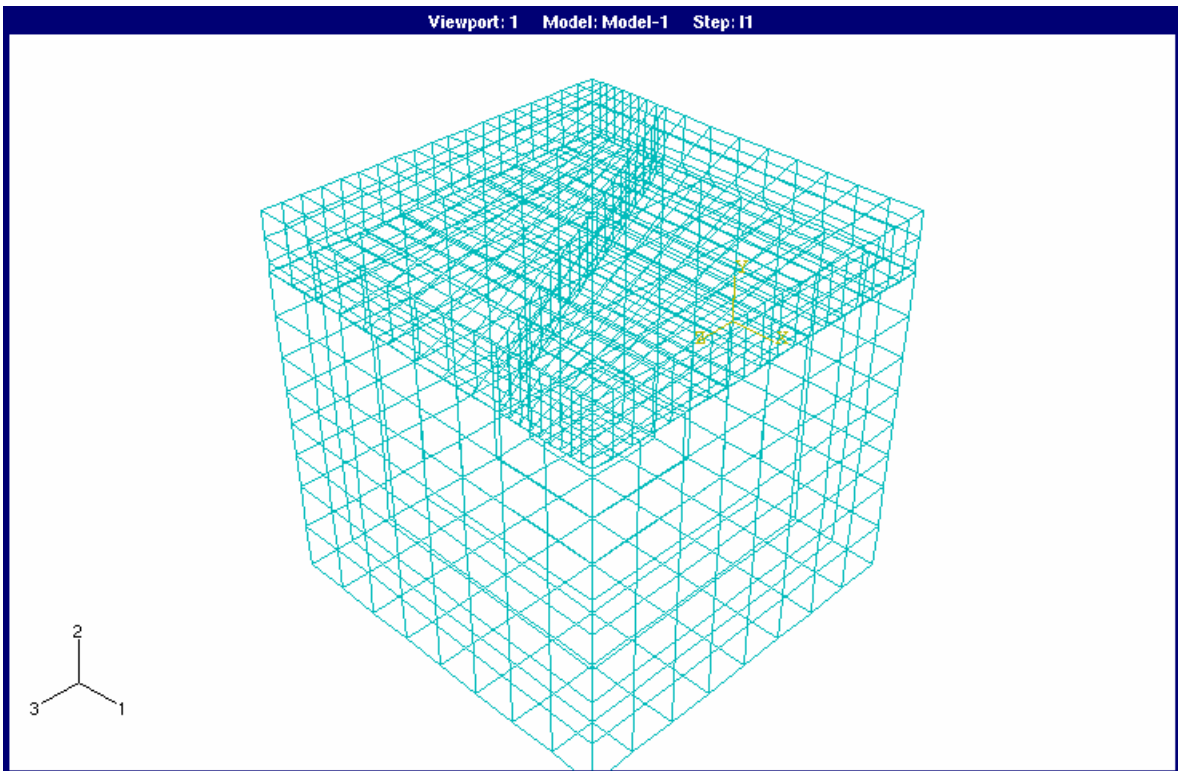


FIG 5.2d Meshed Model

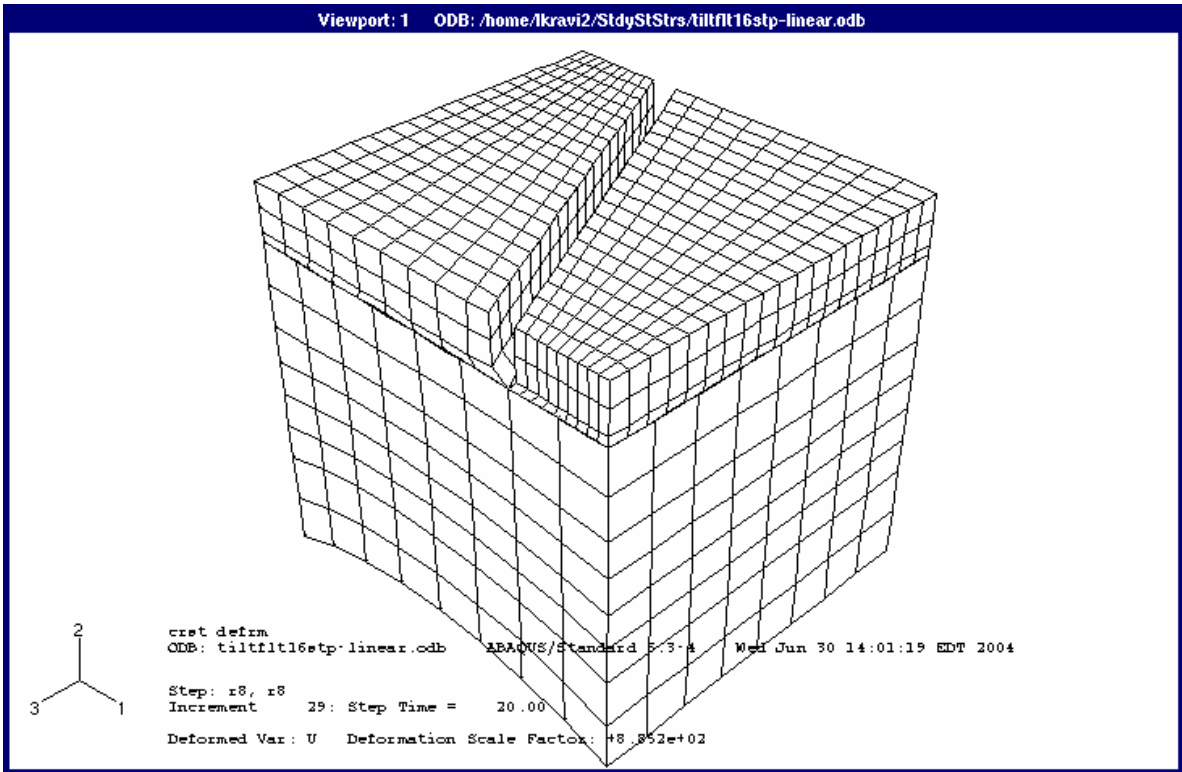


FIG 5.2e Final Deformation of the Model at the End of the 16<sup>th</sup> Step.

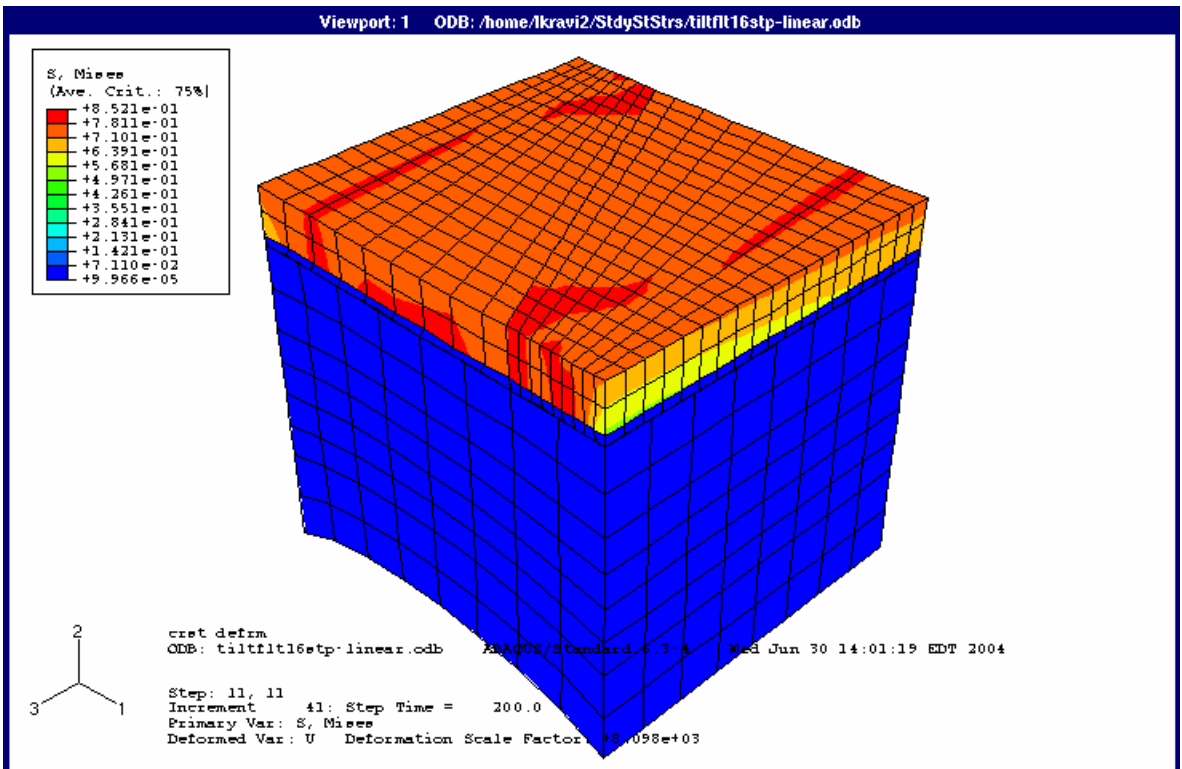


FIG 5.2f Model Mises Stresses at the End of the 1<sup>st</sup> Loading Step

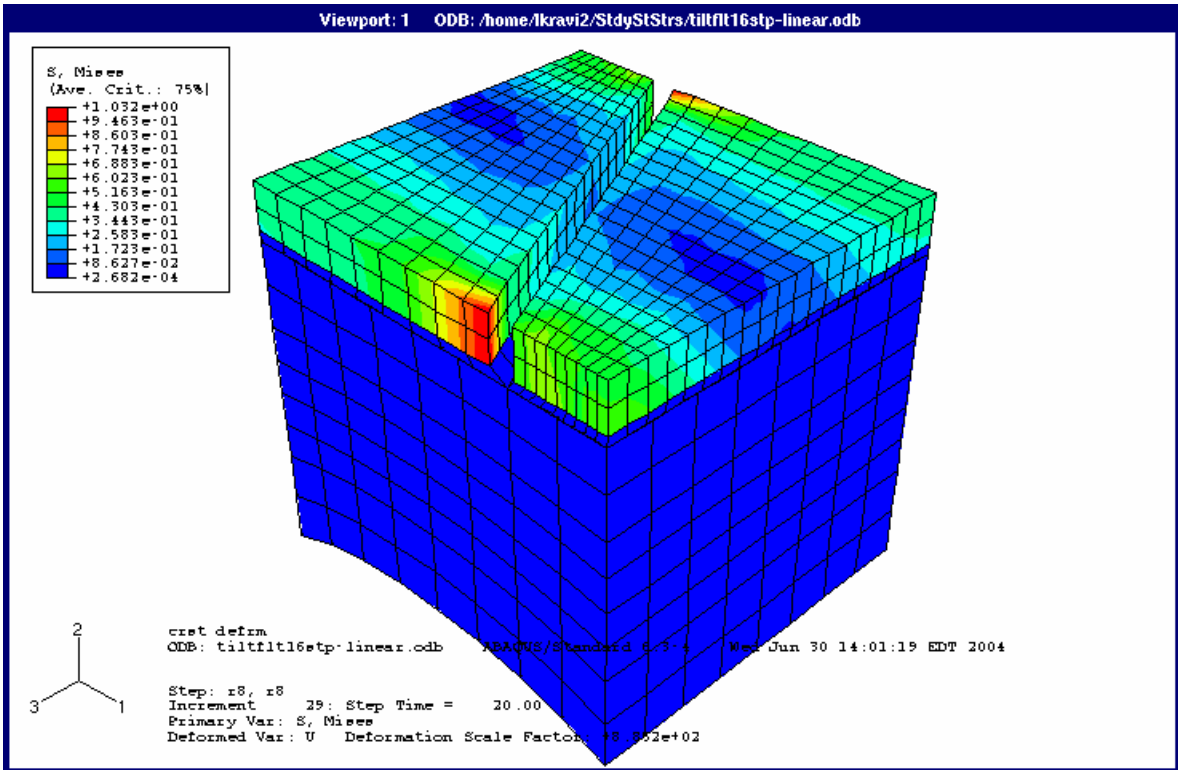


FIG 5.2g Model Mises stresses at the End of the 8<sup>th</sup> Rifting Step

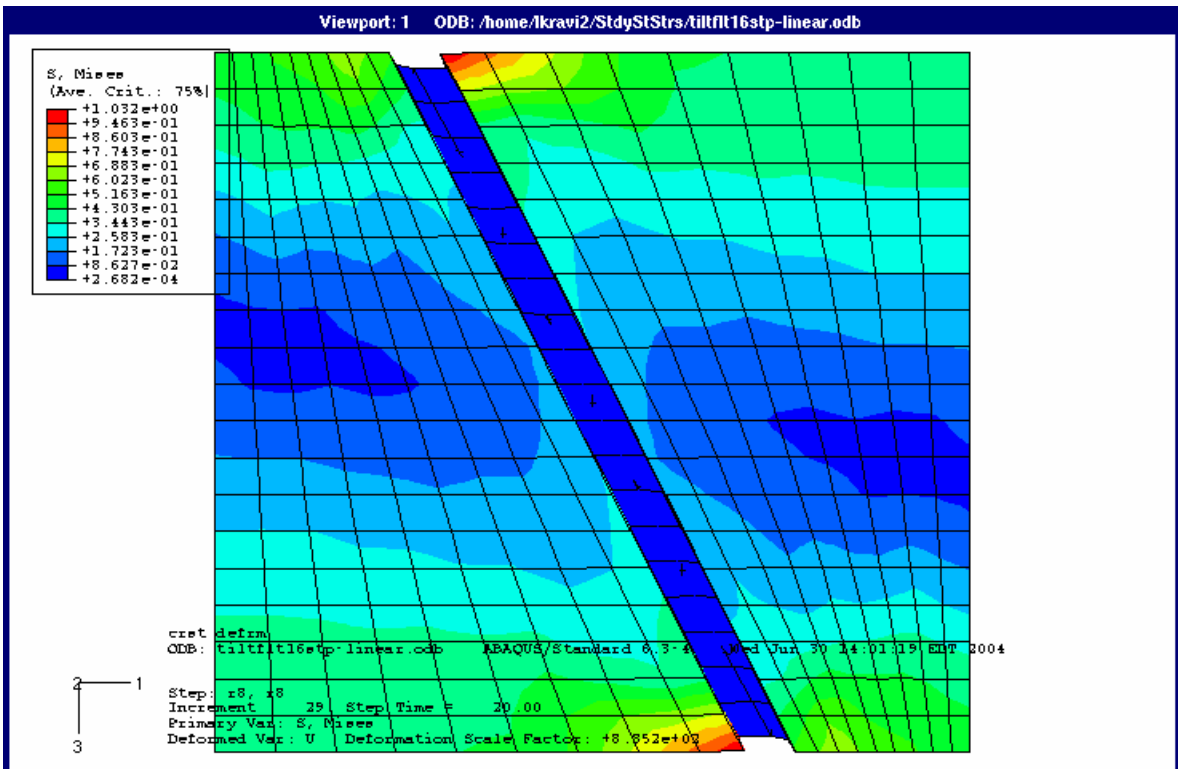


FIG 5.2h Top View of the Rift/Fault with Mises Stresses at the End of 8<sup>th</sup> Rifting Step

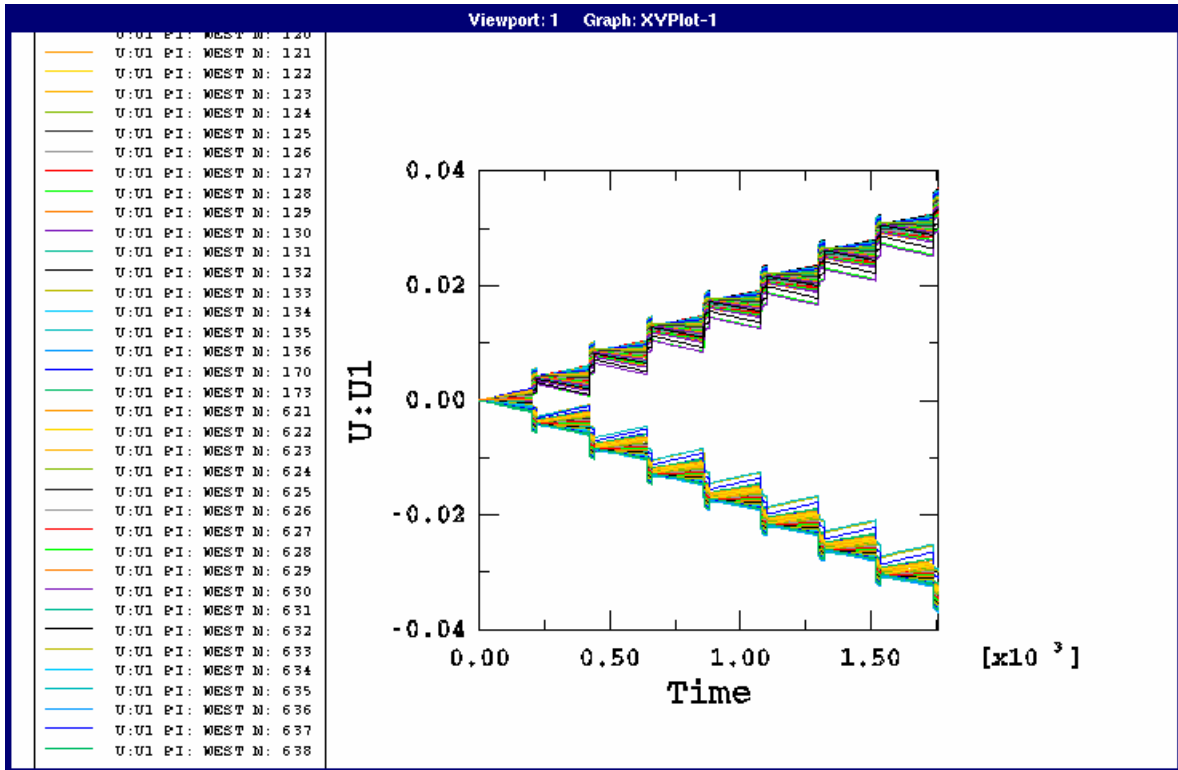


FIG 5.2i Displacement of the Nodes on the Rift During the 16 Step Analysis

Figure 5.2i gives displacement of each node on the fault but differs from the straight fault model because of asymmetry. Some nodes move in one direction during loading and the opposite direction during rifting. Initially we have nodes on either sides of the line of symmetry and that is the reason why displacements are of different slopes.

Figures 5.2j, 5.2k, and 5.2l represent the Time Vs Mises Stress distribution during the 16 step cycle (8 loading and 8 rifting steps) of the entire model at different locations. They represent the steady state stress attained and the number of cycles it took to reach the steady state stress.

Figure 5.2j represents steady State Mises Stress and the number of cycles it took to reach the steady state stress for the right hand bottom node on the front face of the model. The steady state Mises stresses for this node is  $19.5 \times 10^{-3}$  MPa and its corresponding cycle time is 12 cycles.

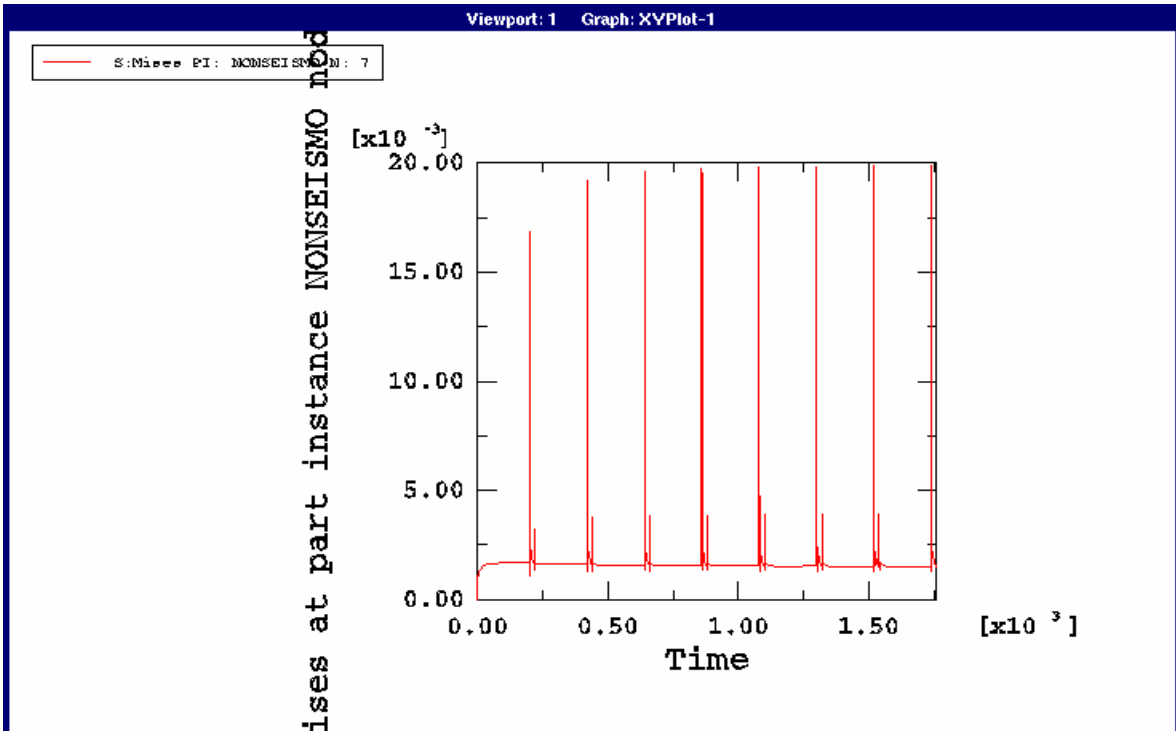


FIG 5.2j Cycle-Up and Subsequent steady State Mises Stress for the Right Hand Bottom Node on the Front Face of the Model.

Figure 5.2k represents steady State Mises Stress and the number of cycles it took to reach the steady state stress for the node located at the base of the rift on the front face of the model. The steady state Mises stresses for this node is 1.25 MPa and its corresponding cycle time is 14 cycles.



Figure 5.2l represents steady State Mises Stress and the number of cycles it took to reach the steady state stress for the node located in the middle of the front face of the model. The steady state Mises stresses for this node is  $22.05 \times 10^{-3}$  MPa and its corresponding cycle time is 6 cycles.

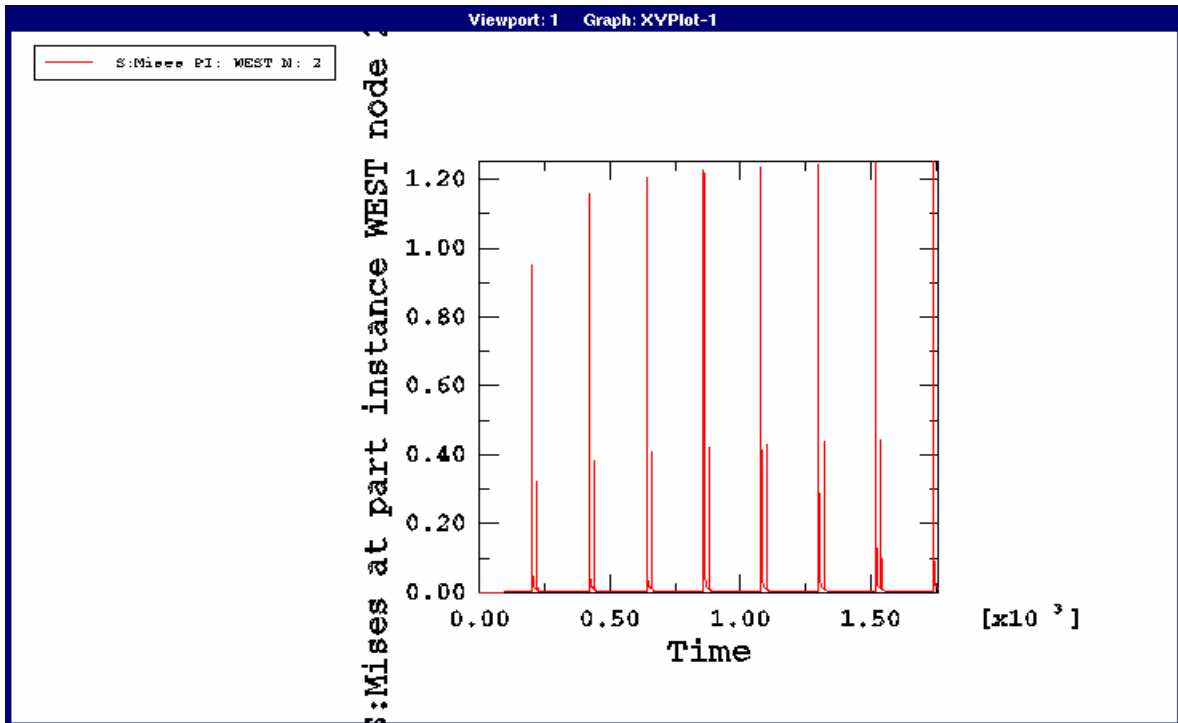


FIG 5.2k Cycle-Up and Subsequent Steady State Mises Stress for a Node Located at the Base of the Rift on the Front Face of the Model.

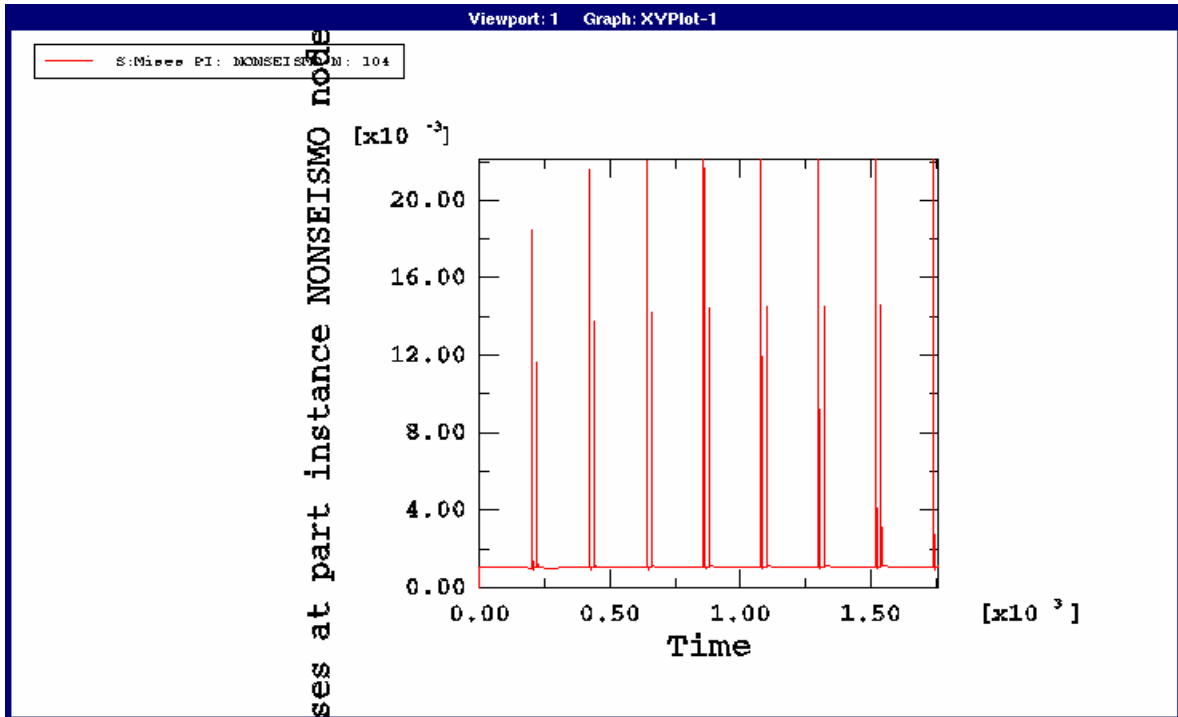


FIG 5.21 Cycle-Up and Subsequent Steady State Mises Stress for a Node Located in the Middle of the Front Face of the Model.

### 5.3 EXPERIMENT 3: INTERSECTING RIFT MODEL

This experiment is conducted to better understand the behavior of intersecting rifts. We have considered two individual rift patterns intersecting at a point. This drives the complexity to a higher level. We have used virtual topology to generate a better mesh to handle the meshing issues more thoroughly. Using virtual topology we have generated the same corresponding nodes on either side of the rift to ensure proper functionality of the user-subroutine. Plots in this experiment are similar to the those explained in the experiment 1. The middle pattern in the displacement plot (fig 5.3i) represents the displacement of the nodes along the angular rift pattern. The pattern on the top and bottom represents the displacement of the nodes on the east and west sides of the straight part of the rift.

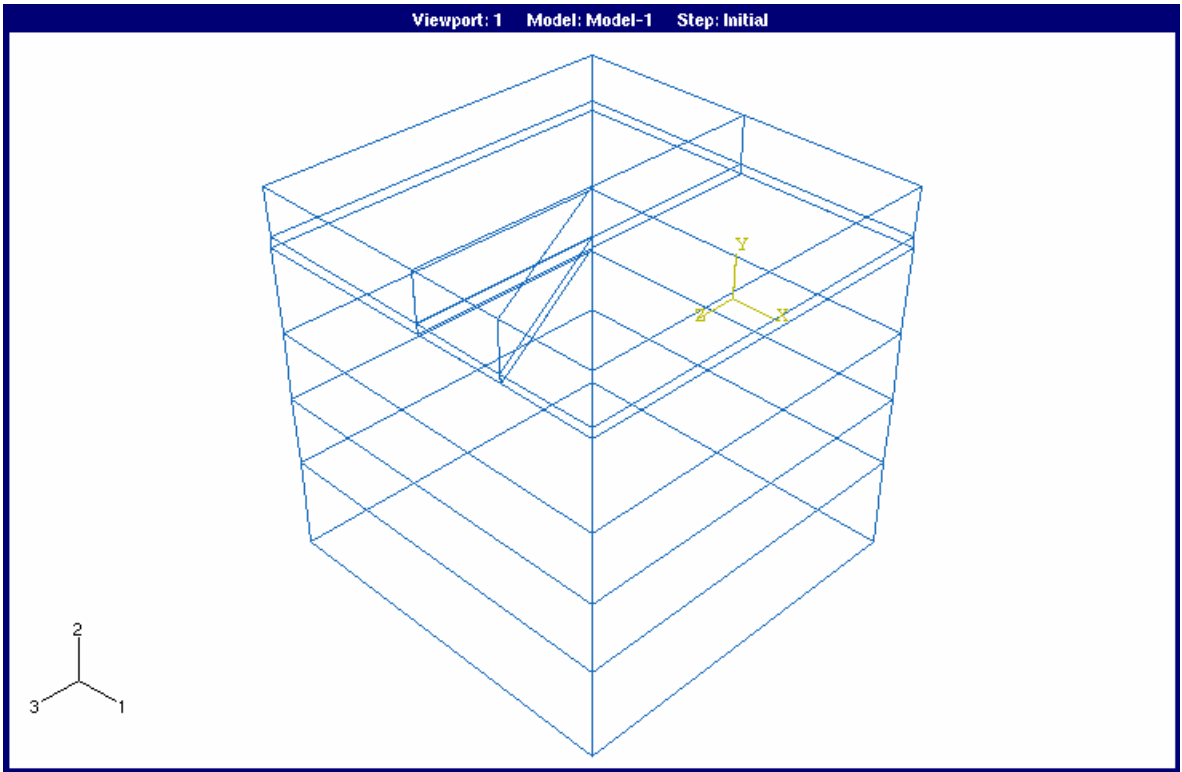


FIG 5.3a Intersecting Rift Model Assembly

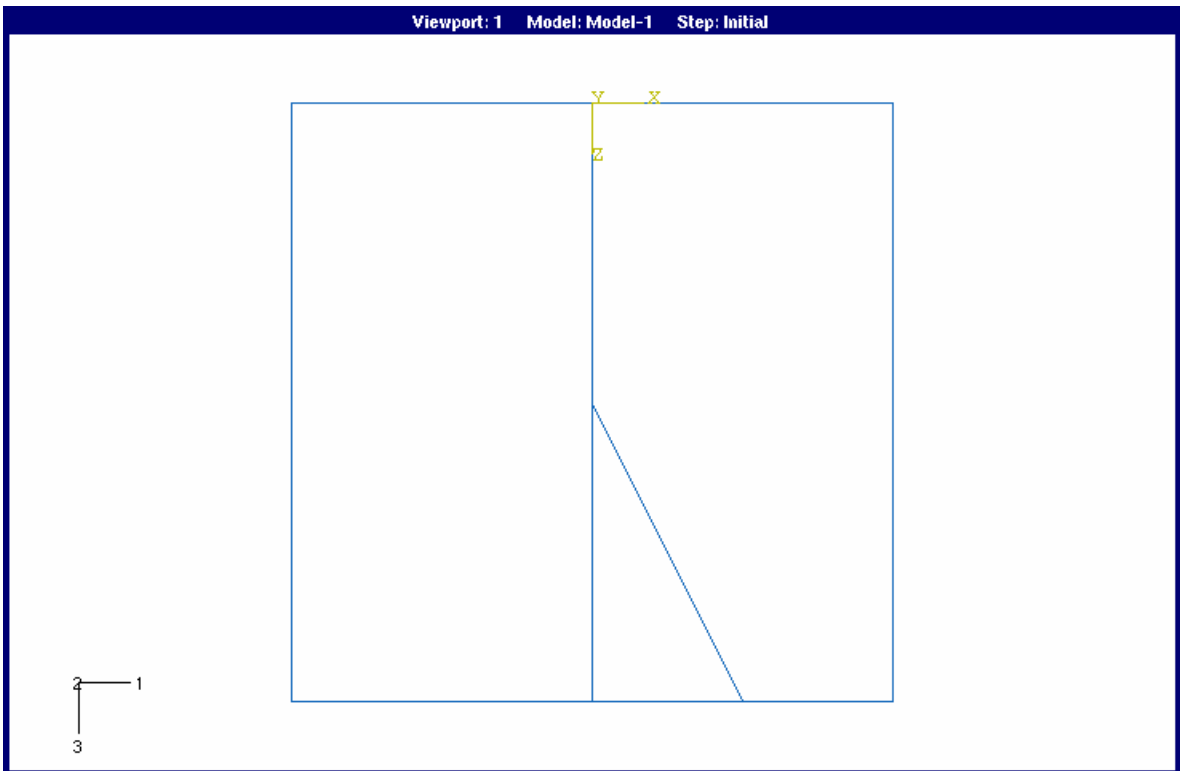


FIG 5.3b Top View of the Intersecting Rift Model

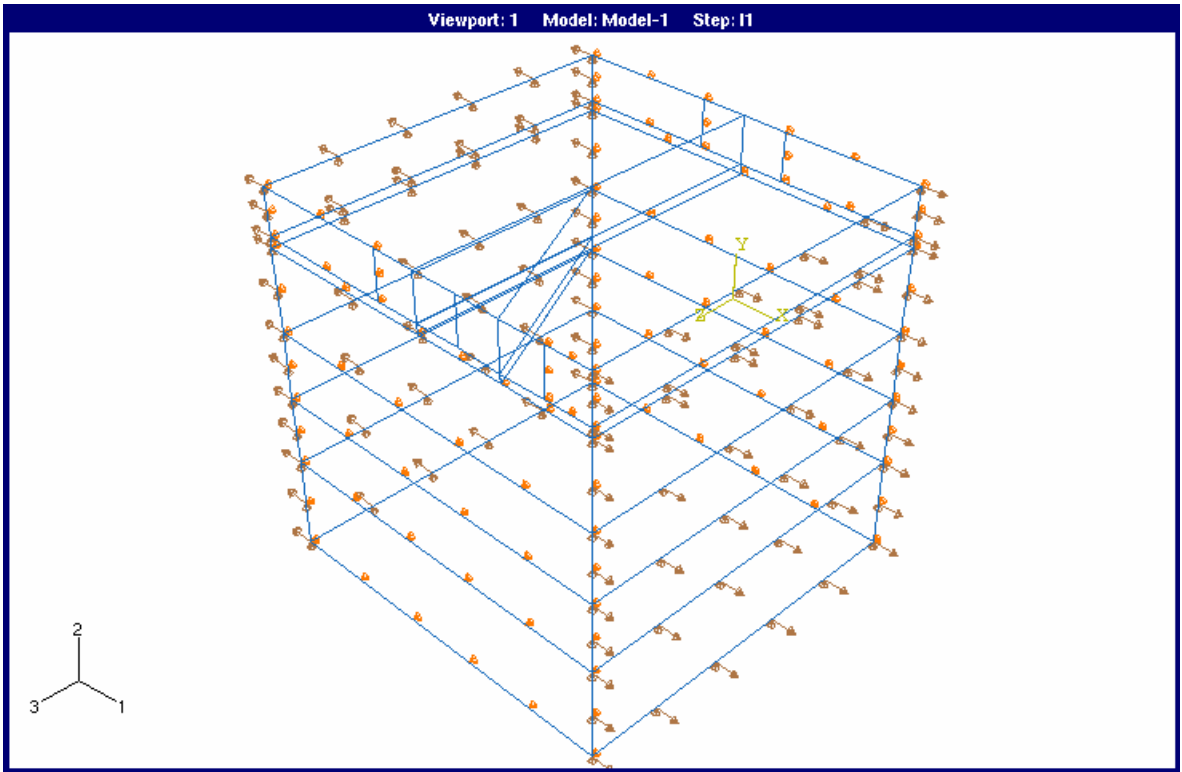


FIG 5.3c Model with Loads and Boundary Conditions

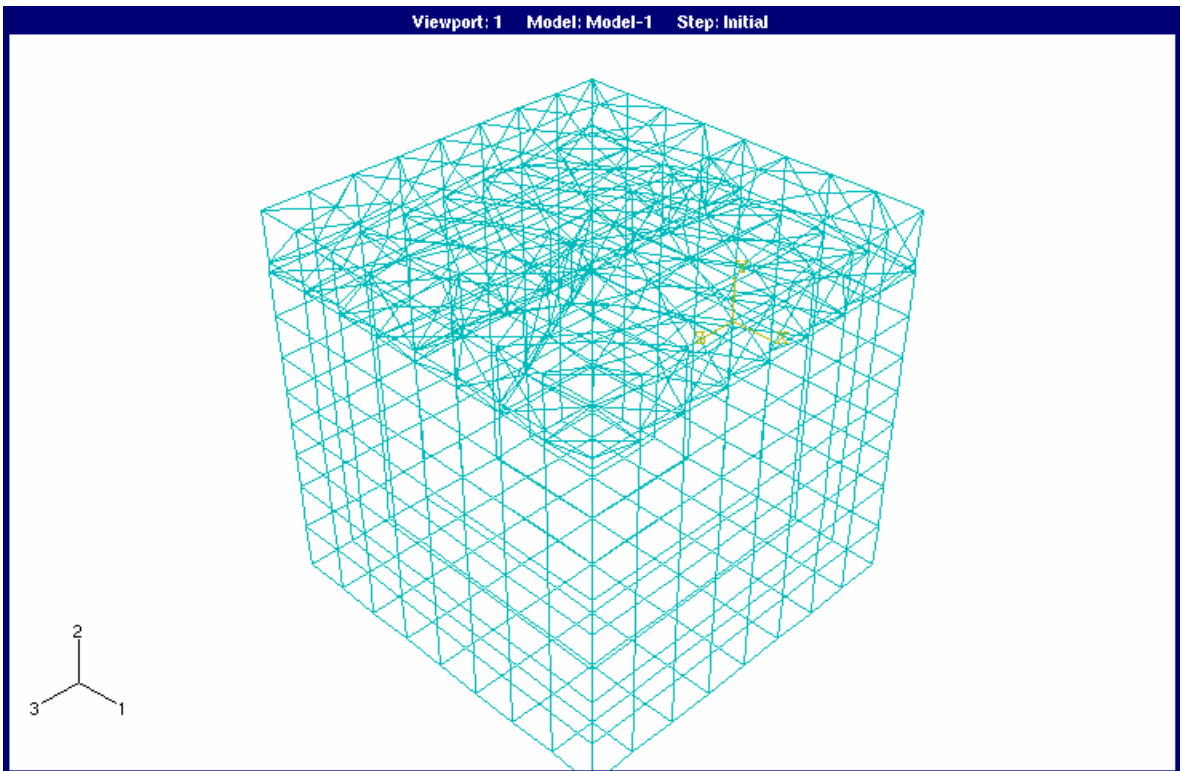


FIG 5.3d Meshed Model Using Virtual Topology

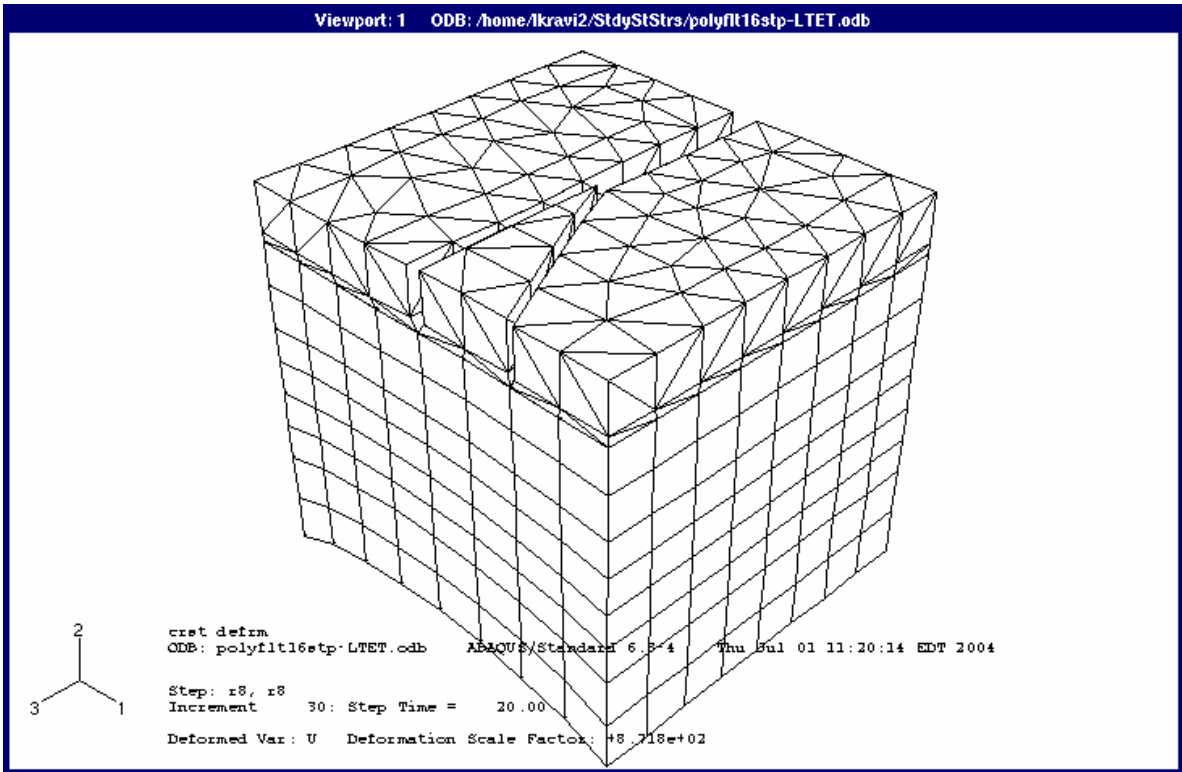


FIG 5.3e Final Deformation of the Model at the End of the 16<sup>th</sup> Step.

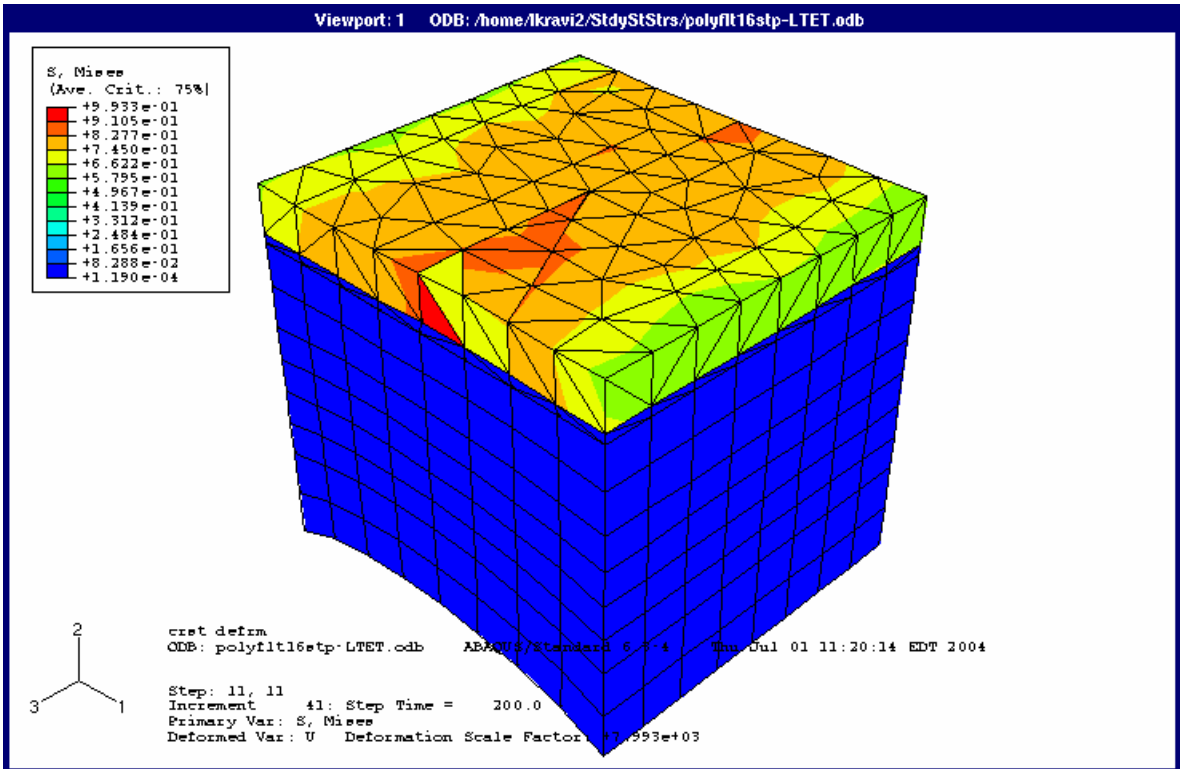


FIG 5.3f Model Mises Stresses at the End of the 1<sup>st</sup> Loading Step

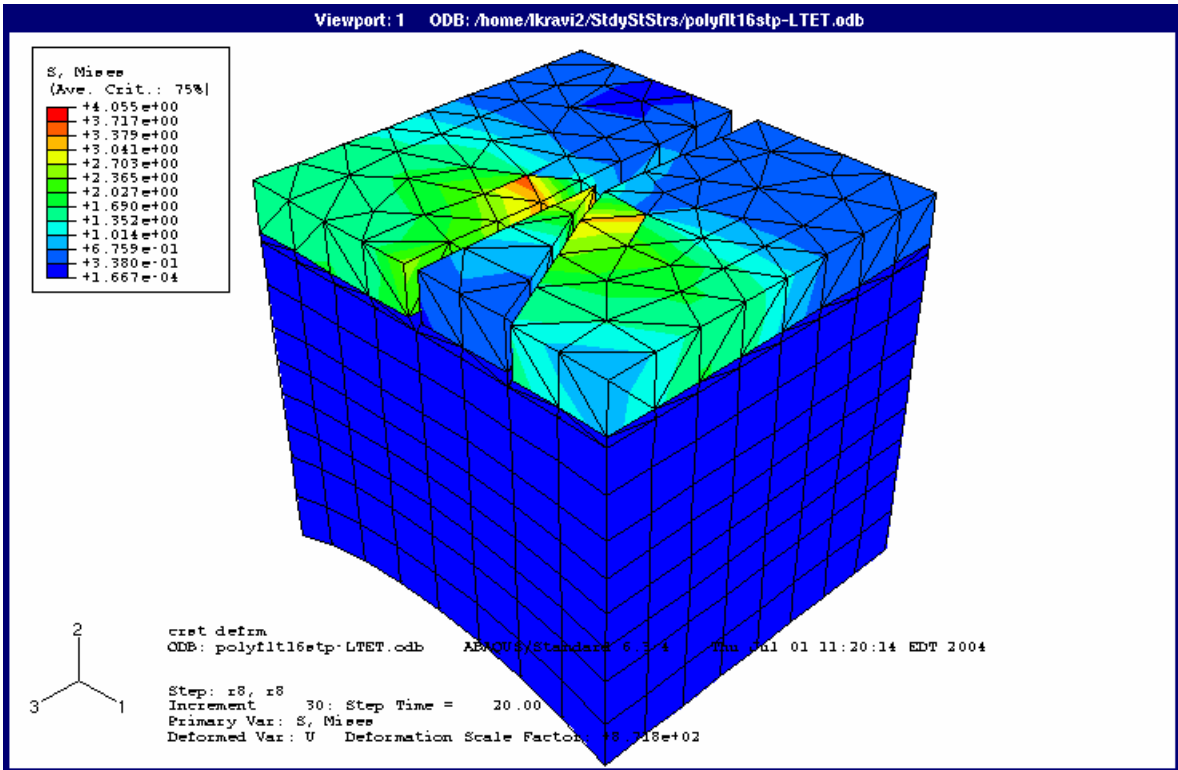


FIG 5.3g Model Mises stresses at the End of the 8<sup>th</sup> Rifting Step

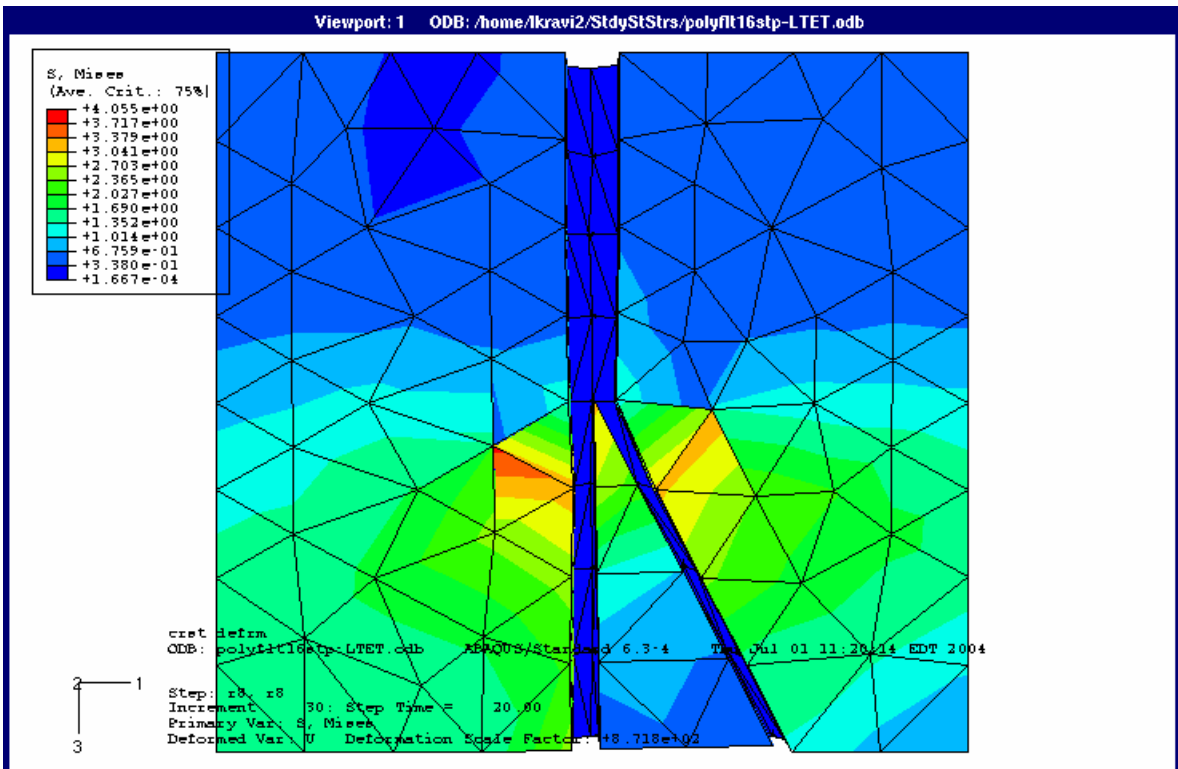


FIG 5.3h Top View of the Rift/Fault with Mises Stresses at the End of 8<sup>th</sup> Rifting Step

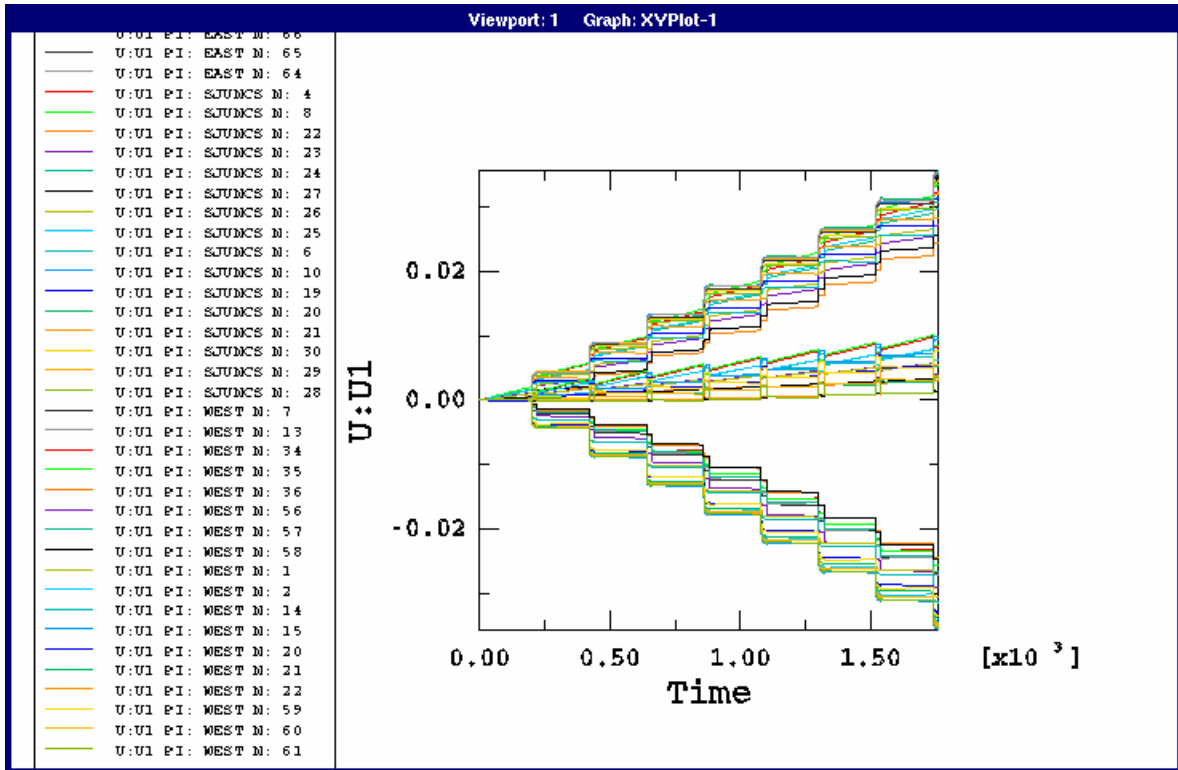


FIG 5.3i Displacement of the Nodes on the Rift During the 16 Step Analysis

Figures 5.3j, 5.3k, and 5.3l represent the Time Vs Mises Stress distribution during the 16 step cycle (8 loading and 8 rifting steps) of the entire model at different locations. They represent the steady state stress attained and the number of cycles it took to reach the steady state stress.

Figure 5.3j represents steady State Mises Stress and the number of cycles it took to reach the steady state stress for the right hand bottom node on the front face of the model. The steady state Mises stresses for this node is  $22.5e10^{-3}$  MPa and its corresponding cycle time is 14 cycles.

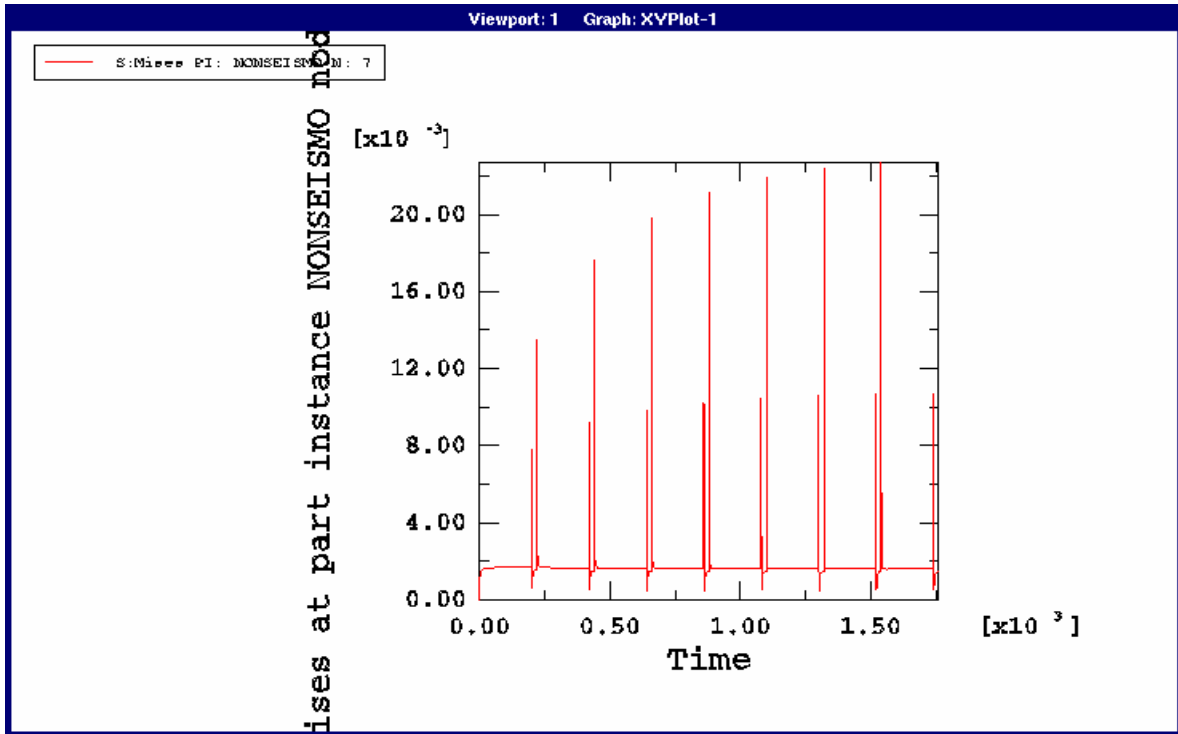


FIG 5.3j Cycle-Up and Subsequent steady State Mises Stress for the Right Hand Bottom Node on the Front Face of the Model.

Figure 5.3k represents steady State Mises Stress and the number of cycles it took to reach the steady state stress for the node located at the base of the rift on the front face of the model. The steady state Mises stresses for this node is 1.3 MPa and its corresponding cycle time is 16 cycles.

Figure 5.3l represents steady State Mises Stress and the number of cycles it took to reach the steady state stress for the node located in the middle of the front face of the model. The steady state Mises stresses for this node is  $33.0 \times 10^{-3}$  MPa and its corresponding cycle time is 14 cycles.



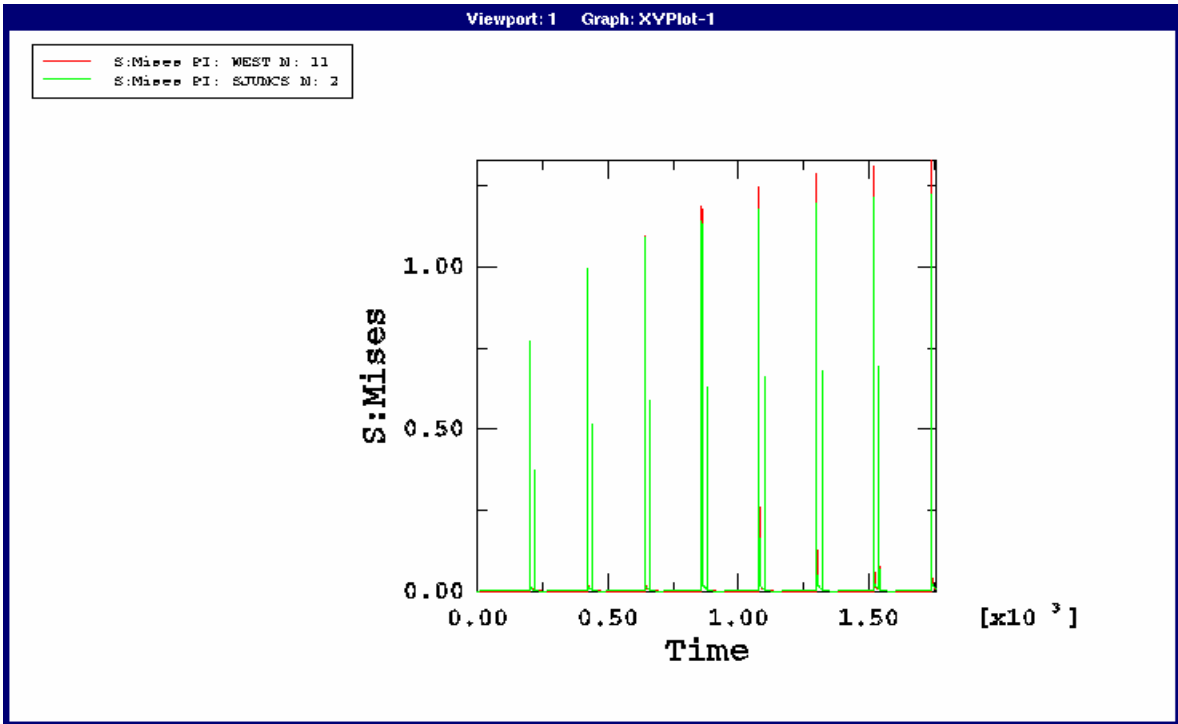


FIG 5.3k Cycle-Up and Subsequent Steady State Mises Stress for a Node Located at the Base of the Rift on the Front Face of the Model.

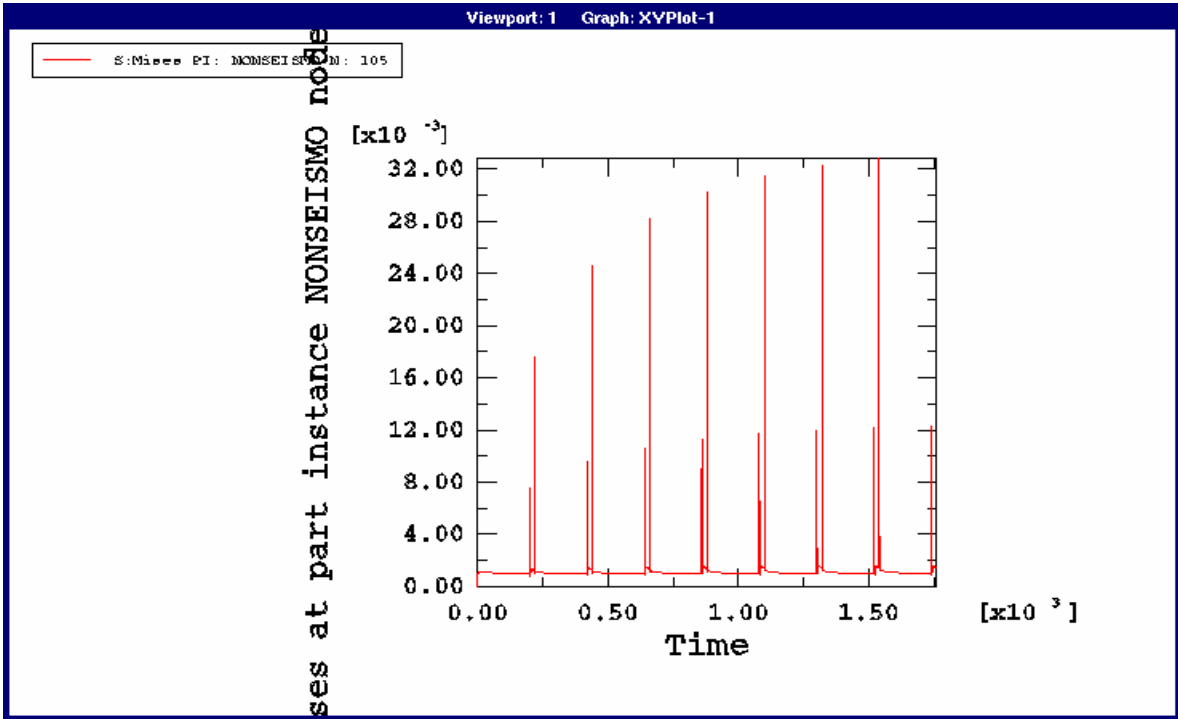


FIG 5.3l Cycle-Up and Subsequent Steady State Mises Stress for a Node Located in the Middle of the Front Face of the Model.

#### 5.4 EXPERIMENT 4: BOX RIFT MODEL

This model increases the complexity and is important for further development of Iceland models that have similar geometries. The box rifting problem has a rift pattern close to the 1<sup>st</sup> order model Dr. Kenner and Dr. Simons would compare to real data. In these models we have a straight rift intersected at two different location by “U” rift pattern. These models help us understand rifting issues that involve corners, multiple polygons, and intersecting rifts.

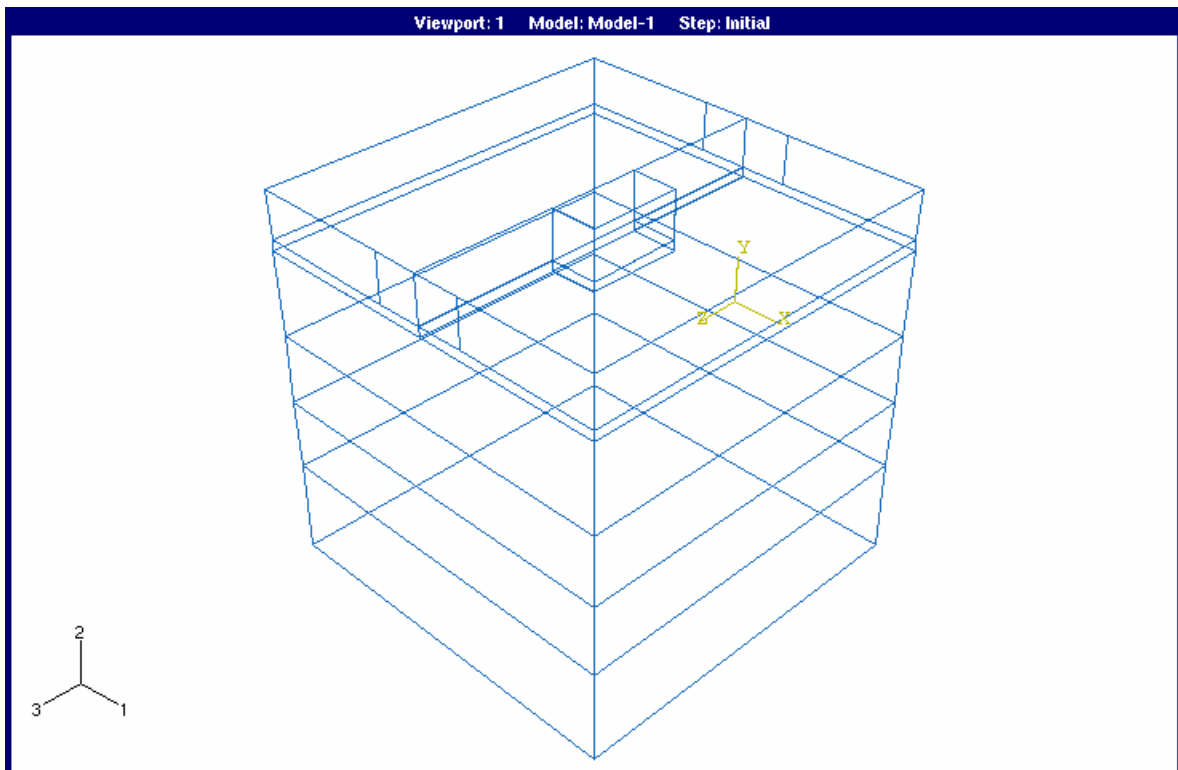


FIG 5.4a Box Rift Model Assembly

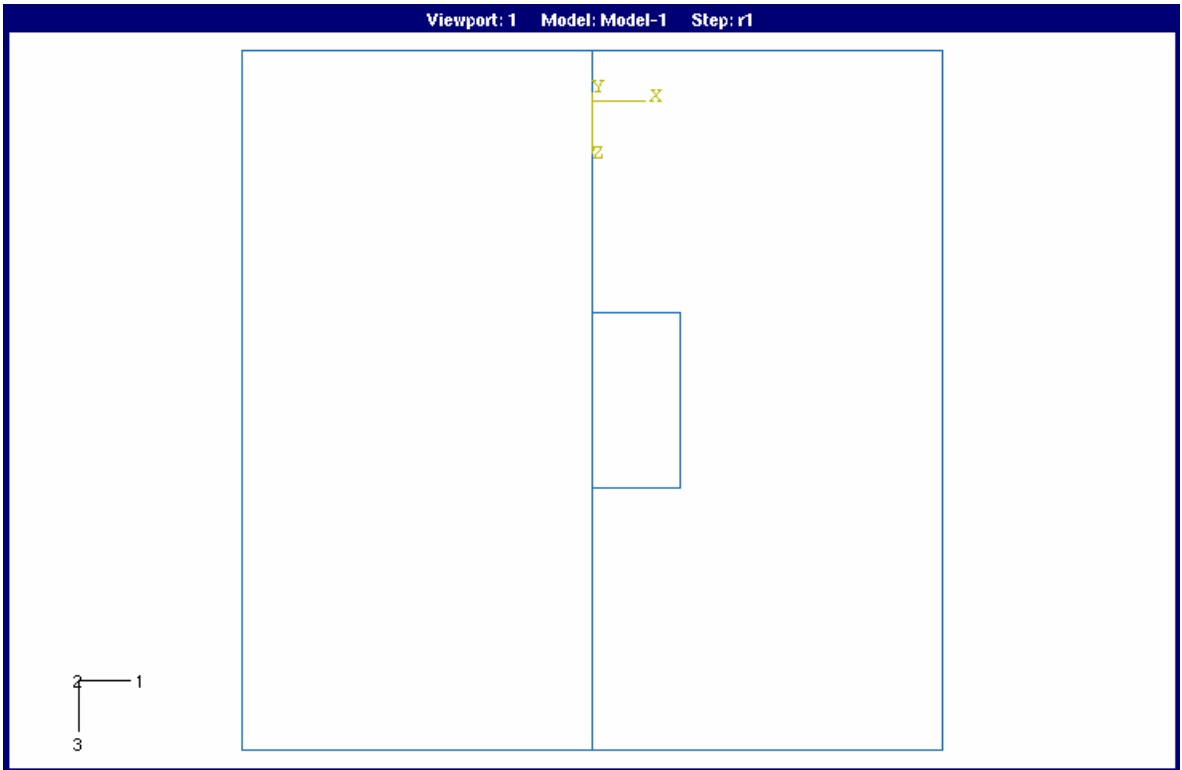


FIG 5.4b Top View of the Box Rift Model

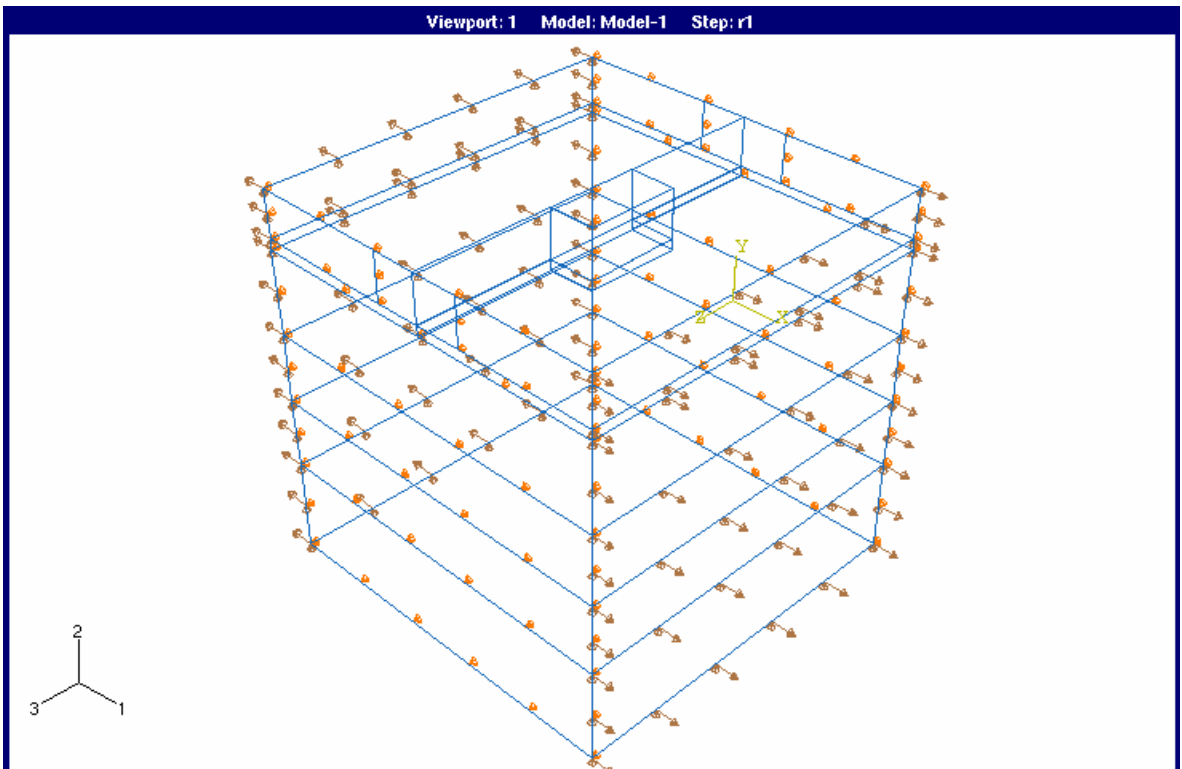


FIG 5.4c Model with Loads and Boundary Conditions

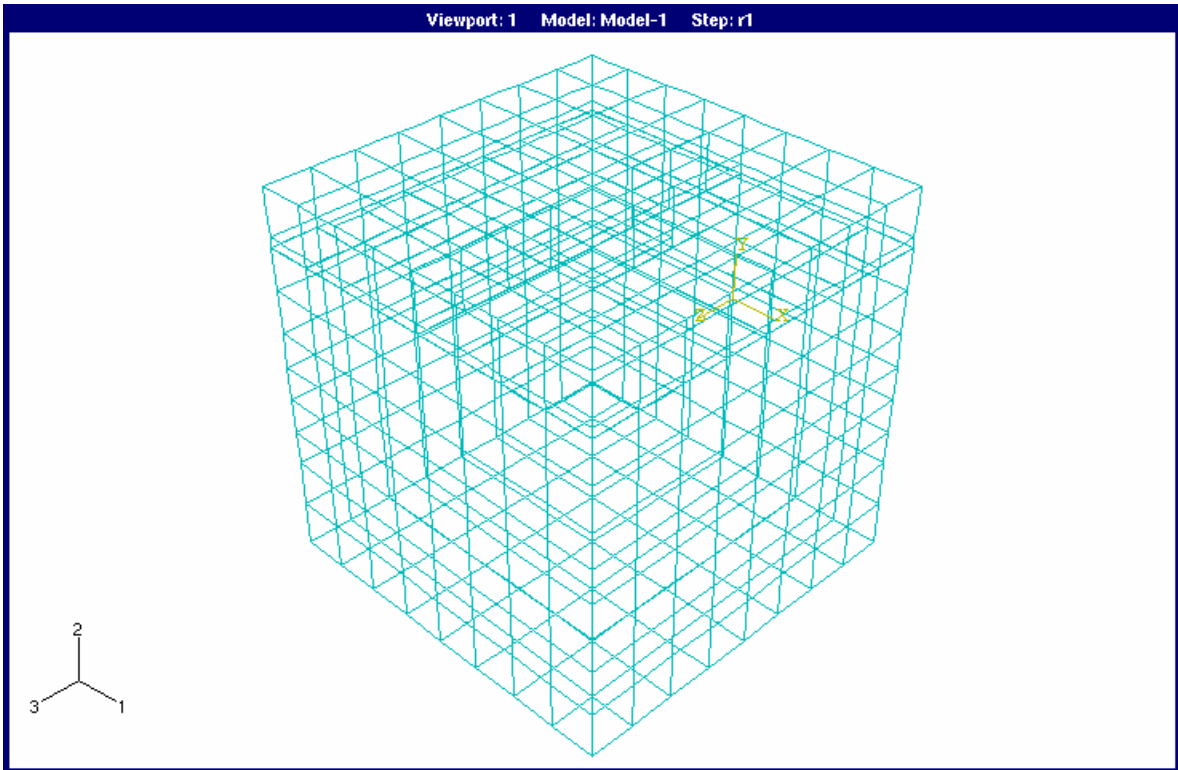


FIG 5.4d Meshed Model

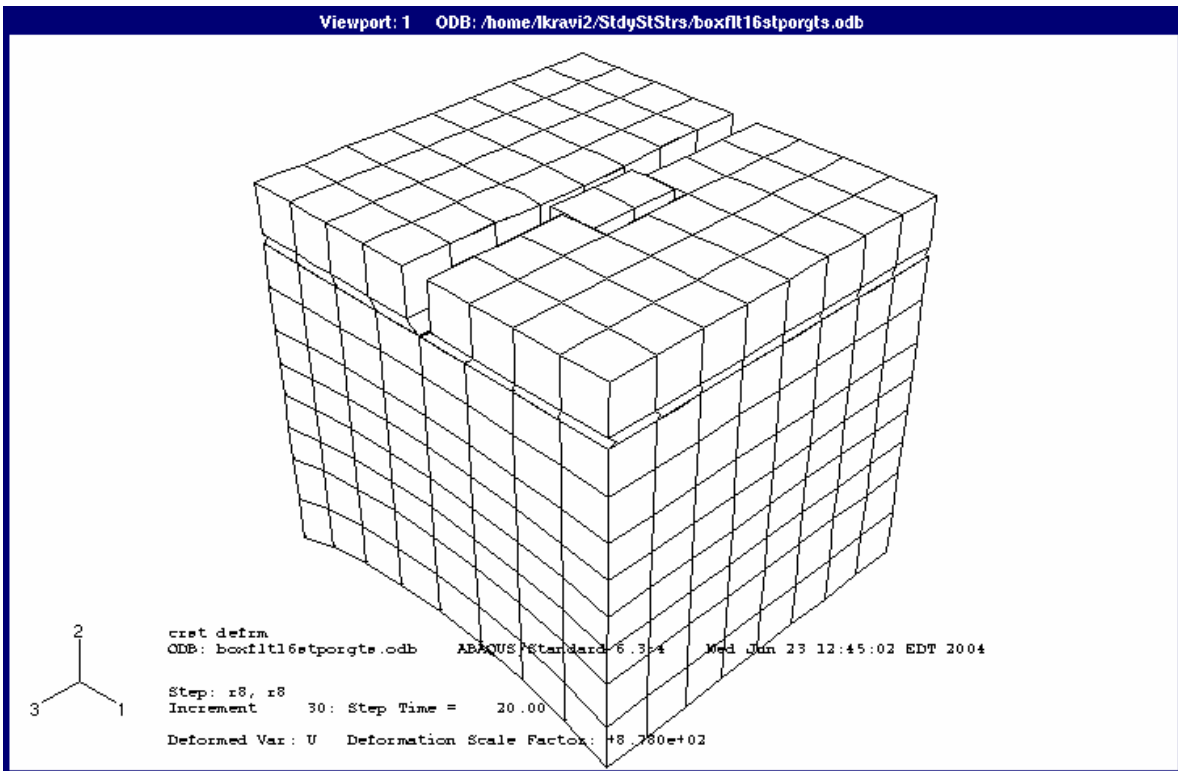


FIG 5.4e Final Deformation of the Model at the End of the 16<sup>th</sup> Step.

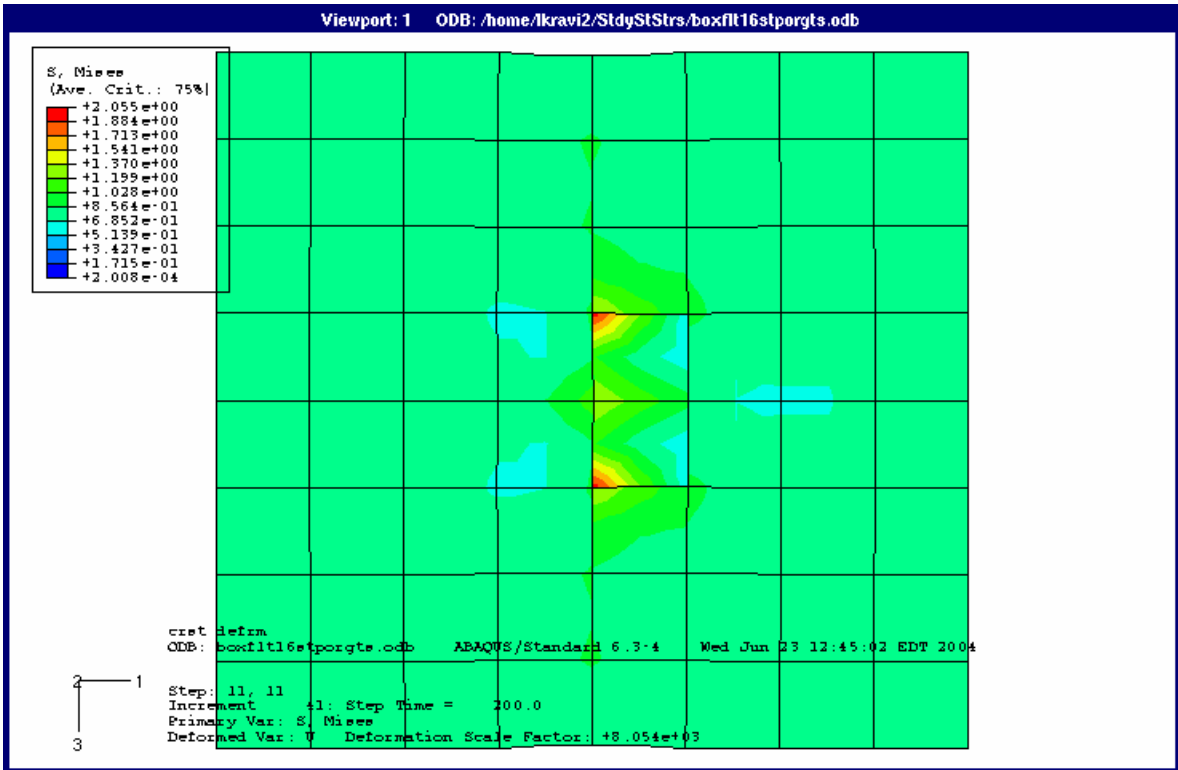


FIG 5.4f Top View of the Model Mises Stresses at the End of the 1<sup>st</sup> Loading Step

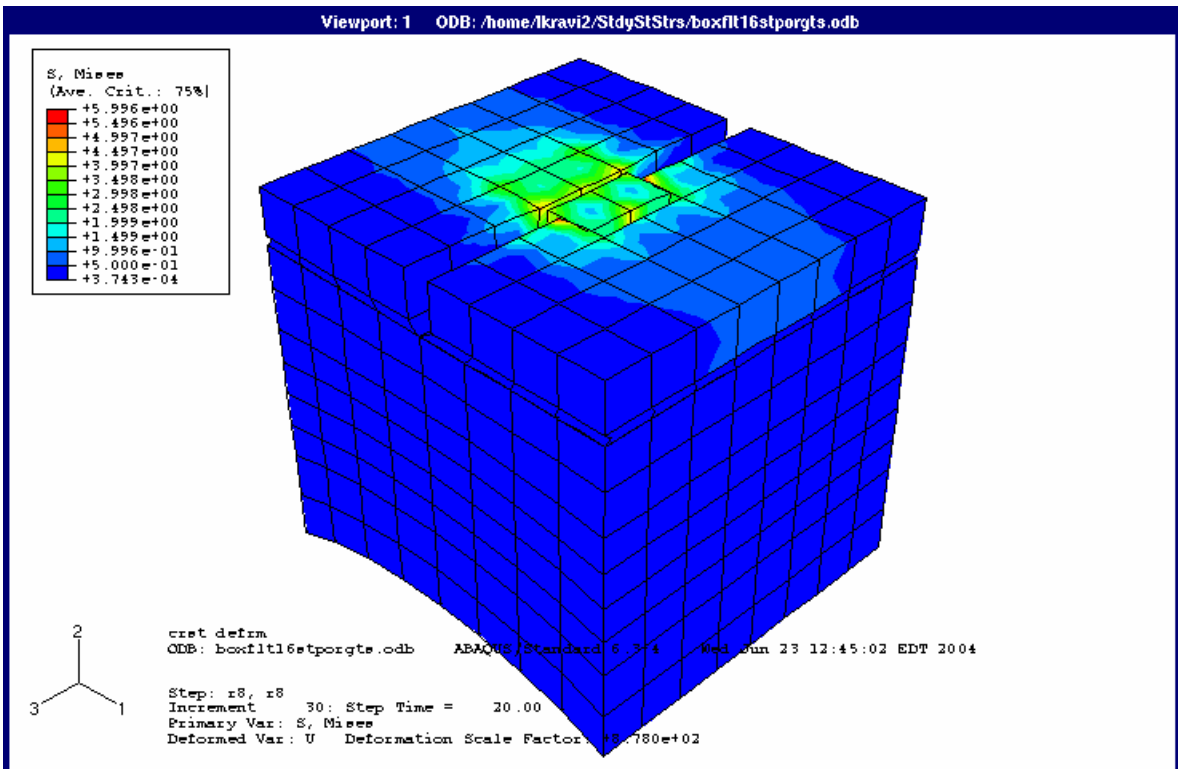


FIG 5.4g Model Mises stresses at the End of the 8<sup>th</sup> Rifting Step

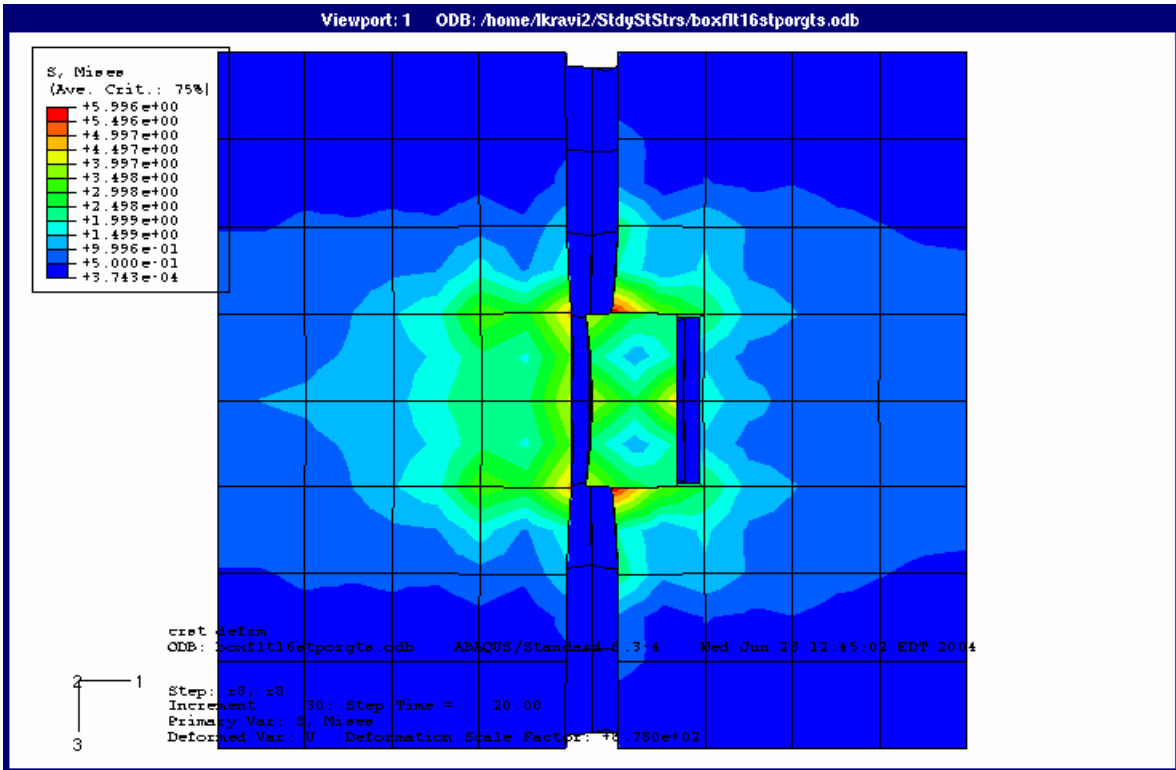


FIG 5.4h Top View of the Rift/Fault with Mises Stresses at the End of 8<sup>th</sup> Rifting Step

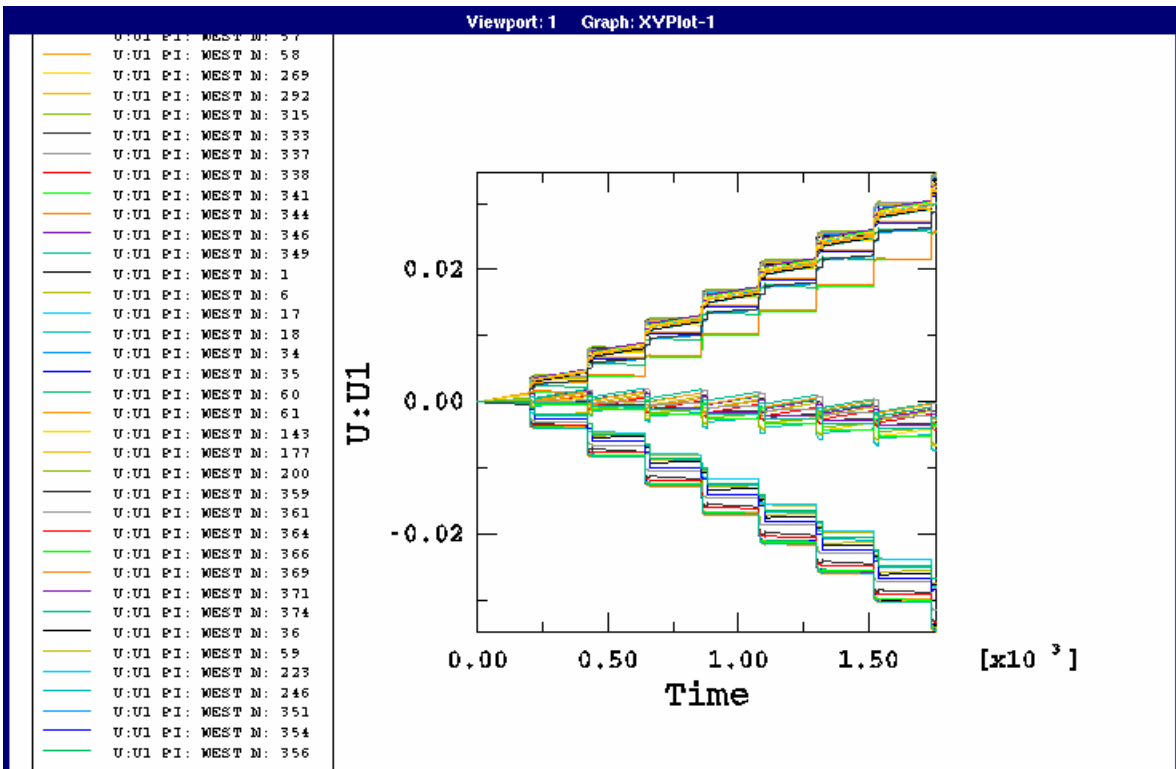


FIG 5.4i Displacement of the Nodes on the Rift During the 16 Step Analysis

Figure 5.4i is similar to figure 5.3i. The top and bottom lines represent displacements along the straight fault segment and the middle displacement comes from the nodes along the sides of the box.

Figures 5.4j, 5.4k, and 5.4l represent the Time Vs Mises Stress distribution during the 16 step cycle (8 loading and 8 rifting steps) of the entire model at different location. They represent the steady state stress attained and the number of cycles it took to reach the steady state stress.

Figure 5.4j represents steady State Mises Stress and the number of cycles it took to reach the steady state stress for the right hand bottom node on the front face of the model. The steady state Mises stresses for this node is  $21.25 \times 10^{-3}$  MPa and its corresponding cycle time is 14 cycles.

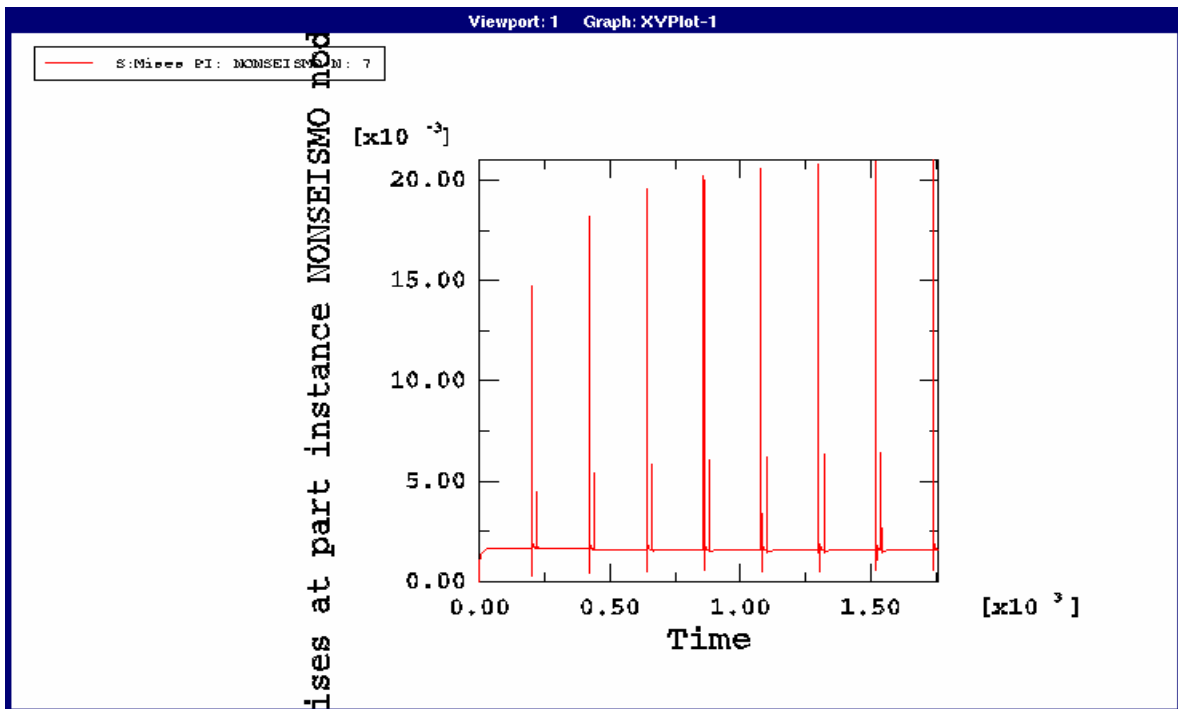


FIG 5.4j Cycle-Up and Subsequent steady State Mises Stress for the Right Hand Bottom Node on the Front Face of the Model.

Figure 5.4k represents steady State Mises Stress and the number of cycles it took to reach the steady state stress for the node located at the base of the rift on the front face of the model. The steady state Mises stresses for this node is 1.75 MPa and its corresponding cycle time is 10 cycles.

Figure 5.4l represents steady State Mises Stress and the number of cycles it took to reach the steady state stress for the node located in the middle of the front face of the model. The steady state Mises stresses for this node is  $19.25 \times 10^{-3}$  MPa and its corresponding cycle time is 14 cycles.

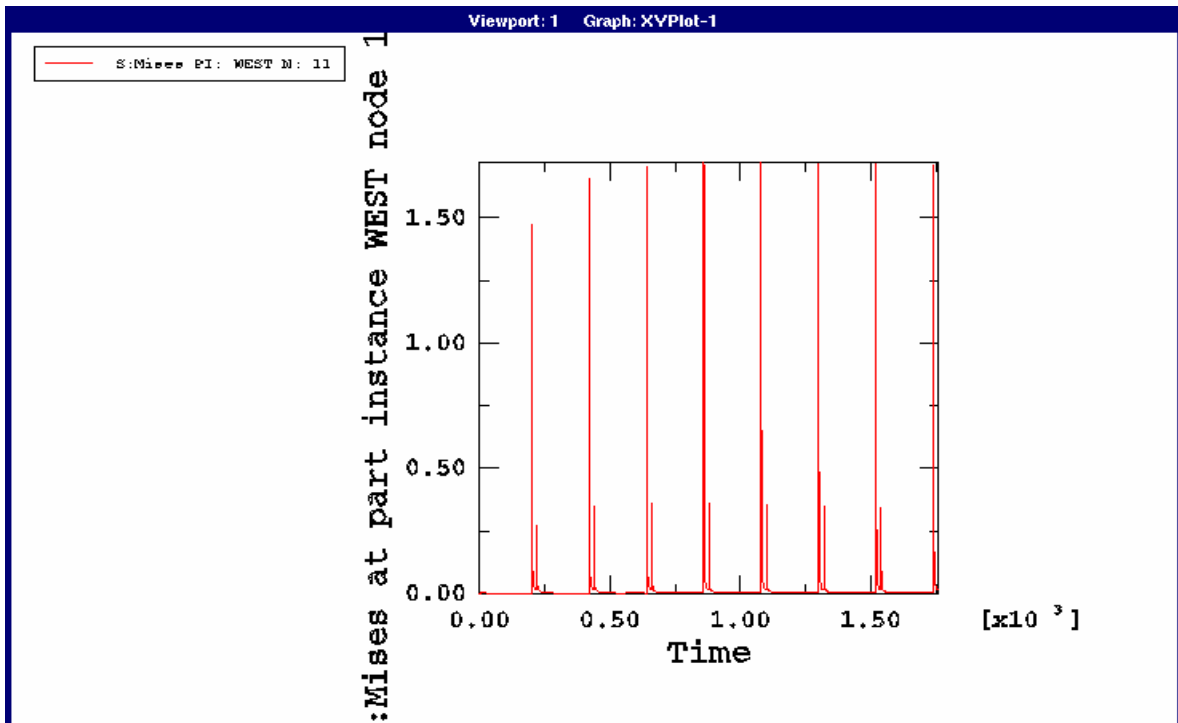


FIG 5.4k Cycle-Up and Subsequent Steady State Mises Stress for a Node Located at the Base of the Rift on the Front Face of the Model.



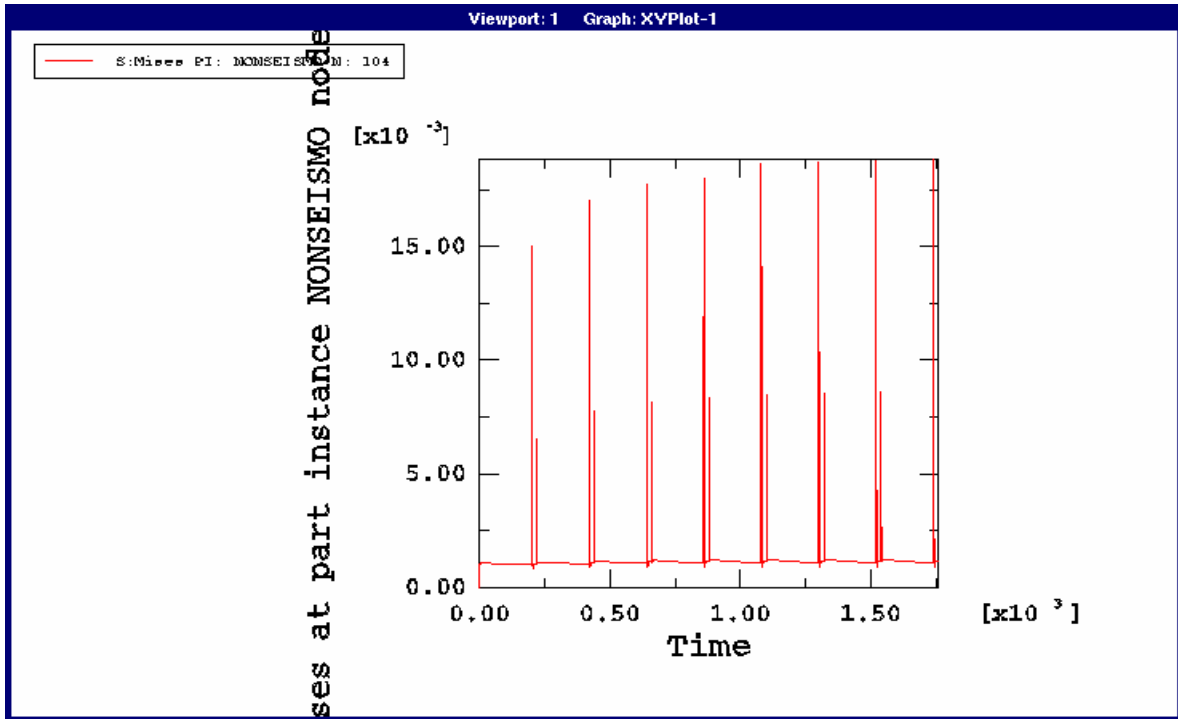


FIG 5.4I Cycle-Up and Subsequent Steady State Mises Stress for a Node Located in the Middle of the Front Face of the Model.

**5.5 EXPERIMENT 5&6: SKEWED RIFT MODEL & DOUBLE KINK MODEL:**

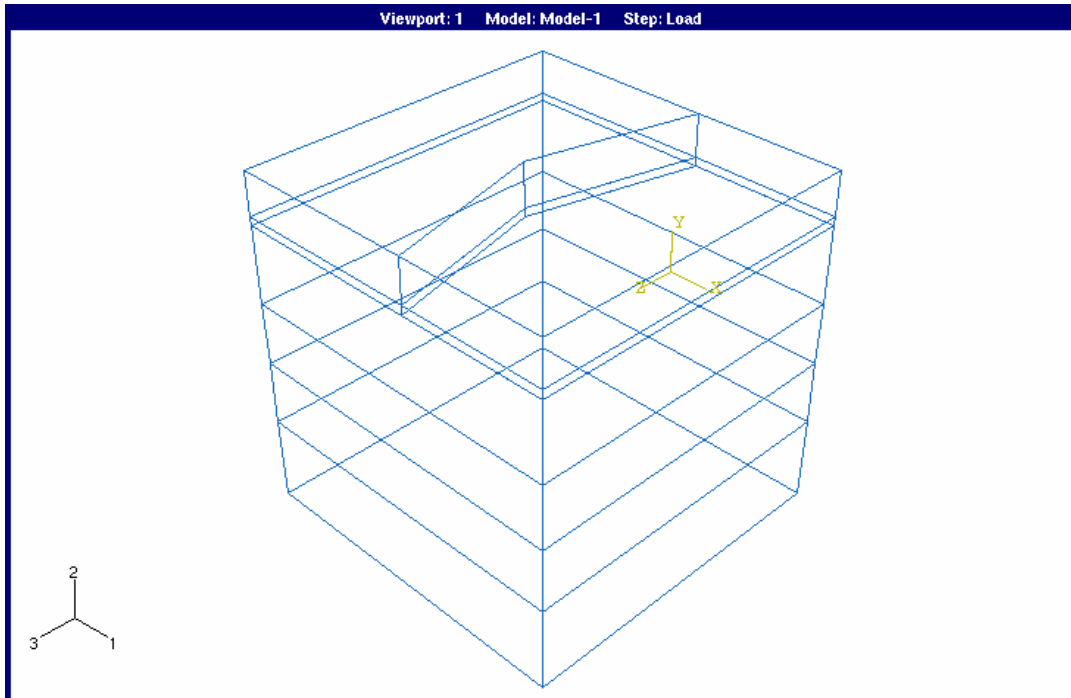


FIG 5.5a Skewed Rift Model

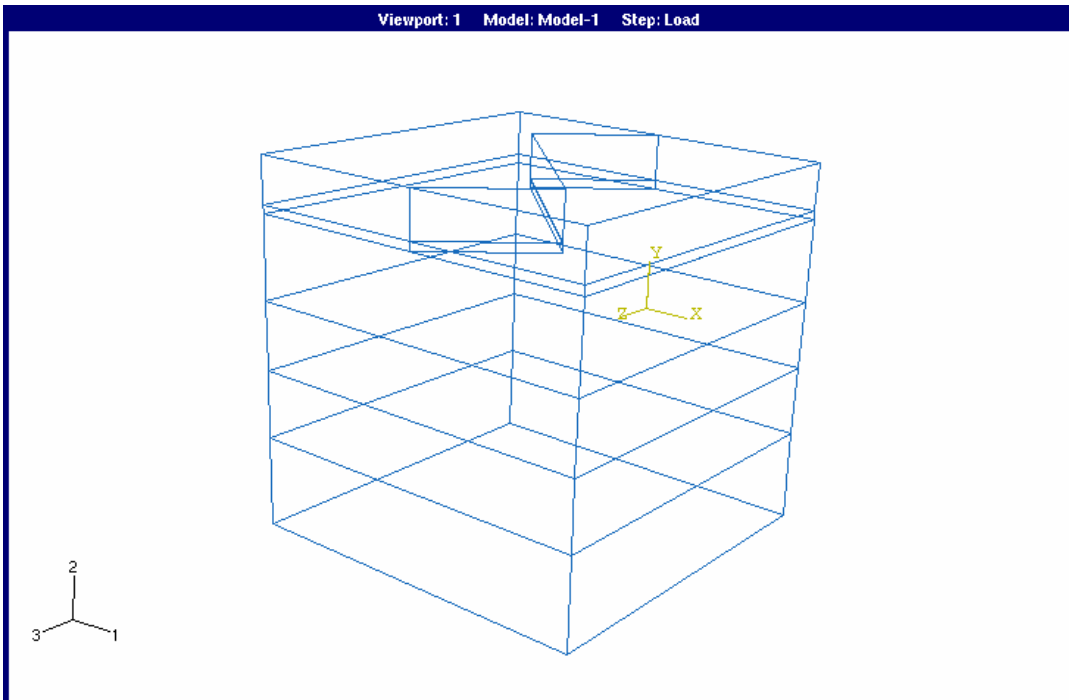


FIG 5.5b Double Kink Model

These models were also successfully run but for expediency the results are not shown here.

In summary the stress in all models at the downward tip of the rift is highest. This result is expected. As for cycle-up times there is no clear trend. These cycle-up times clearly depend on the geometry of the model and rheology of the model at various depths.

**CHAPTER SIX**

***CONCLUSION***

6.1 CONCLUSIONS.....89

## 6.1 CONCLUSIONS:

The steady state Mises stresses for the node located at the right hand bottom of the models considered in experiments 1, 2, 3, and 4 are  $23.5 \times 10^{-3}$  MPa,  $19.5 \times 10^{-3}$  MPa,  $22.5 \times 10^{-3}$  MPa, and  $21.25 \times 10^{-3}$  MPa respectively. Their corresponding cycle times are 10 cycles, 12 cycles, 14 cycles and 14 cycles. Reference FIG 5.1j, 5.2j, 5.3j, and 5.4j

The steady state Mises stresses for the node located at the base of the rift (120 km) on the front face of the models considered in experiments 1, 2, 3, and 4 are 0.9 MPa, 1.25 MPa, 1.3 MPa, and 1.75 MPa respectively. Their corresponding cycle times are 8 cycles, 14 cycles, 16 cycles and 10 cycles. Reference FIG 5.1k, 5.2k, 5.3k, and 5.4k

The steady state Mises stresses for the node located in the middle of the front face of the models considered in experiments 1, 2, 3, and 4 are  $21.0 \times 10^{-3}$  MPa,  $22.05 \times 10^{-3}$  MPa,  $33.0 \times 10^{-3}$  MPa, and  $19.25 \times 10^{-3}$  MPa respectively. Their corresponding cycle times are 4 cycles, 6 cycles, 14 cycles and 14 cycles. Reference FIG 5.1l, 5.2l, 5.3l, and 5.4l.

Based on the above study and all the experiments conducted we conclude that:

- Different locations in the model have different cycle-up times and steady state stress values. These values are a function of model geometry; however stresses at the fault tip as expected are always larger than other locations in the model.

- Changes in Rheology, far-field boundary conditions, and rift/fault pattern causes variation in cycle-up time and steady state stress value at different locations in the model.
- Multiple rifting events can be successfully modeled using an ABAQUS \*MPC user-defined subroutine.
- Complex rifting patterns, as required for Iceland models, can be successfully modeled using ABAQUS, User-Subroutine, and Virtual topology.
- Actual discrete rifting events, as described in this document, are the first of their kind.

**CHAPTER SEVEN**

***SCOPE OF FUTURE WORK***

7.1 FUTURE WORK.....92

## 7.1 FUTURE WORK:

One thing that can be said about this project is that, it is never ending. There are many factors that are still to be considered and have to be dealt in detail. These include complexity in the rift/fault pattern in Iceland, the orientations of the rift/fault, the force exerted by the upcoming magma beneath the rift/fault, proper far-field boundary conditions and many others.

The efforts we have made towards future work include working on models of greater complexity to more fully describe the tectonics of Iceland as seen below. Based on Dr. Shelley J. Kenner and Dr. Mark Simons work we have the capabilities to develop this model. Below is the 1<sup>st</sup> order model that Kenner and Simons will use to compare with real data. If this works the order of complexity could even get more precise and march toward reality.

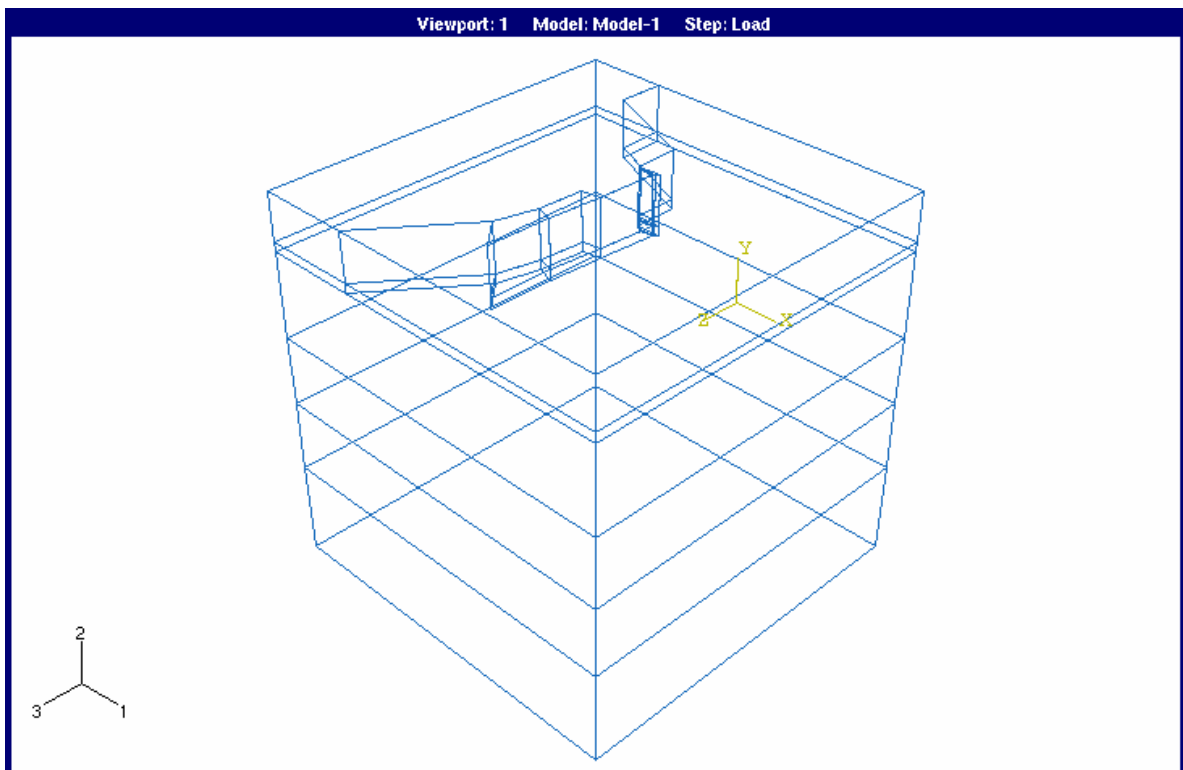


FIG 7.1 Model with a complex rift pattern.

The 1<sup>st</sup> order model (fig.7.1) is generated from the following sub-assemblies. They are East part, West part, SJuncS, SJuncN, NJuncS, NJuncN, and Non-seismogenic zone is located beneath these sections.

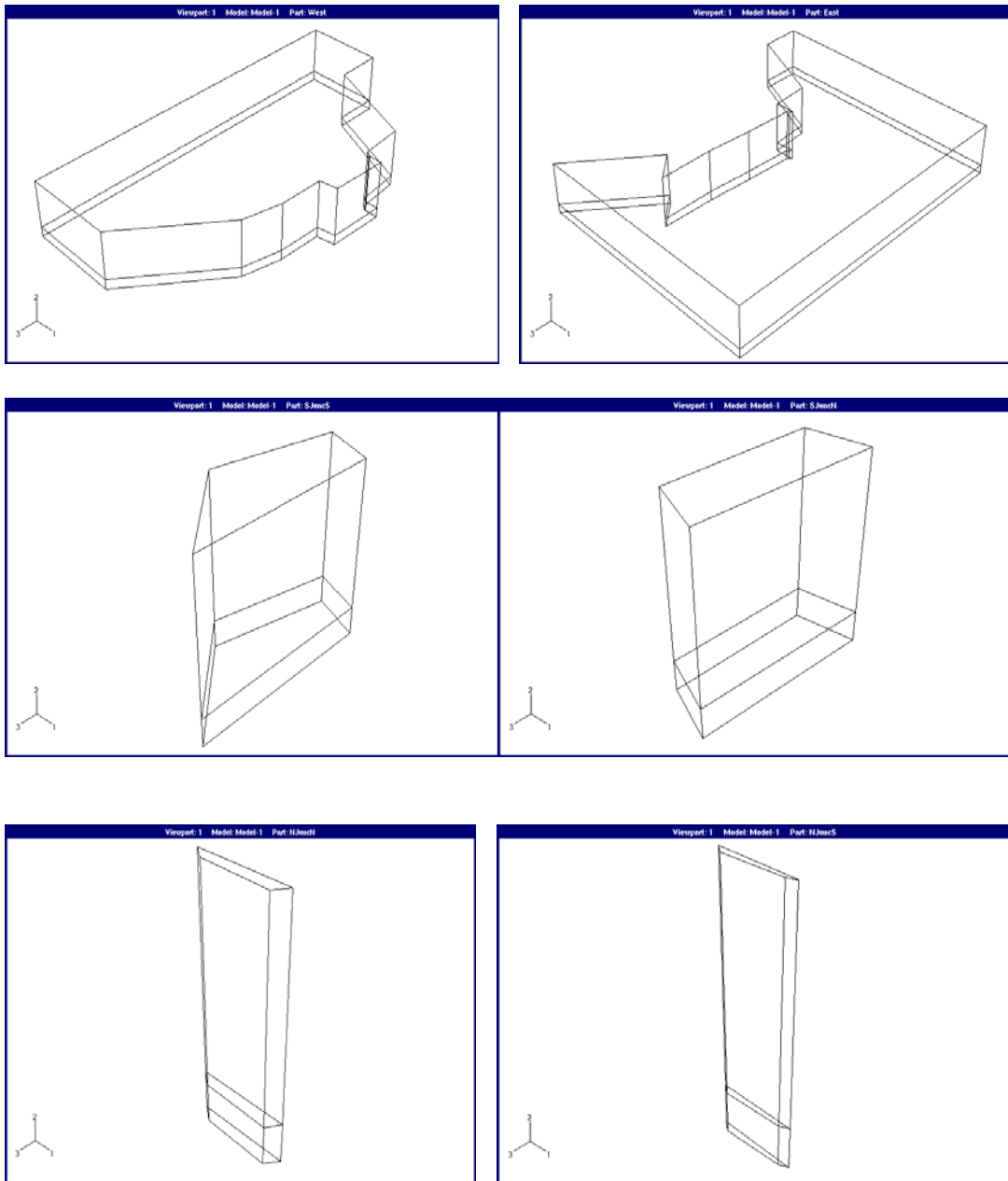


FIG 7.2 Parts of the complex model



## Appendix A

### GLOSSARY:

**Asthenosphere:** The shell within the earth, some tens of kilometers below the surface and of undefined thickness, which is a shell of weakness where plastic movements take place to permit pressure adjustments. It is located beneath the lithosphere.

**Basalt:** A Volcanic rock (or lava) that characteristically is a medium-gray to black igneous rock, contains 45% to 54% silica, and generally is rich in iron and magnesium. Basalt is world's most abundant lava and is the chief constituent of isolated oceanic islands.

**Dike:** A sheet like body of igneous rock that cuts across layering or contacts in the rock into which it intrudes.

**Fissures:** Elongated fractures or cracks on the slopes of a volcano. Fissure eruptions typically produce liquid flows, but pyroclastics may also be ejected.

**Flood Basalt:** Extremely fluid basaltic lava that erupts as a series of horizontal flows in rapid succession (geologically), covering vast areas; generally believed to be the product of fissure eruption. Flood basalts are extruded along mid-oceanic ridges during crustal extension.

**Generation of Magma:** The temperature of the mantle is lower than its melting point. Hence the mantle is usually solid. If there is a hot mass of mantle , the specific gravity of

the mass is slightly lighter than the surrounding part, and it gradually goes up. Because the mantle is of low heat-conductivity it is not easy to conduct heat. The mass of mantle hardly cools while it rises up, this is called adiabatic rising. Continuing to rise up, it would finally begin to melt and this is how magma is generated.

**Graben:** An elongate crustal block that is relatively depressed (downdropped) between two fault systems.

**Hot Spot:** A heat source or a volcanic center deep within the earth's mantle, 60 to 120 miles (100 to 200 km) across and persistent for at least a few tens of million of years. It is thought to be the surface expression of a persistent rising plume of hot mantle material.

**Hot-spot Volcanoes:** Volcanoes related to a persistent heat source in the mantle.

**Hyaloclastite:** A deposit formed by the flowing or intrusion of lava or magma into water, ice, or water-saturated sediment and its consequent granulation or shattering into small angular fragments.

**Igneous Rock:** One of the main groups of rocks that comprise the earth's crust. They constitute about 15% of the earth's surface, and are formed of molten material (magma) that flows up from the deeper part of the crust.

**Lava:** Magma which has reached the surface through a volcanic eruption. The term is most commonly applied to streams of liquid rock that flow from a crater or fissure. It also refers to cooled and solidified rock.

**Left Lateral:** If you were to stand on the fault and look along its length, this is a type of strike-slip fault where the left block moves toward you and the right block moves away.

**Lithosphere:** The rigid crust and uppermost mantle of the earth. Thickness is on the order of 60 miles (100 km). Stronger than the underlying asthenosphere.

**Mantle Plume:** A persistent column of magma rising upwards from the earth's mantle to the crust; it appears to be the main contributing factor to hot spots.

**Magma:** Molten rock beneath the surface of the earth.

**Mid-ocean Ridge:** A continuous feature that extends through the Atlantic, Indian, Antarctic, and South Pacific Oceans, the Norwegian Sea, and the Arctic Basin. It's the greatest mountain range on the earth, with a total distance of over 35,000 miles. Magma is extruded at these location to form new lithosphere.

**Mid-Atlantic Ridge:** It is that portion of the mid-oceanic ridge which lies within the Atlantic Ocean. Occasionally, the ridge reaches above the ocean surface as islands or reefs as in Iceland.

**Slow-spreading:** According to plate tectonics, when two crustal plates separate, basaltic material wells up through the spreading center and produces a ridge. Rapid separation of plates builds ridges with gentle slopes and broad elevations, such as those of East Pacific Rise. The steep flanks of the Mid-Atlantic Ridge were formed by slow spreading.

**Shield Volcano:** A gently sloping volcano, resembling a flattened dome. It is built by flows of very fluid basaltic lava erupted from numerous, closely placed vents and fissures. It is generally of smaller area than a flood basalt.

**Ridge:** An elongate, narrow, steep-sided elevation of the earth's surface or the ocean sea floor. A major submarine mountain range.

**Right Lateral:** If you were to stand on the fault and look along its length, this is a type of strike-slip fault where the right block moves toward you and the left block moves away.

**Rifting:** Rifting is the process by which the continental lithosphere stretches. A Continental rift is the belt or zone of the continental lithosphere where the extensional deformation (rifting) is occurring. These zones have important consequences and geological features, and if the rifting is successful, lead to the formation of new ocean basins.

**Rift System:** The oceanic ridges formed where tectonic plates are separating and a new crust is being created; also, their on-land counterparts such as the East African Rift.

**Rift Valley:** A valley that was developed along a tectonic rift resulting from plate separation. Where the plates are separating rapidly, as along the East Pacific Rise, the rift is filled by magma that wells up to form a new sea floor that migrates along the sloping flanks on either side of the original fissure. When separation of the plates is slower, as along the Atlantic and Indian ridges, the up welling magma doesn't cover over the fissure; instead, it adheres to the trailing edge of the plate on either side of the rift, creating precipitous scraps\* on each side. The original rift has now become a *rift valley*,

which marks the center of the ridge. The deep cleft along the crest of the mid-oceanic ridge is called the mid-ocean rift.

**Rift Zone:** A zone of volcanic features associated with underlying dikes. The location of the rift is marked by cracks, faults, and vents.

REFERENCE:

1. The facts on file dictionary of Geology and Geophysics by Dorothy Farris  
Lapidus; Donald Coates, Ph.D
2. McGraw-Hill Dictionary of Earth Science by Sybil P. Parker
3. U.S Geological Survey.([www.usgs.gov](http://www.usgs.gov))

## Appendix B

% USRMKTSTMPVW is user input file where the specifications of the model to be

% generated are given by the user

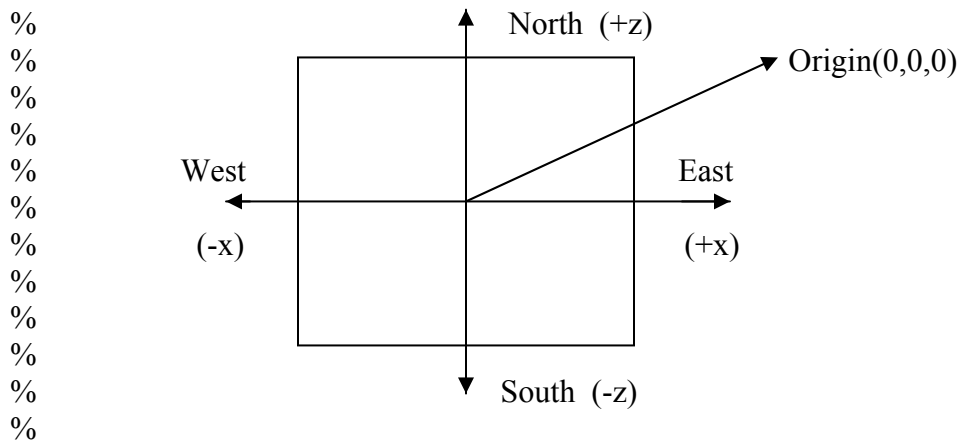
% X-direction assumed to run E-W (+1 direction is east)

% Y-direction assumed to run UP-DOWN (+2 direction is up)

% Z-direction assumed to run N-S (+3 direction is south)

% Specify required model parameters with origin (0,0,0) being at the center of the top

% rectangular face as shown.



% Specify the corners of the rectangle

xmax = ;

xmin = - ;

zmax = ;

zmin = - ;

% Enter the depth to the base of the model

ymin = - ;

% Specify the crustal depth with respect to the top surface

pcrstdpth = ;

% Specify the number of layers in the non-seismogenic zone

nlyrs = ;

% Specify the crack pattern by entering the point list in an M\*2 matrix form which

% results in the entire crack inclusive of the top face corner points.

%

%

%

%

%

%

%

%

%

%

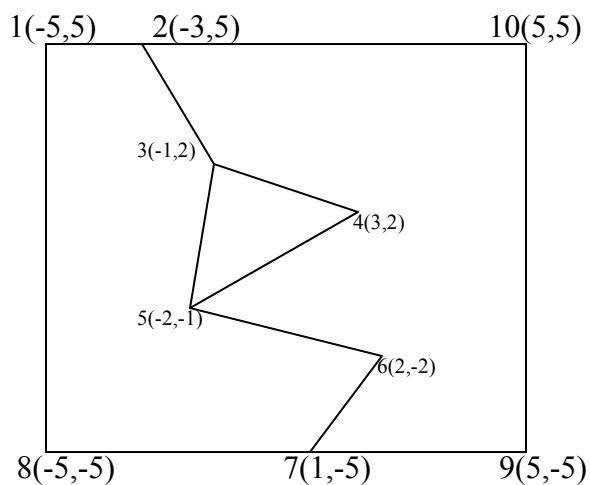
%

%

%

%

%



```

% Example: ptlst = [-5,5; ...
%                -3,5; ...
%                -1,2; ...
%                3,2; ...
%                -2,-1; ...
%                2,-2; ...
%                1,-5; ...
%                -5,-5; ...
%                5,-5; ...
%                5,5];
%

```

```

ptlst = [      ];

```

```

% Specify the connectivity matrix which defines the connectivity of each cell, with the
% eastern most cell defined at the bottom.

```

```

% Example: connect = [01,02,03,05,06,07,08,00,00; ...
%                   03,04,05,00,00,00,00,00,00; ...
%                   02,10,09,07,06,05,04,03,00];
%

```

```

connect = [      ];

```

```

% Specify the point list of the layers in the non-seismogenic zone in N*2 matrix form

```

```

%lyrptlst = [      ];

```

```

% Specify the depths of the layers in the non-seismogenic zone in 1*N matrix form

```

```

dpths = [      ];

```

```

% Specify the crack tip depth

```

```

deltacarck =      ;

```

```

% Specify the rheology of each layer in the non-seismogenic zone from rheology 1 till

```

```

% rheology(n+1)

```



% Number of rheologies in the non-seismogenic zone will be no:of layers+1 (i.e) n+1.

Rheology1

E =

$\eta$  =

$\nu$  =

% Till

Rheology(n+1)

E =

$\eta$  =

$\nu$  =

% Specify the rheology of each cell in the crustal layer from rheology cell1 till

% rheology cell(k)

% Number of cell will be the no:of rows(k) in the connect matrix.

Rheology cell1

E =

$\eta$  =

$\nu$  =

% Till

Rheology cell(k)

E =

$\eta$  =

$\nu$  =

## Appendix C

### GEOLOGICAL TIME SCALE

(mya = million years ago)

<b>Phanerozoic Eon</b> (543 mya to present)	Cenozoic Era (65 mya to today)	Quaternary (1.8 mya to today) Holocene (10,000 years to today) Pleistocene (1.8 mya to 10,000 yrs) Tertiary (65 to 1.8 mya) Pliocene (5.3 to 1.8 mya) Miocene (23.8 to 5.3 mya) Oligocene (33.7 to 23.8 mya) Eocene (54.8 to 33.7 mya) Paleocene (65 to 54.8 mya)
	Mesozoic Era (248 to 65 mya)	Cretaceous (144 to 65 mya) Jurassic (206 to 144 mya) Triassic (248 to 206 mya)
	Paleozoic Era (543 to 248 mya)	Permian (290 to 248 mya) Carboniferous (354 to 290 mya) Pennsylvanian (323 to 290 mya) Mississippian (354 to 323 mya) Devonian (417 to 354 mya) Silurian (443 to 417 mya) Ordovician (490 to 443 mya) Cambrian (543 to 490 mya) Tommotian (530 to 527 mya)
<b>Precambrian Time</b> (4,500 to 543 mya)	Proterozoic Era (2500 to 543 mya)	Neoproterozoic (900 to 543 mya) Vendian (650 to 543 mya) Mesoproterozoic (1600 to 900 mya) Paleoproterozoic (2500 to 1600 mya)
	Archaean (3800 to 2500 mya)	
	Hadean (4500 to 3800 mya)	

REFERENCE:

Geological Society of America (GSA) 1999 Geologic Timescale, compiled by A.R. Palmer and J. Geissman -- S. Rieboldt, Nov. 2002.

## REFERENCES

1. Fred F. Pollitz and Selwyn Sacks, *Viscosity structure beneath northeast Iceland*, Journal of Geophysical Research, Vol. 101, No. B8, Pages 17,771-17,793, August 10, 1996.
2. M. A. Hofton and G. R. Foulger, *Postdrifting anelastic deformation around spreading plate boundaries, north Iceland. 1. Modeling of the 1987-1992 deformation using a viscoelastic Earth structure*, Journal of Geophysical Research, Vol. 101, No. B11, Pages 25,403-25,421, November 10, 1996.
3. John C. Lynch and Mark A. Richards, *Finite element models of stress orientations in well-developed strike-slip fault zones: Implications for the distribution of lower crustal strain*, Journal of Geophysical Research, Vol. 106, No. B11, Pages 26,707-26,729, November 10, 2001.
4. Alex Bjornsson, *Dynamics of Crustal Rifting in NE Iceland*, Journal of Geophysical Research, Vol. 90, No. B12, Pages 10,151-10,162, October 10, 1985.
5. M. Fernandez and G. Ranalli, *The role of rheology in extensional basin formation modeling*, Elsevier Tectonophysics 282(1997) 129-145.
6. Shelley J. Kenner and Mark Simons, *Temporal clustering due to postseismic reloading*, Submitted to Geophysical Journal International.
7. John J. Clague and Peter T. Bobrowsky, *The geological signature of great earthquakes off Canada's west coast*, Geoscience Canada, Vol.26.
8. Pradeep Talwani, *On the nature of reservoir-induced seismicity*, Pure and Applied Geophysics, 150(1997) 473-492.
9. Geoffrey C. P. King et al., *Static stress changes and the triggering of earthquakes*, Bulletin of the Seismological Society of America, Vol. 84, No. 3, pp. 935-953, June 1994.
10. Iain S. Stewart et al., *Glacio-seismotectonics: ice sheets, crustal deformation and seismicity*, Pergamon Quarterly Science Reviews 19(2000) 1367-1389.
11. Andrew M. Freed and Jain Lin, *Delayed triggering of the 1999 Hector Mine earthquake by viscoelastic stress transfer*, Letters to Nature Vol. 411, May 10, 2001.
12. Kurt L. Feigl et al., *Crustal deformation near Hengill volcano, Iceland 1993-1998*, Journal of Geophysical Research, Vol. 105, No. B8, Pages 25,655-25,675, November 10, 2000.

13. Wolfgang R. Jacoby et al., *Geodetic and geophysical evidence for magma movement and dyke injection during the Krafla rifting episode in north Iceland*, International Union of Geodesy and Geophysics and American Geophysical Union.
14. M. A. Hofton and G. R. Foulger, *Post-rifting anelastic deformation around spreading plate boundaries, north Iceland. 2. Implications of model derived from 1987-1992 deformation field.*, Journal of Geophysical Research, Vol. 101, No. B11, Pages 25,403-25,421, November 10, 1996.
15. G. R. Foulger et al., *Post-rifting stress relaxation at the divergent plate boundary in northeast Iceland*, Letters to Nature Vol. 358, August 6, 1992.
16. Freysteinn Sigmundsson et al., *The 1994-1995 seismicity and deformation at the Hengill triple junction, Iceland.*, Journal of Geophysical Research, Vol. 102, No. B7, Pages 15,7151-15,161, July 10, 1997.
17. Carolina Pagli et al., *Triggered fault slip on June 17, 2000 on the Reykjanes Peninsula, SW-Iceland captured by radar interferometry*, Geophysical Research Letters, Vol. 30, No. 6, 1273, 2003.
18. Freysteinn Sigmundsson and Pall Einarsson, *Glacio-isostatic crustal movements caused by historical volume change of the Vatnajokull ice cap, Iceland*, Geophysical Research Letters, Vol. 19, No. 21, pp. 2123-2126, 1992.
19. Agust Gudmundsson, *Ocean-ridge discontinuities in Iceland*, Journal of Geophysical Research, Vol. 152, Pages 1011-1015, 1995.
20. Yijun Du and Atilla Aydin, *Three-dimensional characteristics of dike intrusion along the northeast Iceland rift from inversion of geodetic data*, Elsevier Science Publishers, Tectonophysics, 204, 1992.
21. Freysteinn Sigmundsson, *Post-glacial rebound and asthenosphere viscosity in Iceland*, Geophysical Research Letters, Vol. 18, No. 6, pp. 1131-1134, 1991.
22. Cook, R.D., Malkus, D.S., and Plesha, M.E., *Concepts and Applications of Finite Element Analysis*, J Wiley and Sons, pp. 14-15, 2000.
23. M.A Hofton et al., *Horizontal surface deformation due to dyke emplacement in an elastic-gravitational layer overlying a viscoelastic-gravitational half-space*, Journal of Geophysical Research, Vol. 100, No. B4, Pages 6329-6338, April 20, 1995.

24. Wolfgang R. Jacoby et al., *Geodetic and geophysical evidence for magma movement and dyke injection during the Krafla rifting episode in north Iceland*, American Geophysical Union, 1989.
25. M. Christina Hackman et al., The mechanics of the south Iceland seismic zone, *Journal of Geophysical Research*, Vol. 95, No. B11, Pages 17,339-17,353, Oct.20, 1990.
26. W. Jacquelyne Kious and Robert I. Tilling, *This Dynamic Earth: The Story of Plate Tectonics*, published by United States Geological Survey in 1996.
27. Abaqus/Standard User Manual Version 6.3, by HKS.
28. U.S. Geological Survey. [www.usgs.gov](http://www.usgs.gov).

# VITA

## **Date and Place of Birth**

- January 26, 1980 at Khammam, Andhra Pradesh, INDIA.

## **Education**

- Bachelor of Engineering (B.E) in Mechanical Engineering, Chaitanya Barathi Institute of Techonoly, Osmania University, Hyderabad, INDIA.

## **Work Experience**

- Research Assistant, Department of Geological Sciences, University of Kentucky, Lexington, KY. (August 2002- December 2004).